



LUND UNIVERSITY

Identification of the Linear Steering Dynamics of the Sea Splendour

Källström, Claes

1977

Document Version:

Publisher's PDF, also known as Version of record

[Link to publication](#)

Citation for published version (APA):

Källström, C. (1977). *Identification of the Linear Steering Dynamics of the Sea Splendour*. (Technical Reports TFRT-7129). Department of Automatic Control, Lund Institute of Technology (LTH).

Total number of authors:

1

General rights

Unless other specific re-use rights are stated the following general rights apply:

Copyright and moral rights for the publications made accessible in the public portal are retained by the authors and/or other copyright owners and it is a condition of accessing publications that users recognise and abide by the legal requirements associated with these rights.

- Users may download and print one copy of any publication from the public portal for the purpose of private study or research.
- You may not further distribute the material or use it for any profit-making activity or commercial gain
- You may freely distribute the URL identifying the publication in the public portal

Read more about Creative commons licenses: <https://creativecommons.org/licenses/>

Take down policy

If you believe that this document breaches copyright please contact us providing details, and we will remove access to the work immediately and investigate your claim.

LUND UNIVERSITY

PO Box 117
221 00 Lund
+46 46-222 00 00

IDENTIFICATION OF THE LINEAR STEERING
DYNAMICS OF THE SEA SPLENDOUR

CLAES KÄLLSTRÖM

Institutionen för Reglerteknik
Lunds Tekniska Högskola
December 1977

Dokumentutgivare
Lund Institute of Technology
Handläggare
Department of Automatic Control
Claes G. Källström
Författare
Claes G. Källström

Dokumentnamn
REPORT
Utgivningsdatum
Dec 1977

Dokumentbeteckning
LUTFD2/(TRT67129)/1-85/(1977)
Arendebeteckning
STU 73 4128 U
STU 75 40 53

10T4

Dokumenttitel och undertitel

10T4 Identification of the linear steering dynamics of the Sea Splendour

Referat (sammandrag)

System identification techniques are applied to determine the linear steering dynamics of the tanker Sea Splendour from two full-scale experiments. The output error method and the maximum likelihood method are applied using the identification program LISPID. The data have several defects, but it is shown that it is nevertheless possible to determine the linear steering dynamics. The maximum likelihood method is proved to be advantageous compared to the output error method.

Referat skrivet av
author

Förslag till ytterligare nyckelord

Ship, ship steering, ship dynamics

Klassifikationssystem och -klass(er)

50T0

Indextermer (ange källa)

52T0

Omfång

85 pages

Övriga bibliografiska uppgifter

56T2

Språk

English

Sekretessuppgifter

60T0

ISSN

60T4

ISBN

60T6

Dokumentet kan erhållas från

62T0
Department of Automatic Control
Lund Inst of Technology
PO Box 725, S-220 07 LUND 7, Sweden

Mottagarens uppgifter

62T4

Pris

66T0

DOKUMENTATABLAD enligt SIS 62 10 12

SIS-
DB 1

IDENTIFICATION OF THE LINEAR STEERING
DYNAMICS OF THE SEA SPLENDOUR

Claes G. Källström

TABLE OF CONTENTS

	Page
1. INTRODUCTION	1
2. EXPERIMENTS	2
3. IDENTIFICATION RESULTS FROM EXPERIMENT 1	7
4. IDENTIFICATION RESULTS FROM EXPERIMENT 2	62
5. CONCLUSIONS	79
6. ACKNOWLEDGEMENTS	81
7. REFERENCES	82

1. INTRODUCTION

System identification techniques are applied to determine the linear steering dynamics of the Sea Splendour from full-scale experiments. The identification program LISPID (see Källström, Essebo and Åström (1976)) is used to analyse the experiments. The output error method and the maximum likelihood method are applied.

The Sea Splendour is an oil tanker of 255 000 tdw built for the Salén Shipping Companies in Stockholm by Kockums Shipyard in Malmö. Two experiments performed in ballast condition are analysed.

2. EXPERIMENTS

The Sea Splendour is a single-screw turbine tanker of 255 000 tdw with a half-spade rudder. The maximum power at 85 rpm is 32 000 shp and the trial speed at full draught is 15.7 knots. The length between perpendiculars L is 329.2 m, the breadth is 51.8 m, and the mean draught is 20.1 m when the ship is fully loaded. The displacement at full draught is 285 000 m³.

The two experiments were performed in ballast condition with a displacement of 163 700 m³. The draught at bow and stern was 10.0 m and 13.0 m, respectively.

The first experiment was performed on the 4th of June, 1972, north of Stavanger, Norway. The wind was blowing on starboard with a speed of about 10 m/s (fresh breeze). The ship speed V was approximately 15.9 knots and the propeller rate of revolution was about 80 rpm. The experiment lasted for about 50 min. In the middle of the experiment the course was changed by 20°. The rudder input was originally chosen as a PRBS signal, but it was necessary to make many manual changes to avoid large deviations from the desired course. The sampling interval was 30 s. At every sample instant the process computer measured rudder servo position, rudder deflection, fore and aft sway velocities, yaw rate, course, forward speed, number of propeller revolutions, power, and printed them on a typewriter. The input-output data used for the system identification are shown in Fig 2.1. The rudder angles are positive towards port. Seven consecutive readings were missed between 1520 - 1700 s, and the sampling interval was furthermore a few seconds too long sometimes. The number of recorded samples are 97.

The second experiment was performed on the 10th of June, 1972, west of Portugal. A wind of about 4 - 5 m/s (gentle breeze) was blowing from astern. The ship speed V was approximately 16.5 knots and the propeller rate of revolution was about 80 rpm. The experiment lasted for about 30 min. The rudder input was generated manually in an arbitrary manner. The sampling interval was 15 s. Measurements

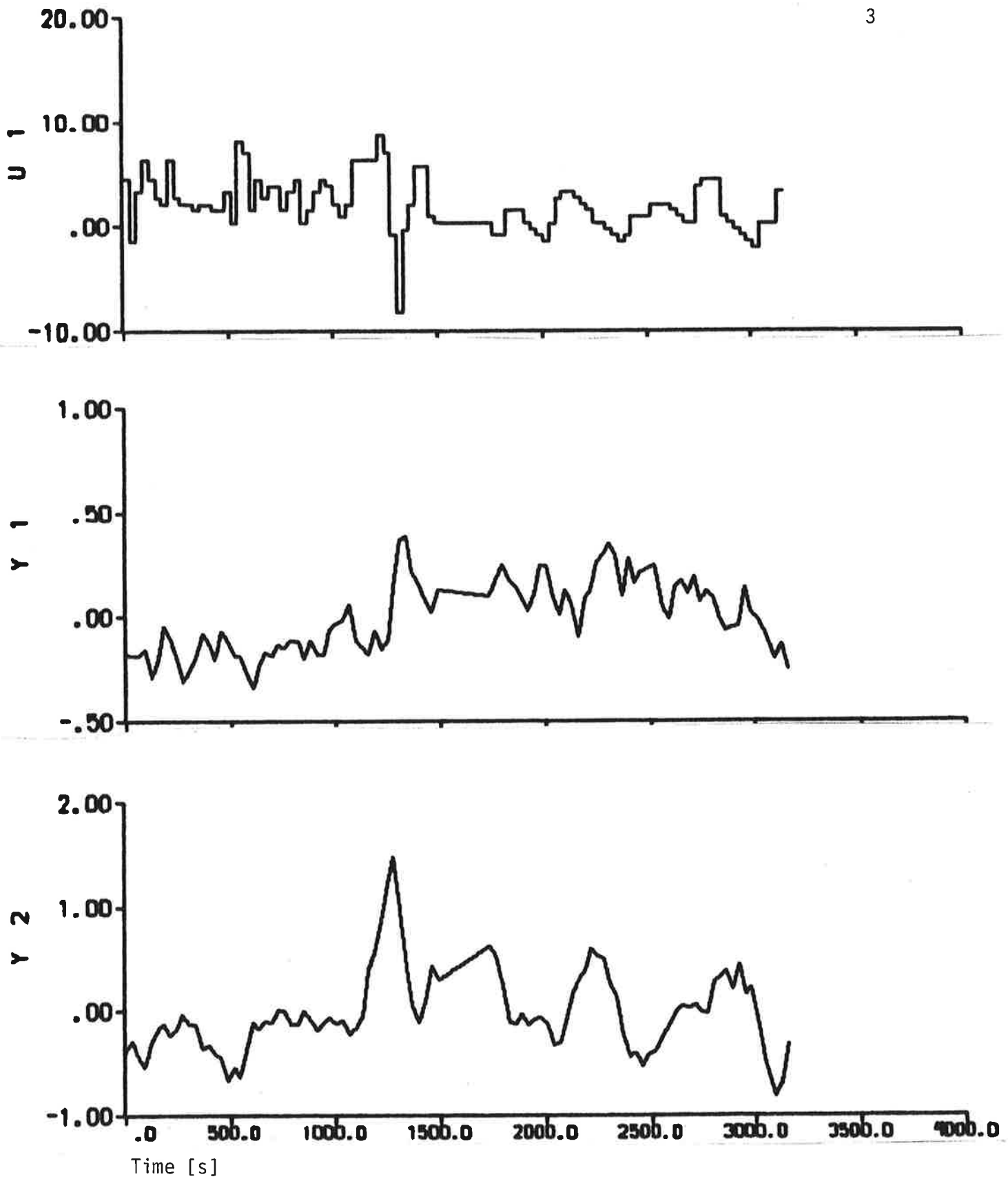


Fig 2.1 a - Input-output data obtained from the first experiment. The input is the rudder deflection $U1$ [deg] and the outputs are the fore sway velocity $Y1$ [knots], the aft sway velocity $Y2$ [knots], the yaw rate $Y3$ [deg/s], and the course $Y4$ [deg].

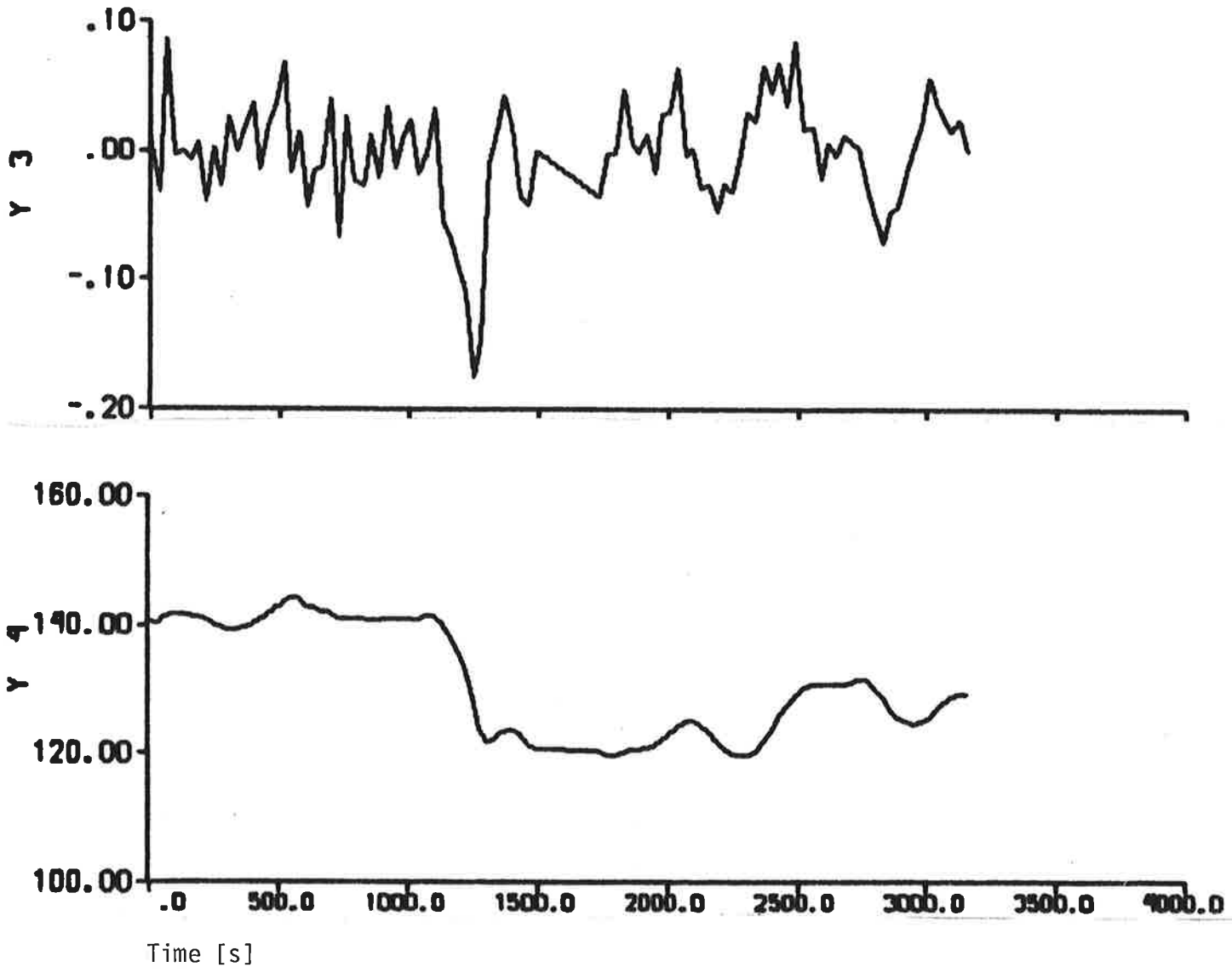


Fig 2.1 b

of rudder servo position, rudder deflection, yaw rate, course and forward speed were recorded at each sample instant. Fig 2.2 shows the input-output data used for the identification. The rudder angles are positive towards port. Seven consecutive readings were missed between 600 - 690 s, and the sampling interval was furthermore a few seconds too long sometimes. The number of recorded samples are 122.

The standard measurement equipment of the Sea Splendour was used for the experiments, which were easy to perform because the ship had an onboard process computer. The sway velocities of experiment 1 were measured by a doppler sonar equipment, type *Ametek Straza* with a resolution of about 0.02 knots. The distance from midship to the fore doppler log L_1 and to the aft doppler log L_2 was 154.6 m and 124.1 m, respectively. Notice that the values of L_1 and L_2 used in the identifications of Section 3 differ slightly from these values. The yaw rates and the headings of both experiments were measured by a rate gyro from AB ATEW, Flen, Sweden, and a Sperry gyro compass, respectively. The drift rate for the rate gyro given by the manufacturer is 3 deg/h (0.0008 deg/s). However, the quality of the rate gyro signal varies with the sea conditions and the way the gyro is mounted, and an accuracy of about 0.005 deg/s seems to be realistic. The resolution of the gyro compass is 1/6 deg. Notice that the doppler sonar and the rate gyro may have biases. The resolution of the rudder angles of experiment 1 is 0.6 deg and the resolution of the rudder servo positions of experiment 2 is 0.1 deg.

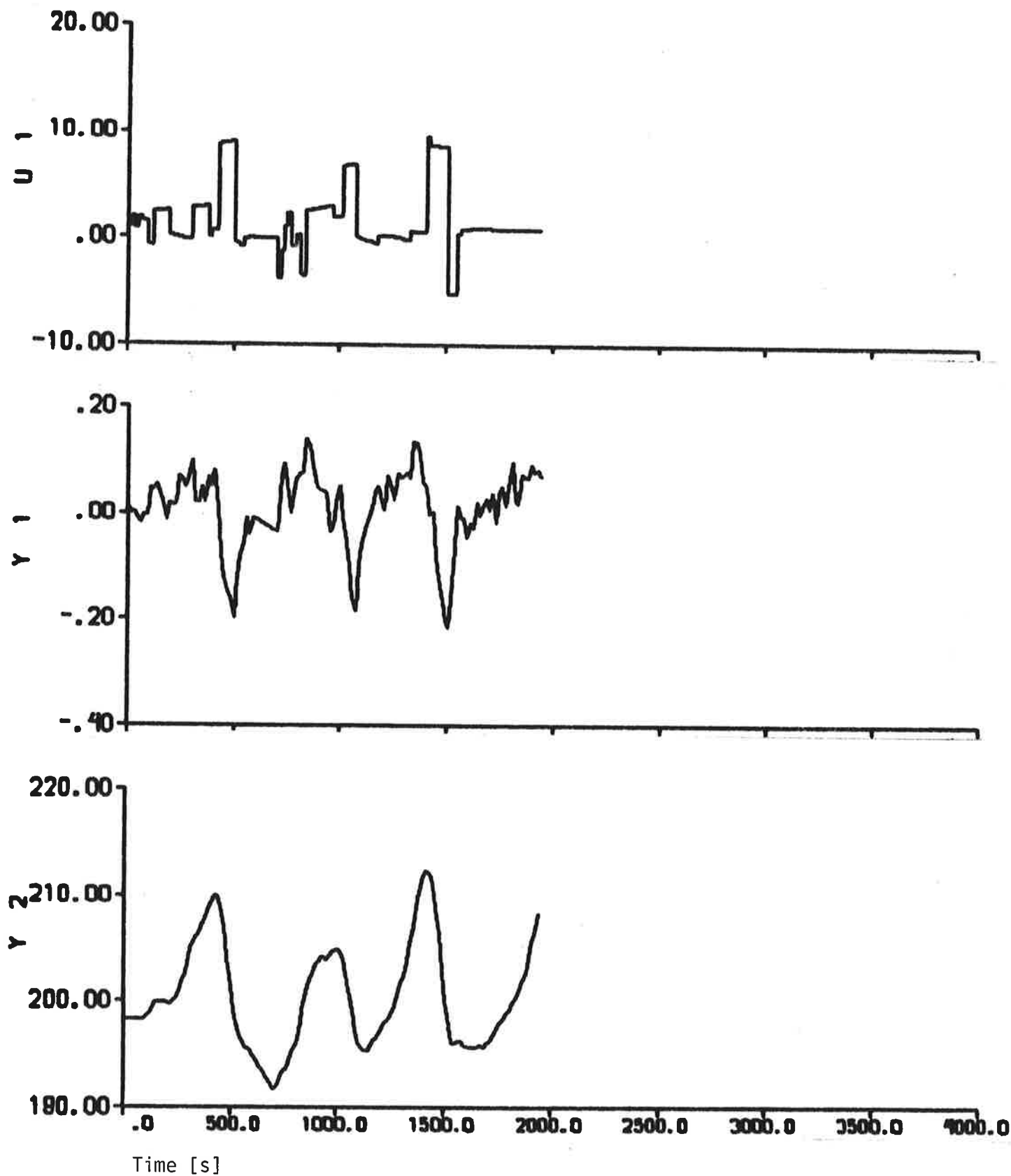


Fig 2.2 - Input-output data obtained from the second experiment. The input is the rudder servo position $U1$ [deg], and the outputs are the yaw rate $Y1$ [deg/s], and the course $Y2$ [deg].

3. IDENTIFICATION RESULTS FROM EXPERIMENT 1

The data from the first experiment have partly been analysed before (see Åström and Källström (1973), (1976) and Åström, Källström, Norrbin and Byström (1975)). A more complete summary of the identification results from the program LISPID is given in this section.

The identifications are based on the following linear model of the steering dynamics (cf Åström, Norrbin, Källström and Byström (1974), and Åström, Källström, Norrbin and Byström (1975))

$$\begin{aligned}
 & \begin{bmatrix} \frac{L}{V^2} \theta_1 & \frac{L^2}{V^2} \theta_2 & 0 \\ \frac{L}{V^2} \theta_3 & \frac{L^2}{V^2} \theta_4 & 0 \\ 0 & 0 & 1 \end{bmatrix} \begin{bmatrix} dv \\ dr \\ d\psi \end{bmatrix} = \begin{bmatrix} \frac{1}{V} \theta_5 & \frac{L}{V} \theta_6 & \theta_9 \\ \frac{1}{V} \theta_7 & \frac{L}{V} \theta_8 & \theta_9 \theta_{10} \\ 0 & 1 & 0 \end{bmatrix} \begin{bmatrix} v(t) \\ r(t) \\ \psi(t) \end{bmatrix} dt + \\
 & + \begin{bmatrix} \alpha_1 \theta_{11} & \theta_{13} \\ -\alpha_1 \theta_{11} \theta_{12} & \theta_{14} \\ 0 & 0 \end{bmatrix} \begin{bmatrix} \delta(t - T_D) \\ U \end{bmatrix} dt + dw \\
 & \begin{bmatrix} v_1(t_k) \\ v_2(t_k) \\ r_m(t_k) \\ \psi_m(t_k) \end{bmatrix} = \begin{bmatrix} \alpha_2 & L_1 \alpha_2 & 0 \\ \alpha_2 & -L_2 \alpha_2 & 0 \\ 0 & 1/\alpha_1 & 0 \\ 0 & 0 & 1/\alpha_1 \end{bmatrix} \begin{bmatrix} v(t_k) \\ r(t_k) \\ \psi(t_k) \end{bmatrix} + \\
 & + \begin{bmatrix} 0 & \theta_{15} \\ 0 & \theta_{16} \\ 0 & \theta_{17} \\ 0 & 0 \end{bmatrix} \begin{bmatrix} \delta(t_k - T_D) \\ U \end{bmatrix} + e(t_k) \quad k = 0, 1, \dots, N-1
 \end{aligned} \tag{3.1}$$

The Wiener process w has the incremental covariance $R_1 dt$, where

$$R_1 = \begin{bmatrix} |\theta_{18}| & \sqrt{|\theta_{18}||\theta_{19}|} \sin \theta_{20} & 0 \\ \sqrt{|\theta_{18}||\theta_{19}|} \sin \theta_{20} & |\theta_{19}| & 0 \\ 0 & 0 & 0 \end{bmatrix}$$

The measurement errors $\{e(t_k)\}$ are assumed to be independent and gaussian with zero mean and covariance R_2 , where

$$R_2 = \begin{bmatrix} |\theta_{21}| & 0 & 0 & 0 \\ 0 & |\theta_{22}| & 0 & 0 \\ 0 & 0 & |\theta_{23}| & 0 \\ 0 & 0 & 0 & |\theta_{24}| \end{bmatrix}$$

The initial state is given by

$$\begin{bmatrix} v(t_0) \\ r(t_0) \\ \psi(t_0) \end{bmatrix} = \begin{bmatrix} \theta_{25}/\alpha_2 \\ \alpha_1 \theta_{26} \\ \alpha_1 \theta_{27} \end{bmatrix}$$

and the initial covariance matrix of state estimate errors is

$$P(t_0) = P_0 = \begin{bmatrix} |\theta_{28}| & \theta_{31} & \theta_{32} \\ \theta_{31} & |\theta_{29}| & \theta_{33} \\ \theta_{32} & \theta_{33} & |\theta_{30}| \end{bmatrix}$$

The time delay T_D is computed as

$$T_D = T(1 - |\sin \theta_{34}|)$$

where T is the sampling interval.

The following variables are introduced in (3.1):

Inputs

- δ - rudder angle [deg]
- u - artificial unit step input [-]

States

- v - sway velocity at midship [m/s]
- r - yaw rate [rad/s]
- ψ - heading angle [rad]

Outputs

- v_1 - fore sway velocity [knots]
- v_2 - aft sway velocity [knots]
- r_m - yaw rate [deg/s]
- ψ_m - heading angle [deg]

The model (3.1) is provided with the following fixed parameter values:

- V - ship speed (8.2 m/s)
- L - ship length (329.2 m)
- L_1 - distance from midship to fore doppler log (147.6 m)
- L_2 - distance from midship to aft doppler log (131.1 m)
- α_1 - conversion factor from degrees to radians (0.01745)
- α_2 - conversion factor from m/s to knots (1.944)

The parameters $\theta_1 - \theta_{34}$ can be estimated in LISPID. Notice, however, that it is possible to estimate only a subset of the 34 parameters and to give the other parameters arbitrary fixed values. It is concluded from (3.1) that $\theta_1 - \theta_4$ are normalized acceleration hydro-

dynamic derivatives, $\theta_5 - \theta_8$, θ_{11} and $-\theta_{11}\theta_{12}$ are normalized linear hydrodynamic derivatives, θ_9 and θ_{10} are wind parameters, θ_{13} and θ_{14} are force and moment biases, and $\theta_{15} - \theta_{17}$ are measurement biases.

The maximum likelihood estimates of the unknown parameters are obtained in LISPID by minimizing the following loss function, if the system and covariance matrices are time-invariant and if the sampling rate is constant:

$$V_1 = \frac{1}{N} \det \left[\sum_{k=0}^{N-1} \varepsilon(t_k) \varepsilon^T(t_k) \right] \quad (3.2)$$

where N is the number of samples and ε is the residuals or innovations. In the general case the loss function

$$V_2 = -\frac{1}{N} \log L \quad (3.3)$$

is minimized, where L is the likelihood function. The one-step prediction errors, i.e. the residuals, are minimized in the maximum likelihood method. The output error method is easily obtained by assuming no process noise in (3.1), i.e. $w = 0$.

Different models can be compared by using Akaike's information criterion (cf Akaike (1972)):

$$AIC = -2 \log \hat{L} + 2\nu \quad (3.4)$$

where \hat{L} is the maximum of the likelihood function, and ν is the number of estimated parameters in the model. According to Akaike the quantity AIC should be minimum for the correct model structure. The following relations are obtained by introducing (3.2) resp (3.3) into (3.4):

$$\begin{aligned} \text{AIC} &= N \log V_1 + 2\nu + (1-n_y)N \log N + n_y N(1+\log 2\pi) \\ \text{AIC} &= 2NV_2 + 2\nu \end{aligned} \quad (3.5)$$

where n_y is the number of outputs, i.e. 4 according to the model (3.1).

The program LISPID allows for both uniform and varying sampling. Three different cases are possible:

ISAMP = 1: Constant sampling interval.

ISAMP = 2: Constant sampling interval, but some samples are missing.

ISAMP = 3: Non-uniform sampling interval.

The most appropriate choice when analysing experiment 1 is ISAMP = 3. However, this requires substantial calculations. Therefore ISAMP = 2 is used instead as an approximation.

The transfer function relating the heading ψ to the rudder angle δ (in radians), when the wind parameters θ_g , θ_{10} and the time delay T_D are zero, is obtained from (3.1):

$$G_{\psi\delta}(s) = \frac{K(1+sT_3)}{s(1+sT_1)(1+sT_2)} = \frac{K_1 (s+1/T_3)}{s(s+1/T_1) (s+1/T_2)} \quad (3.6)$$

where $K_1 = \frac{KT_3}{T_1T_2}$. The corresponding transfer function relating the sway velocity v to the rudder angle (in radians) is

$$G_{V\delta}(s) = \frac{K_V(1+sT_{3V})}{(1+sT_1)(1+sT_2)} = \frac{K_{1V}(s+1/T_{3V})}{(s+1/T_1)(s+1/T_2)} \quad (3.7)$$

where $K_{1V} = \frac{K_V T_{3V}}{T_1 T_2}$. It is customary to normalize the gains and

time constants of (3.6) and (3.7) by use of the 'prime' system:

$$\begin{aligned} K' &= K \cdot L/V & T_1' &= T_1 \cdot V/L \\ K_1' &= K_1 \cdot L^2/V^2 & T_2' &= T_2 \cdot V/L \\ K_V' &= K_V/V & T_3' &= T_3 \cdot V/L \\ K_{1V}' &= K_{1V} \cdot L/V^2 & T_{3V}' &= T_{3V} \cdot V/L \end{aligned} \quad (3.8)$$

The identifiability aspects of the model (3.1) were discussed in Åström and Källström (1973) and (1976). It was concluded that the linear hydrodynamic derivatives $\theta_5 - \theta_8$, θ_{11} and $-\theta_{11}\theta_{12}$ can be determined if the acceleration hydrodynamic derivatives $\theta_1 - \theta_4$ are known and if the heading angle, or the yaw rate, is measured together with the sway velocity. Notice also that all parameters $\theta_{18} - \theta_{24}$ and $\theta_{28} - \theta_{33}$ of the covariance matrices can not be determined when the maximum likelihood method is applied, since it is possible to multiply R_1 , R_2 and P by an arbitrary coefficient and still obtain the same filter gain. Therefore, the parameter θ_{24} is always fixed in the sequel as well as the parameters $\theta_{31} - \theta_{33}$.

The hydrodynamic derivatives of the model (3.1) have been estimated by SSPA from model tests with a tanker similar to the Sea Splendour. The estimates are shown in Table 3.1. The acceleration derivatives $\theta_1 - \theta_4$ are always fixed in the sequel to the values given in Table 3.1.

$m' - Y_{\dot{v}}$	(θ_1)	0.0156
$m' x_G' - Y_{\dot{r}}$	(θ_2)	0
$m' x_G' - N_{\dot{v}}$	(θ_3)	0
$I_z' - N_{\dot{r}}$	(θ_4)	0.00096
Y_v'	(θ_5)	-0.0113
$Y_r' - m'$	(θ_6)	-0.0048
N_v'	(θ_7)	-0.0018
$N_r' - m' x_G''$	(θ_8)	-0.0024
Y_{δ}'	(θ_{11})	0.0018
N_{δ}'	$(-\theta_{11}\theta_{12})$	-0.00086

Table 3.1 - Hydrodynamic derivatives estimated by SSPA.

The estimates are adjusted values from model tests with a tanker similar to the Sea Splendour. The hydrodynamic derivatives are normalized by use of the 'prime' system with mass unit $\rho L^3/2$. The corresponding values in the 'bis' system are obtained by dividing with $m' = 0.00918$. The origin of the co-ordinate system is assumed to be at midship.

A summary of the parameters of the model (3.1) which are given fixed values is:

$$\begin{aligned}\theta_1 &= 0.0156 \\ \theta_2 &= 0 \\ \theta_3 &= 0 \\ \theta_4 &= 0.00096 \\ \theta_{24} &= 0.01 \text{ deg}^2 \\ \theta_{31} &= 0 \\ \theta_{32} &= 0 \\ \theta_{33} &= 0\end{aligned}$$

The performance of SSPA:s model is first investigated by fitting the wind and bias parameters, the initial state and the time delay to the data from experiment 1 by use of the output error method. The result is shown in Fig. 3.1 and the parameter estimates obtained are summarized in Table 3.2. The consistency between the measurements and the model outputs is not too bad, but improvements seem to be possible. Notice that the large biases of the sway velocity measurements obtained ($\theta_{15} = 3.33$ knots and $\theta_{16} = 3.27$ knots) are compensated by a large initial state of the sway velocity ($\theta_{25} = -3.73$ knots). Maybe it would be reasonable to fix one of the parameters θ_{15} , θ_{16} or θ_{25} . The influence of the wind parameters $\theta_9 = -0.039$ and $\theta_{10} = -0.184$ on the performance of the model seems to be negligible, since the transfer function relating the heading to the rudder angle contains almost a pure integrator. The parameters of the transfer functions of SSPA:s model are shown in Table 3.3.

The result of an output error identification where the hydrodynamic derivatives also are estimated is shown in Fig. 3.2. The estimated parameter values are summarized in Table 3.2 and the transfer function parameters are given in Table 3.3. The model outputs and the measurements do not differ too much, but a strange model is obtained. The magnitude of the estimated hydrodynamic derivatives is too small and $Y_{\delta'}$ has even got an incorrect sign.

		Output error (SSPA:s model)	Output error	Maximum likelihood
Figure		3.1	3.2	3.3
Sampling interval T [s]		30	30	30
Number of samples N		96	96	96
Number of estimated parameters ν		11	17	26
ISAMP		2	2	2
Loss function V_1		2.66	1.53	-
Loss function V_2		-	-	-2.92
Akaike's information criterion AIC		-109	-150	-509
Hydrodynamic derivatives ('prime' system, mass unit $\rho L^3/2$)	Y_v' (θ_5)	-0.0113*	-0.0020	-0.0050
	Y_r' (θ_6)	-0.0048*	-0.0021	-0.0013
	N_v' (θ_7)	-0.0018*	-0.0004	-0.0001
	N_r' (θ_8)	-0.0024*	-0.0004	-0.0005
	Y_δ' (θ_{11})	0.0018*	-0.0002	0.0025
	N_δ' ($-\theta_{11}\theta_{12}$)	-0.00086*	-0.00024	-0.00062
Wind parameters	θ_9 [-]	-0.039	-0.006	-0.052
	θ_{10} [-]	-0.184	0.102	-0.121
Biases	θ_{13} [-]	-0.174	0.011	0.155
	θ_{14} [-]	-0.0556	0.0015	-0.0122
	θ_{15} [knots]	3.33	0.28	-1.13
	θ_{16} [knots]	3.27	0.27	-1.08
	θ_{17} [deg/s]	0.0004	-0.0040	-0.0125
Initial state	θ_{25} [knots]	-3.73	-0.64	1.22
	θ_{26} [deg/s]	0.0268	0.0244	-0.0570
	θ_{27} [deg]	140.0	137.4	150.5
Time delay	T_D ($(T-T) \sin\theta_{34} $) [s]	30.0	9.1	15.3

* = fixed value

Table 3.2 - Parameter values from identifications to data from experiment 1.

The corresponding hydrodynamic derivatives in the 'bis' system are obtained by dividing with $m' = 0.00918$.

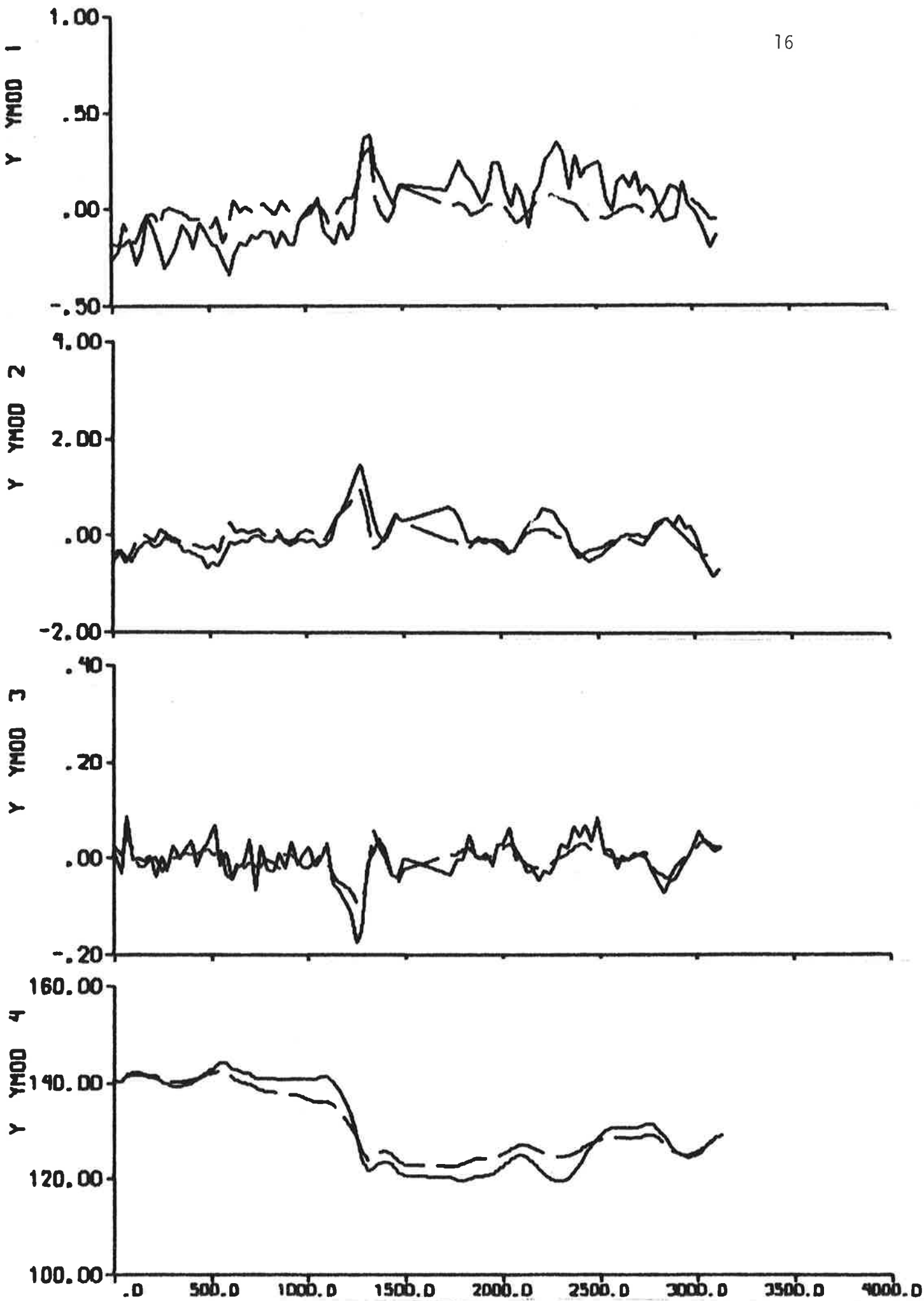


Fig. 3.1 - Result of output error identification to data from experiment 1, when the model is fixed to SSPA:s model. The dashed lines are model outputs. Cf. Fig. 2.1.

	SSPA:s model	Output error	Maximum likelihood
K'	-0.72	9.17	-1.32
K_1'	-0.90	-0.25	-0.65
K_v'	0.47	-9.76	0.85
K_{1v}'	0.12	-0.01	0.16
T_1'	2.30	-189.75	3.38
T_2'	0.36	1.81	1.79
T_3'	1.03	9.40	2.96
T_{3v}'	0.21	-0.46	1.13

Table 3.3 - Normalized ('prime' system) transfer function parameters (cf. (3.6), (3.7) and (3.8)) computed from the models in Table 3.2, when the wind parameters θ_9 and θ_{10} are zero.

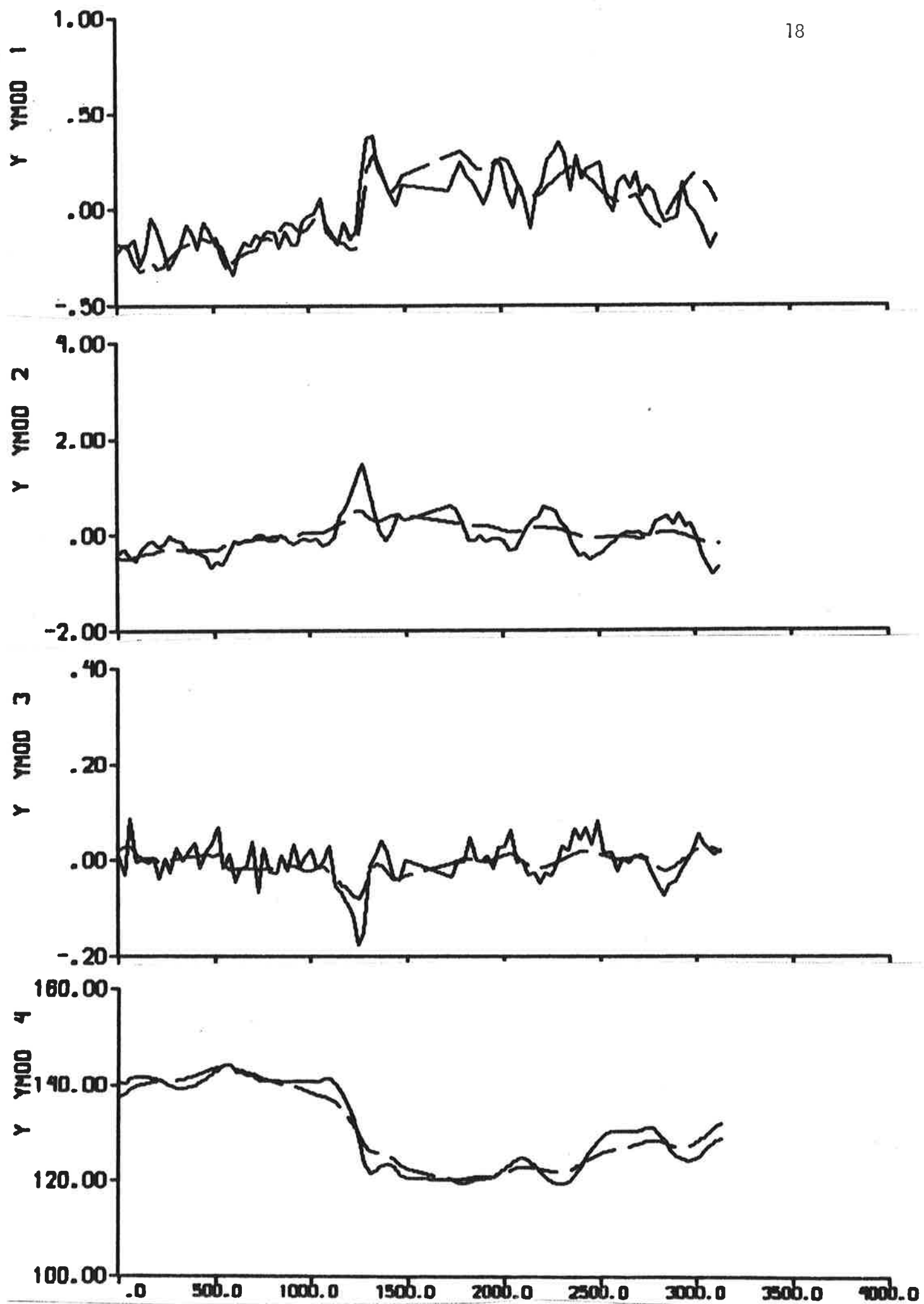


Fig. 3.2 - Result of output error identification to data from experiment 1.
The dashed lines are model outputs. Cf. Fig. 2.1,

The result of a maximum likelihood identification is shown in Fig. 3.3 and the parameter estimates obtained are given in Tables 3.2, 3.3 and 3.4. The loss function V_2 (cf. (3.3)) was minimized. It is concluded from Fig. 3.3a that the model obtained seems to describe the steering dynamics rather well. The estimated hydrodynamic derivatives are more reasonable than those obtained from the output error identification, but they differ very much from SSPA:s values. It is concluded from Akaike's information criterion that the maximum likelihood model is the best one. However, the autocorrelation functions of residuals (Fig. 3.3c) and the cross correlation functions between rudder input and residuals (Fig. 3.3d) show that it is questionable if the residuals corresponding to the aft sway velocity are white and uncorrelated to the rudder input.

There are several possible reasons for the difficulties met when the data from experiment 1 are analysed:

- o The influence of non-linear effects during the course change in the middle of the experiment.
- o The reorientation of wind and wave disturbances after the course change.
- o The missing of seven consecutive readings in the middle of the experiment.

			Maximum likelihood
R_1 (1,1)	(θ_{18})	[-]	$5.4 \cdot 10^{-3}$
R_1 (1,2)	$(\sqrt{ \theta_{18} \theta_{19} } \sin \theta_{20})$	[-]	$-2.9 \cdot 10^{-4}$
R_1 (2,2)	(θ_{19})	[-]	$4.9 \cdot 10^{-5}$
R_2 (1,1)	(θ_{21})	[knots] ²	$1.5 \cdot 10^{-3}$
R_2 (2,2)	(θ_{22})	[knots] ²	$3.8 \cdot 10^{-2}$
R_2 (3,3)	(θ_{23})	[deg/s] ²	$5.8 \cdot 10^{-4}$
P_o (1,1)	(θ_{28})	[m/s] ²	$3.3 \cdot 10^{-2}$
P_o (2,2)	(θ_{29})	[rad/s] ²	$8.3 \cdot 10^{-4}$
P_o (3,3)	(θ_{30})	[rad] ²	$1.3 \cdot 10^{-3}$

Table 3.4 - Parameter values in the covariance matrices from maximum likelihood identification to data from experiment 1.

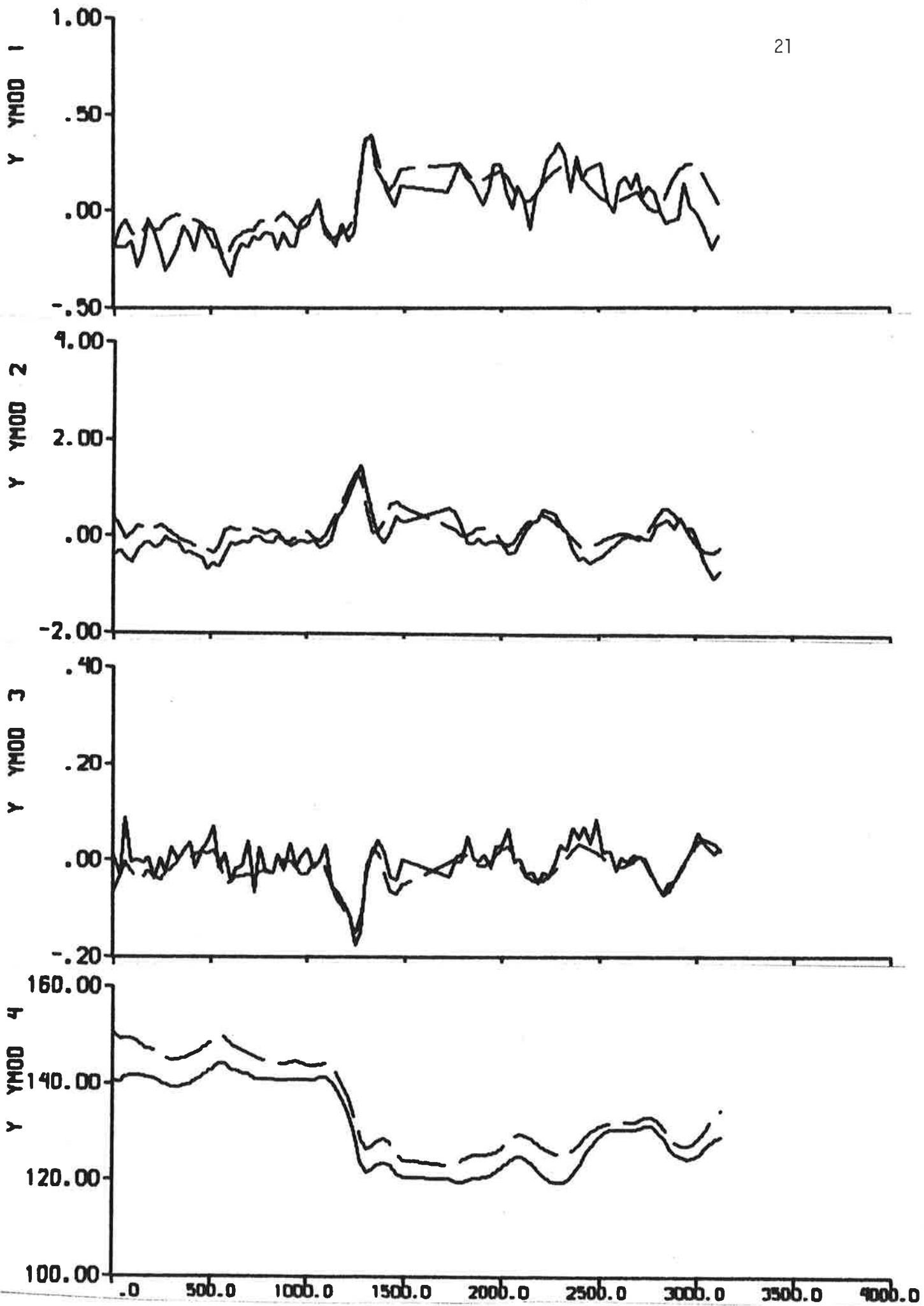


Fig. 3.3 a - Result of maximum likelihood identification to data from experiment 1. The dashed lines are model outputs. Cf. Fig. 2.1.

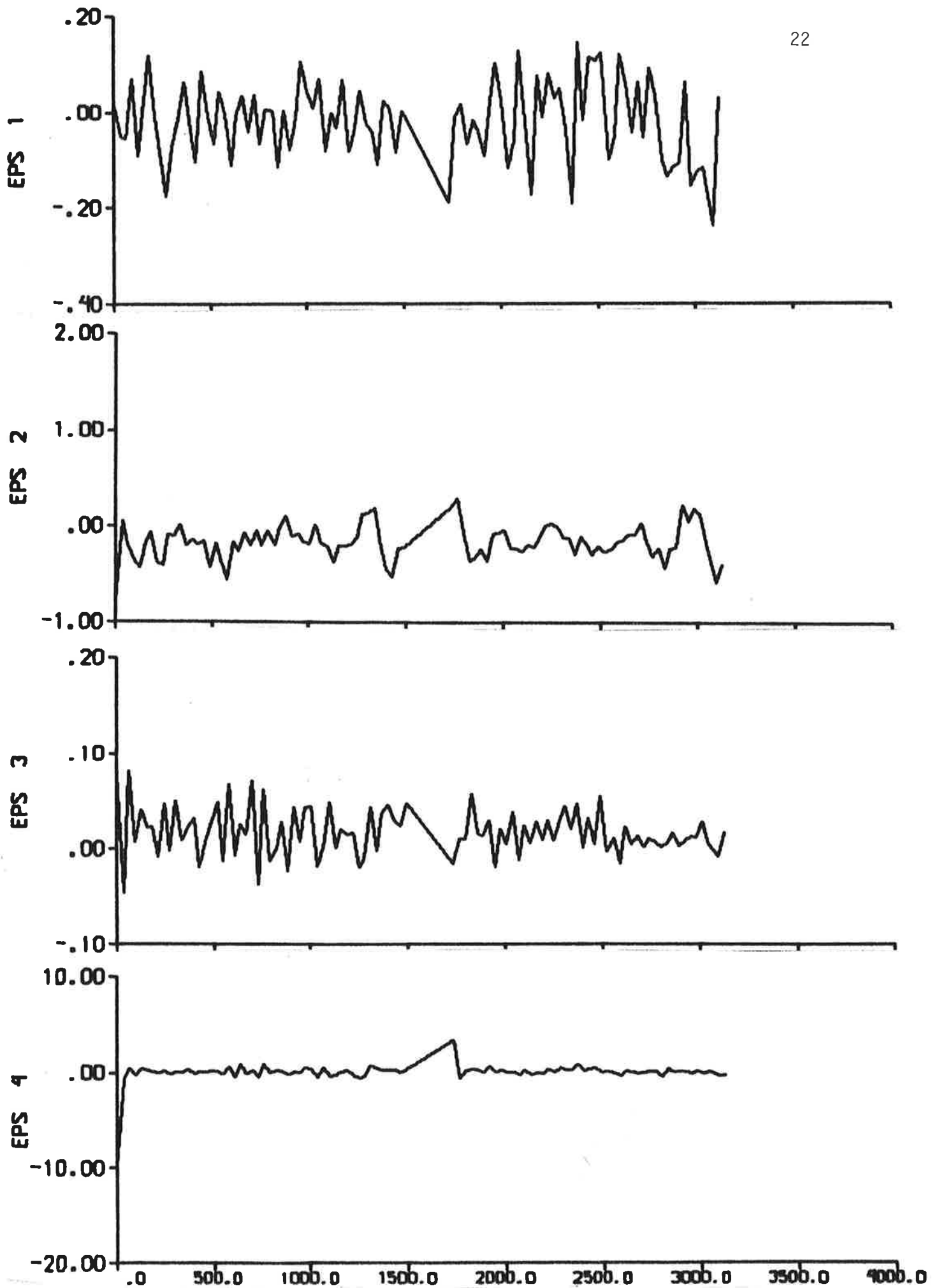


Fig. 3.3 b - Residuals.

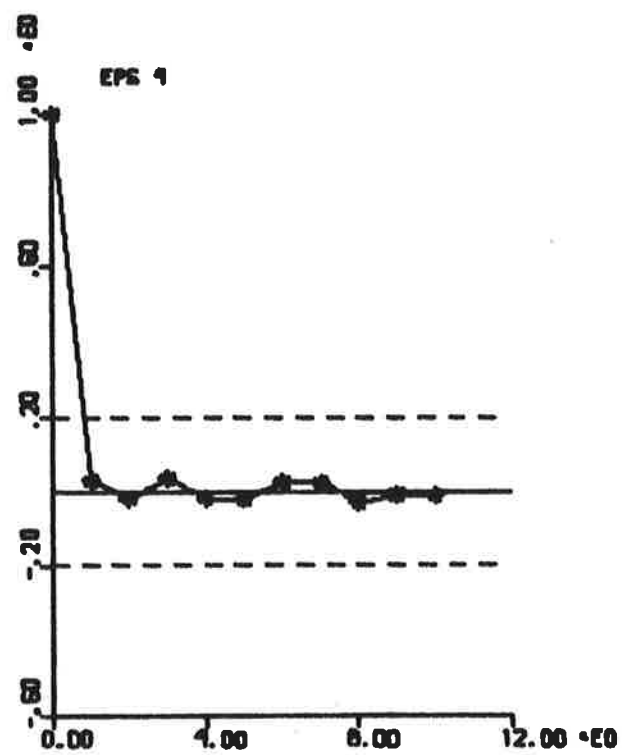
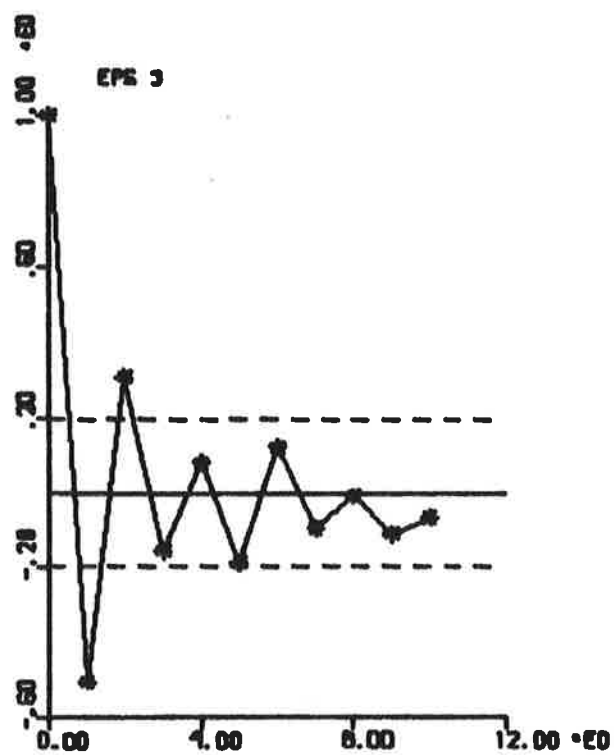
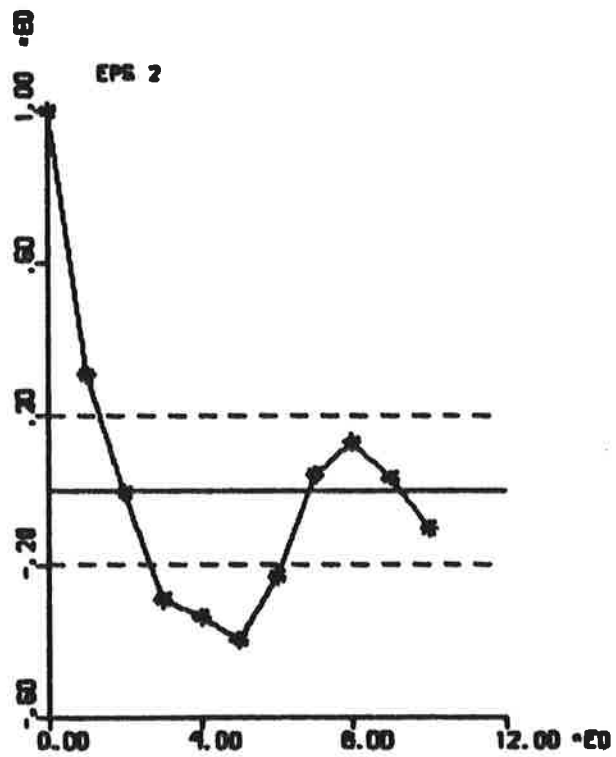
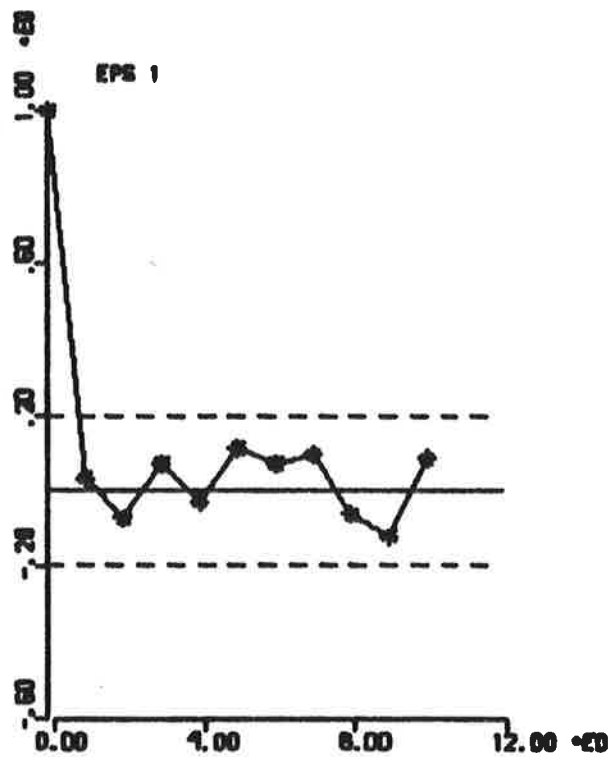


Fig. 3.3 c - Autocorrelation functions of residuals. The dashed lines are $\pm 2\sigma$ limits.

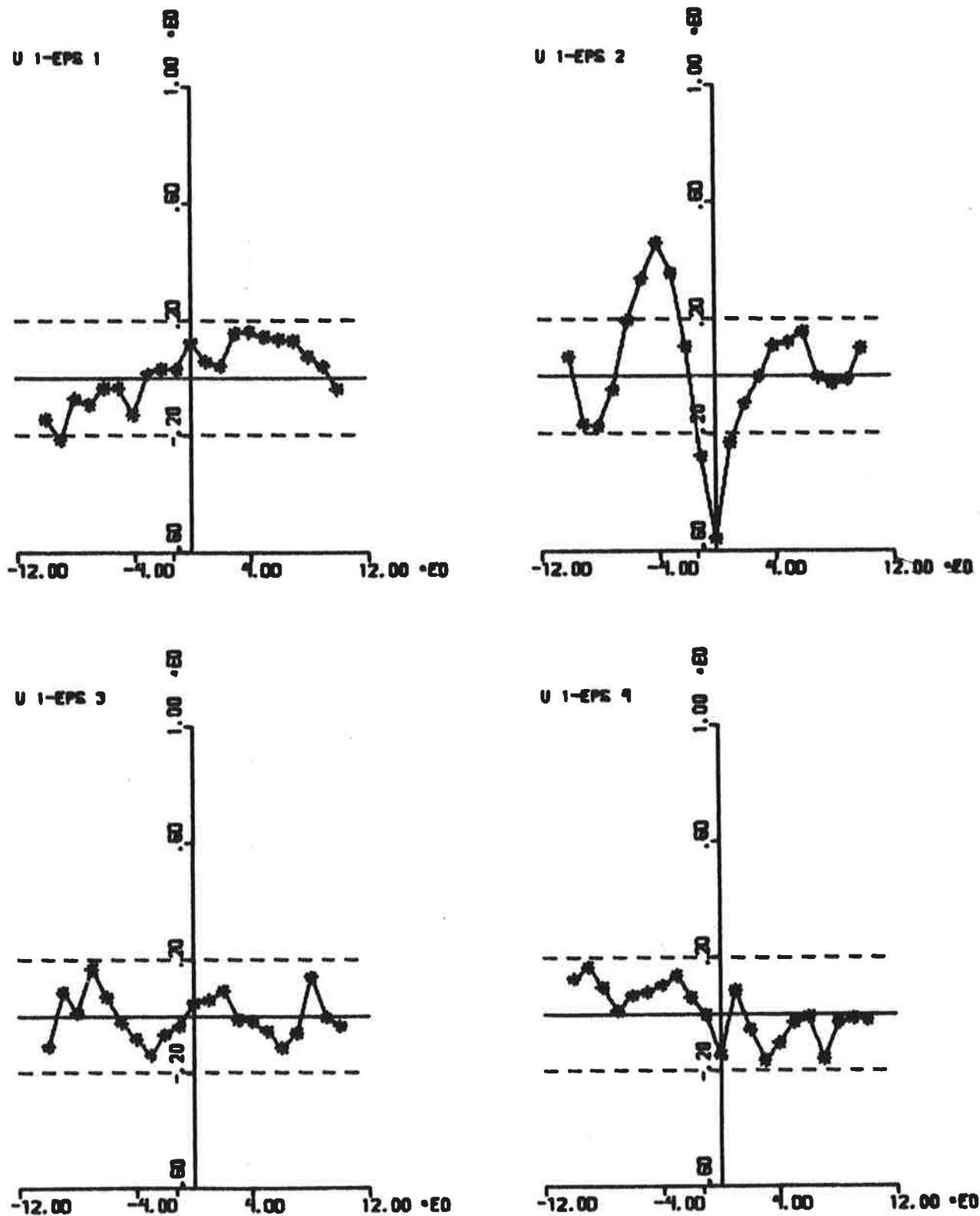


Fig. 3.3 d - Cross correlation functions between rudder input and residuals. The dashed lines are $\pm 2\sigma$ limits.

To avoid these difficulties the experiment 1 is divided into two parts, one before the yaw (0 - 1158 s) and one after (1732 - 3123 s).

The same analysis is performed on each part of experiment 1 as was performed on the entire experiment. The results of output error identifications when the model is fixed to SSPA:s model, output error identifications when the hydrodynamic derivatives also are estimated, and maximum likelihood identifications are shown in Figs. 3.4 - 3.9. The parameter estimates obtained are summarized in Tables 3.5 - 3.7.

		First part of data			Second part of data		
		Output error (SSPA:s model)	Output error	Maximum likelihood	Output error (SSPA:s model)	Output error	Maximum likelihood
Figure		3.4	3.5	3.6	3.7	3.8	3.9
Sampling interval T [s]		30	30	30	30	30	30
Number of samples N		39	39	39	46	46	46
Number of estimated parameters ν		11	17	23	11	17	23
ISAMP		1	1	1	2	2	2
Loss function V_1		0.00156	0.00023	0.00010	0.04269	0.00707	0.00039
Akaike's information criterion AIC		-216	-279	-299	-129	-200	-321
Hydrodynamic derivatives ('prime' system, mass unit $\rho L^3/2$)	Y_v' (θ_5)	-0.0113*	-0.0099	-0.0119	-0.0113*	-0.0131	-0.0146
	$Y_r' - m'$ (θ_6)	-0.0048*	-0.0068	-0.0074	-0.0048*	-0.0049	-0.0057
	N_v' (θ_7)	-0.0018*	-0.0021	-0.0019	-0.0018*	-0.0017	-0.0017
	N_r'						
	$m' \times G'$ (θ_8)	-0.0024*	-0.0017	-0.0014	-0.0024*	-0.0010	-0.0011
	Y_δ' (θ_{11})	0.0018*	0.0018	0.0009	0.0018*	0.0024	0.0018
	N_δ' ($-\theta_{11}\theta_{12}$)	-0.00086*	-0.00067	-0.00070	-0.00086*	-0.00063	-0.00060
Wind parameters	θ_9 [-]	-0.029	-0.028	-0.027	-0.055	-0.055	-0.044
	θ_{10} [-]	-0.058	-0.041	-0.047	0.087	0.074	0.078
Biases	θ_{13} [-]	0.048	0.049	0.048	0.025	0.024	0.015
	θ_{14} [-]	-0.0010	-0.0011	-0.0011	-0.0016	-0.0016	0.0001
	θ_{15} [knots]	0.01	-0.01	-0.01	1.26	1.11	0.86
	θ_{16} [knots]	-0.04	-0.07	-0.08	1.23	1.06	0.81
	θ_{17} [deg/s]	-0.0008	0.0015	0.0010	-0.0019	-0.0005	-0.0005
Initial state	θ_{25} [knots]	0.28	0.22	0.23	-0.93	-0.82	-0.53
	θ_{26} [deg/s]	0.0142	0.0065	0.0051	-0.0466	-0.0433	-0.0441
	θ_{27} [deg]	140.1	139.9	140.3	120.2	121.0	121.0
Time delay	T_D ($T-T \left \sin \theta_{34} \right $) [s]	28.3	21.2	23.4	30.0	9.2	23.8

* = fixed value.

Table 3.5 - Parameter values from identifications to data from the first and second part of experiment 1. The corresponding hydrodynamic derivatives in the 'bis' system are obtained by dividing with $m' = 0.00918$.

	SSPA:s model	First part of data		Second part of data	
		Output error	Maximum likelihood	Output error	Maximum likelihood
K'	-0.72	-3.82	-4.04	-2.82	-1.63
K_1'	-0.90	-0.69	-0.72	-0.65	-0.62
K_v'	0.47	2.84	2.57	1.24	0.76
K_{1v}'	0.12	0.12	0.06	0.15	0.12
T_1'	2.30	13.02	12.90	5.77	3.87
T_2'	0.36	0.43	0.47	0.60	0.54
T_3'	1.03	1.01	1.08	0.80	0.79
T_{3v}'	0.21	0.23	0.14	0.43	0.32

Table 3.6 - Normalized ('prime' system) transfer function parameters (cf. (3.6), (3.7) and (3.8)) computed from the models in Table 3.5, when the wind parameters θ_9 and θ_{10} are zero.

			First part of data	Second part of data
			Maximum likelihood	Maximum likelihood
R_1	(1,1)	($ \theta_{18} $) [-]	$3.2 \cdot 10^{-4}$	$3.3 \cdot 10^{-2}$
R_1	(1,2)	($\sqrt{ \theta_{18} \theta_{19} } \cdot \sin \theta_{20}$) [-]	$4.3 \cdot 10^{-5}$	$1.3 \cdot 10^{-2}$
R_1	(2,2)	($ \theta_{19} $) [-]	$6.0 \cdot 10^{-6}$	$5.4 \cdot 10^{-3}$
R_2	(1,1)	($ \theta_{21} $) [knots] ²	$3.7 \cdot 10^{-3}$	$1.7 \cdot 10^{-7}$
R_2	(2,2)	($ \theta_{22} $) [knots] ²	$4.3 \cdot 10^{-4}$	$1.5 \cdot 10^{-3}$
R_2	(3,3)	($ \theta_{23} $) [deg/s] ²	$5.5 \cdot 10^{-4}$	$1.0 \cdot 10^{-5}$

Table 3.7 - Parameter values in the covariance matrices from maximum likelihood identifications to data from the first and second part of experiment 1.

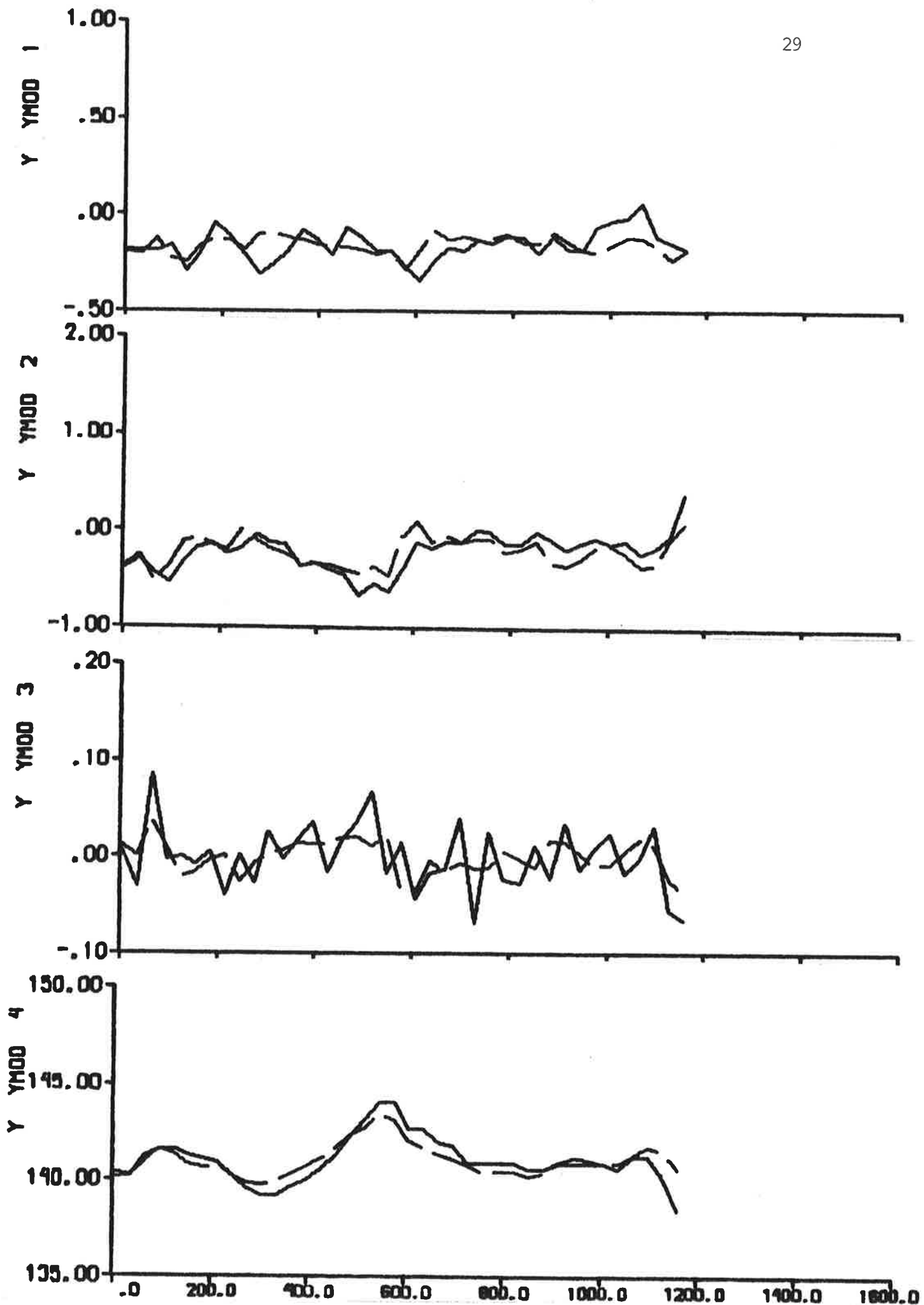


Fig. 3.4 a - Result of output error identification to data from the first part of experiment 1, when the model is fixed to SSPA:s model. The dashed lines are model outputs. Cf. Fig. 2.1.

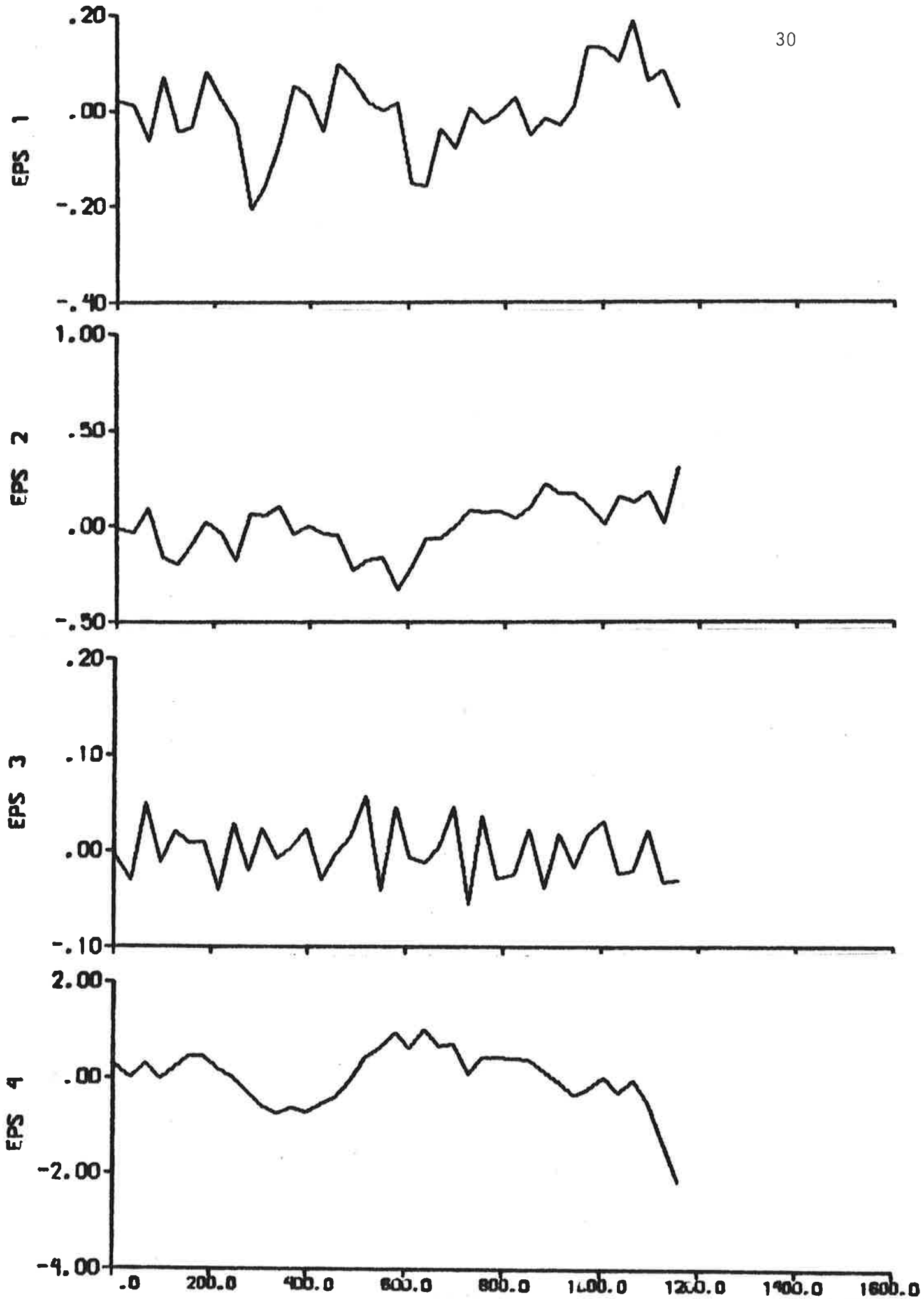


Fig. 3.4 b - Residuals.

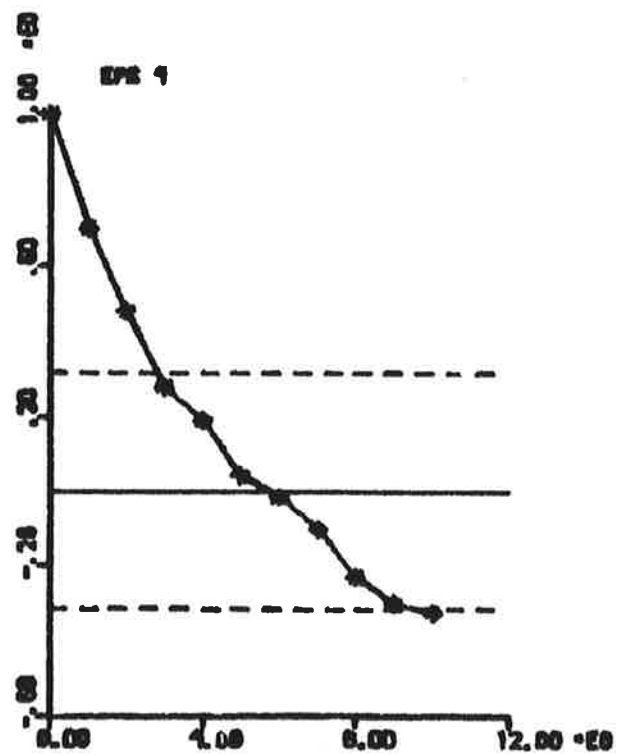
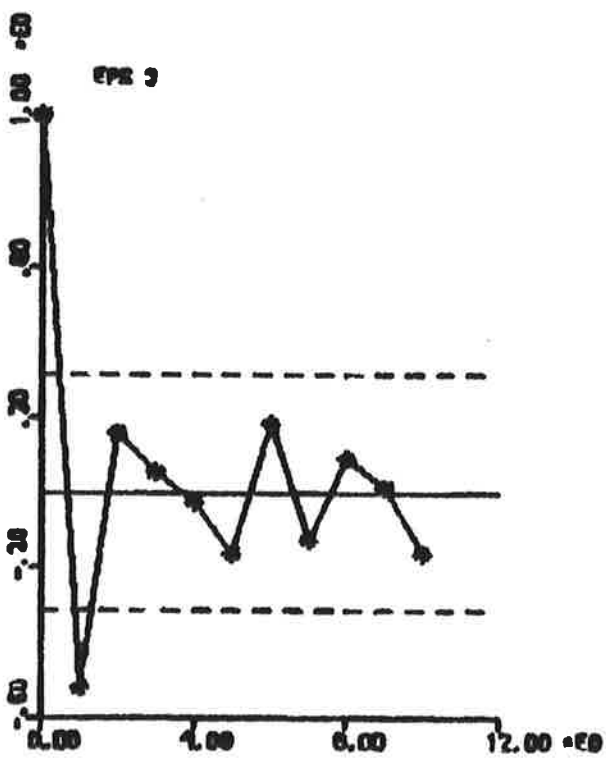
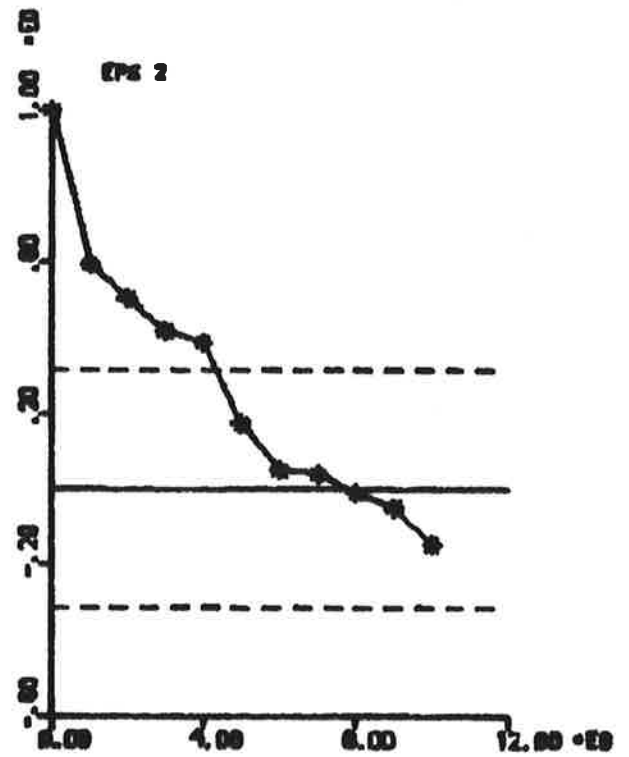
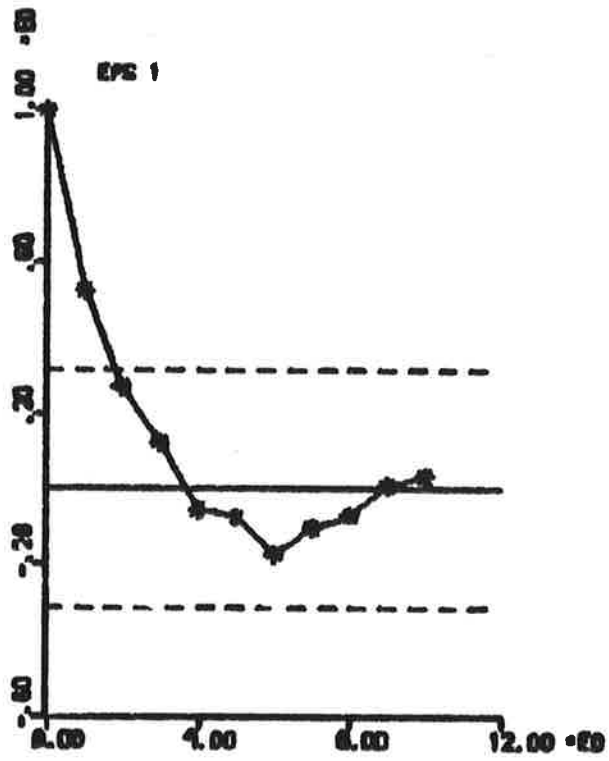


Fig. 3.4 c - Autocorrelation functions of residuals.

The dashed lines are $\pm 2\sigma$ limits.

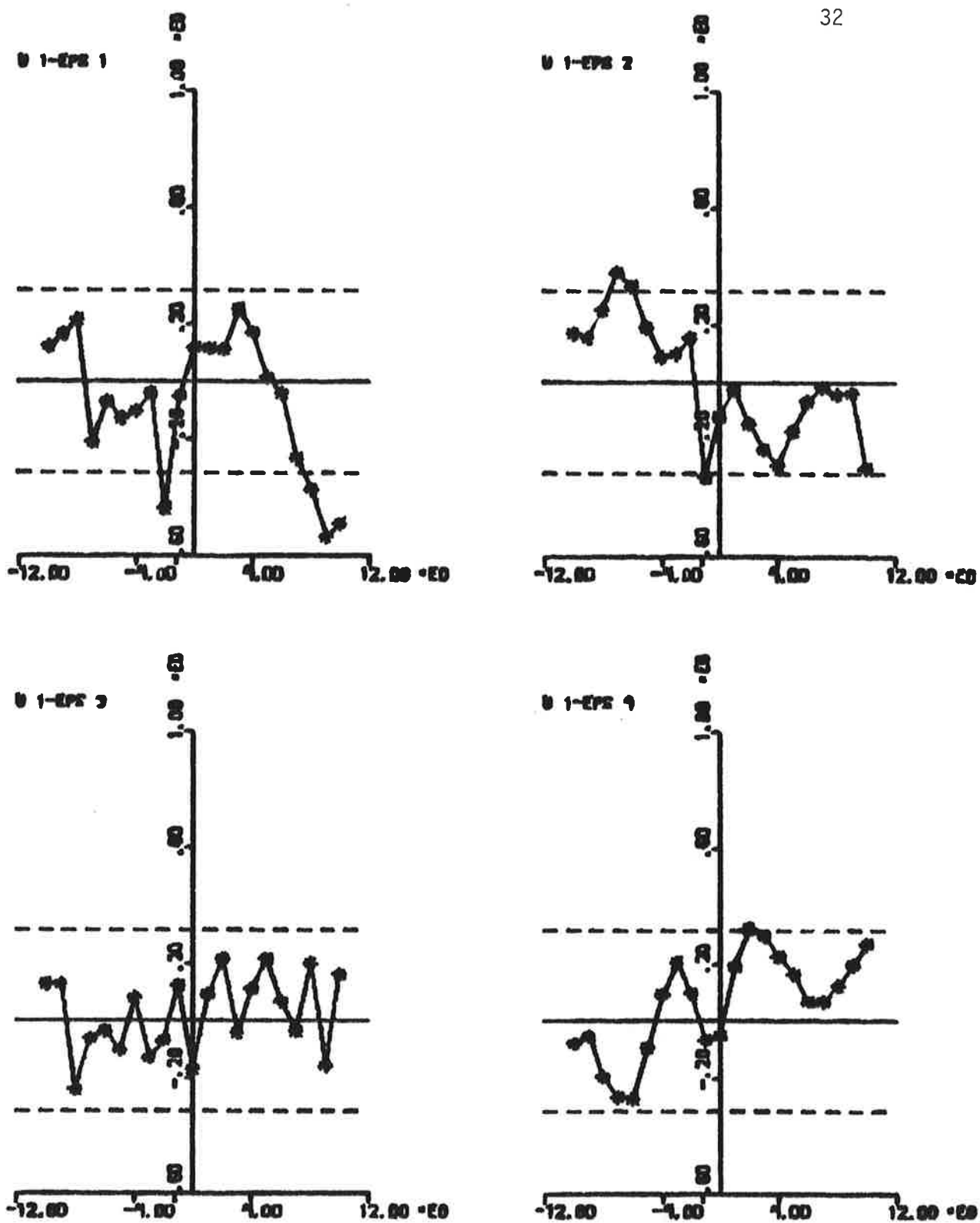


Fig. 3.4 d - Cross correlation functions between rudder input and residuals. The dashed lines are $\pm 2\sigma$ limits.

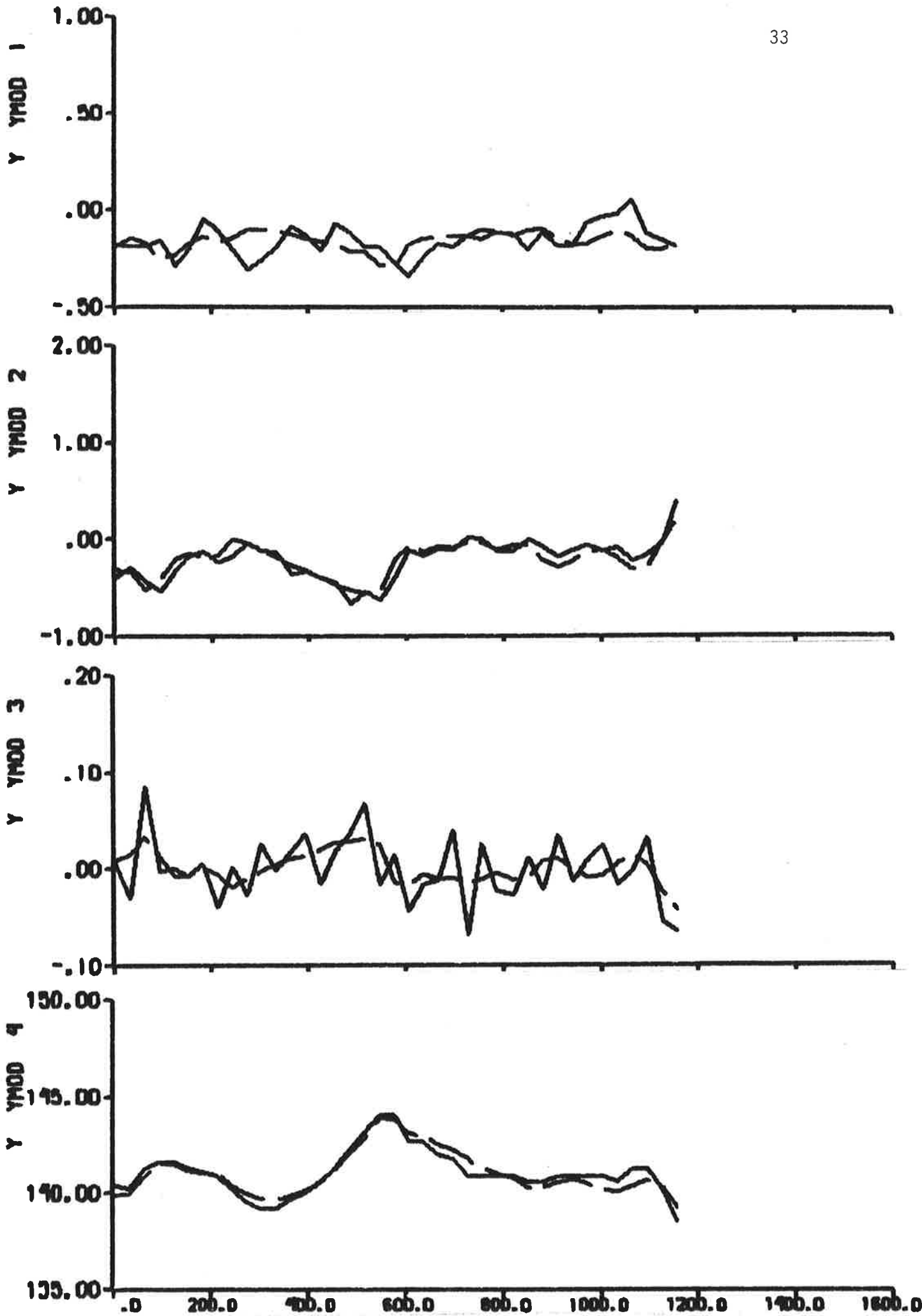


Fig. 3.5 a - Result of output error identification to data from the first part of experiment 1. The dashed lines are model outputs. Cf. Fig. 2.1.

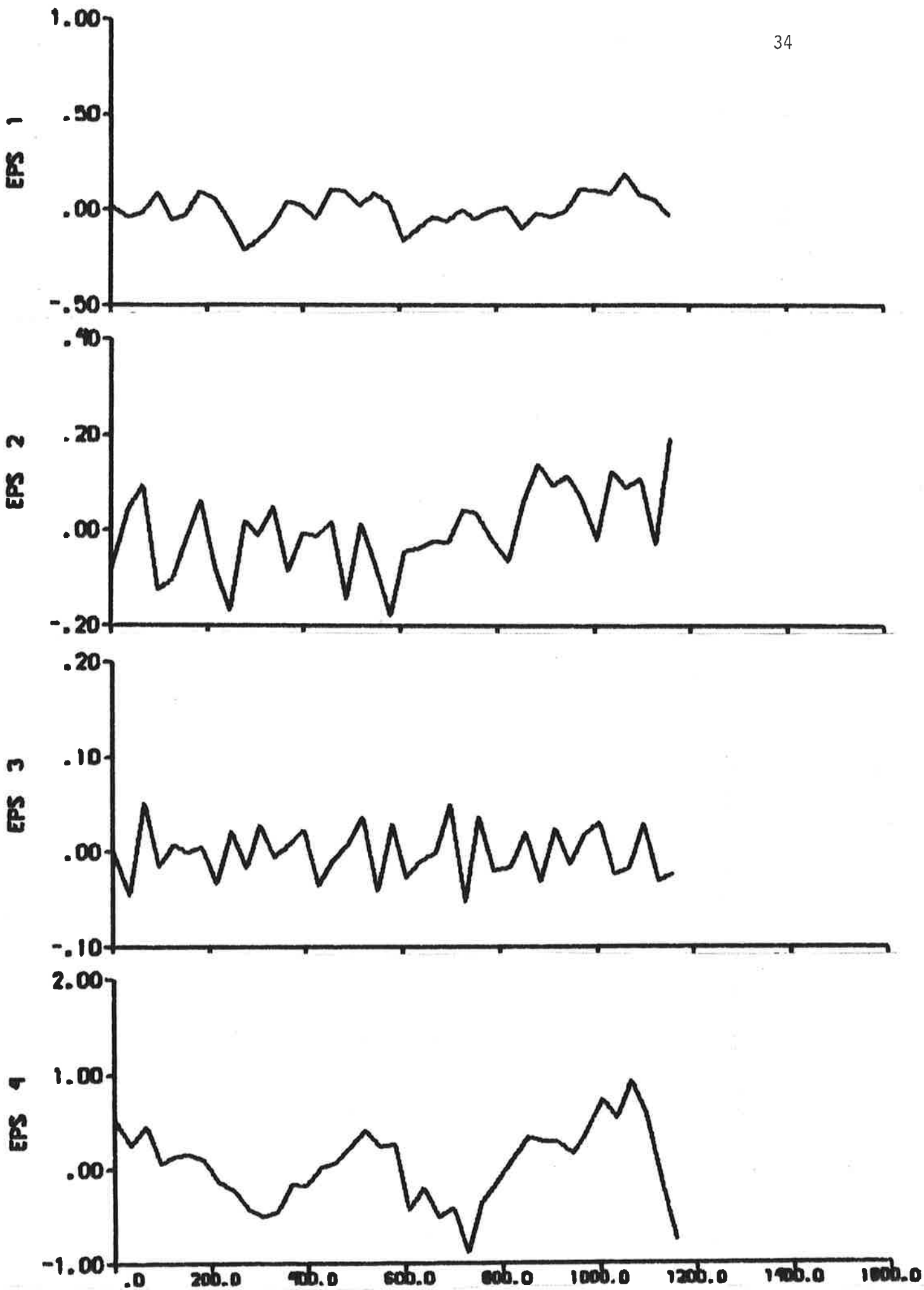


Fig. 3.5 b - Residuals.

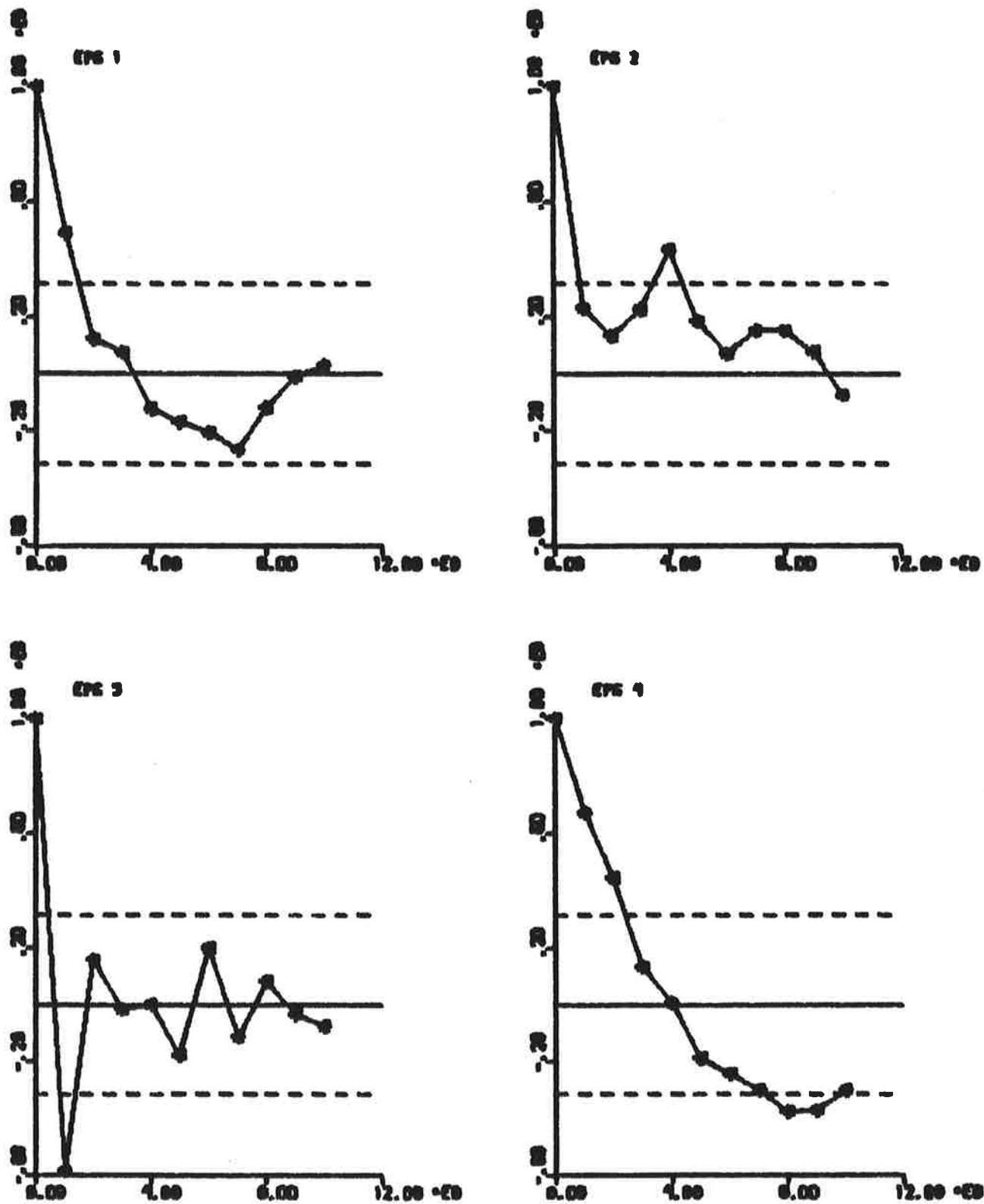


Fig. 3.5 c - Autocorrelation functions of residuals.
The dashed lines are $\pm 2\sigma$ limits.

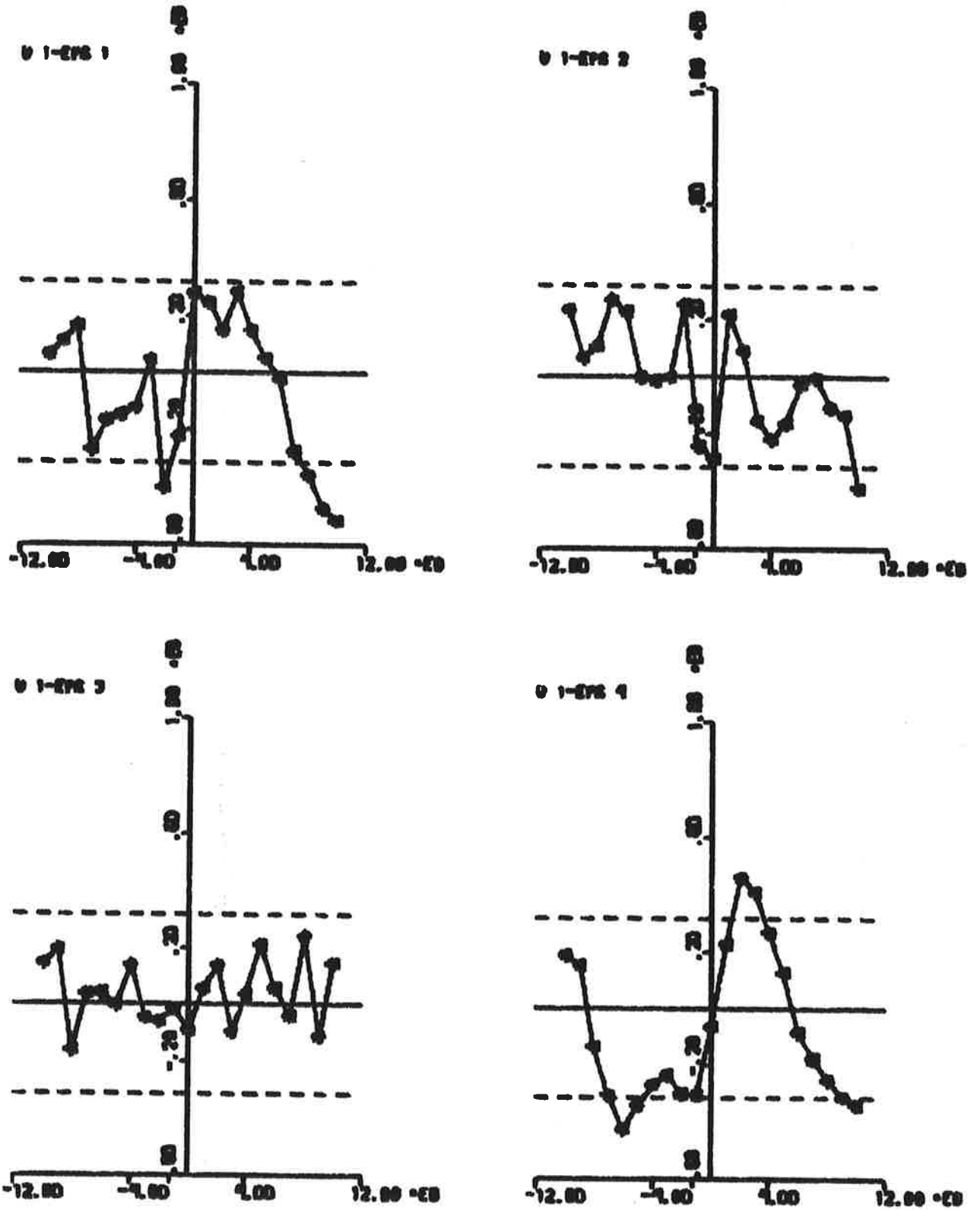


Fig. 3.5 d - Cross correlation functions between rudder input and residuals. The dashed lines are $\pm 2\sigma$ limits.

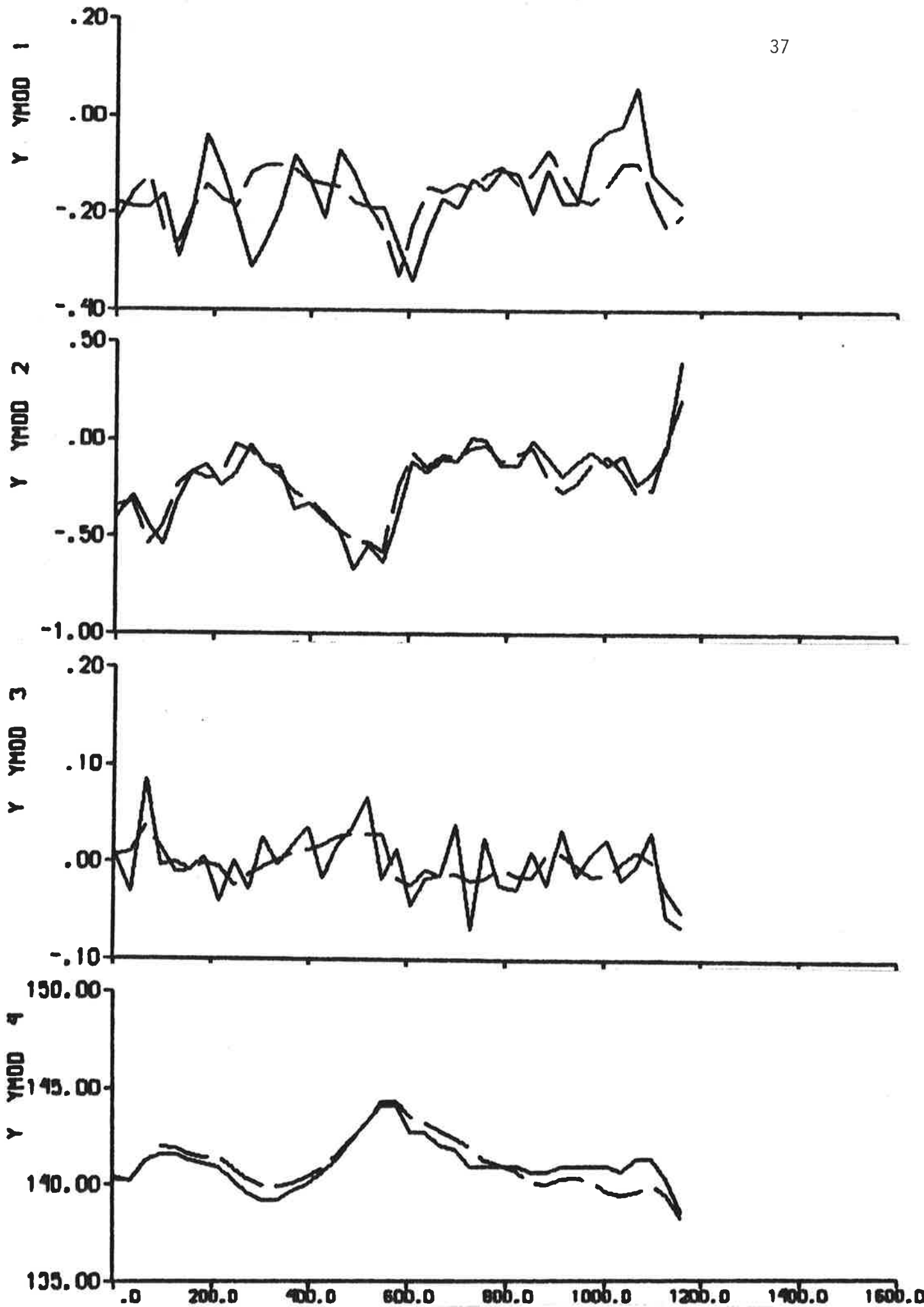


Fig. 3.6 a - Result of maximum likelihood identification to data from the first part of experiment 1. The dashed lines are model outputs. Cf. Fig. 2.1.

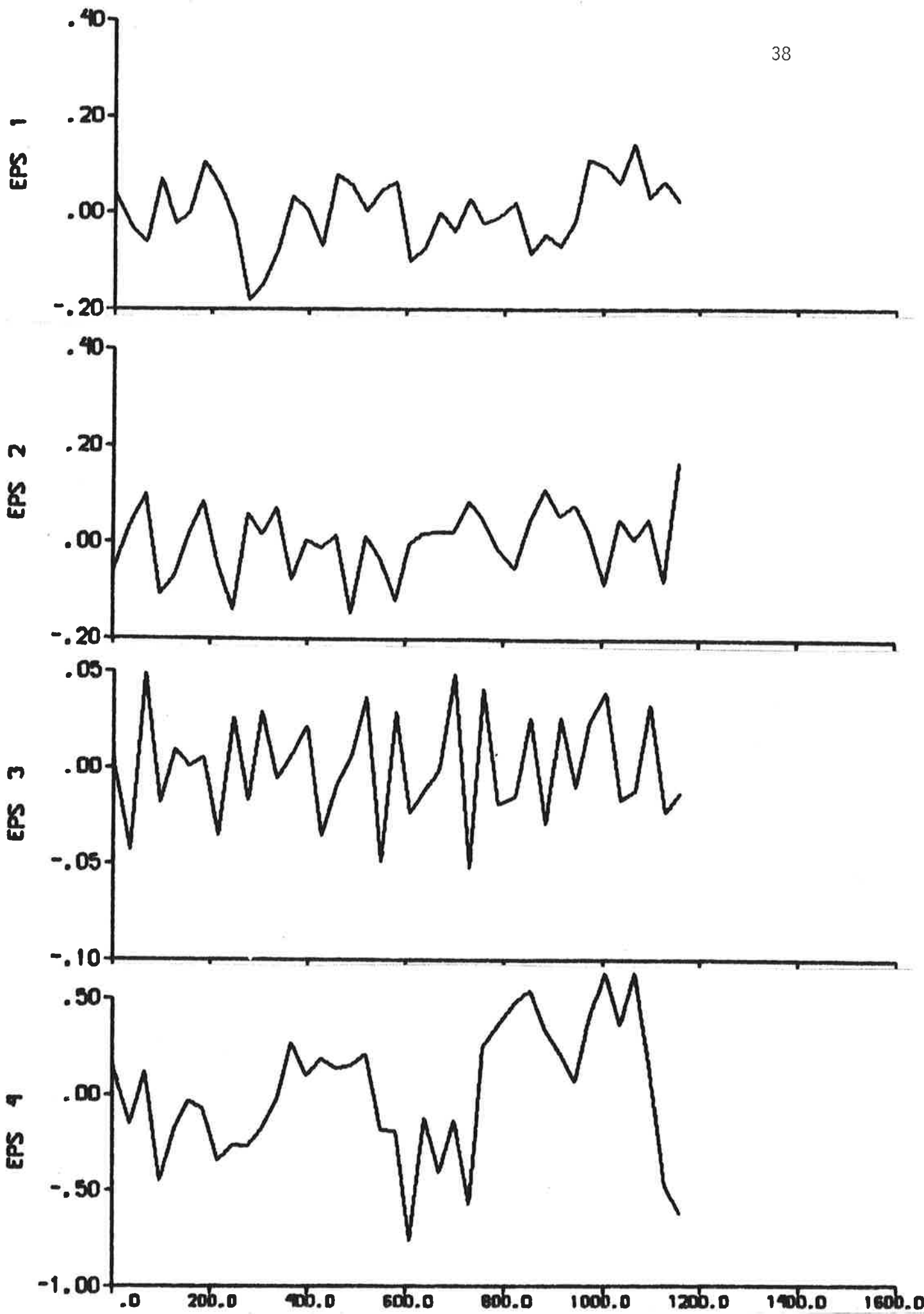


Fig. 3.6 b - Residuals.

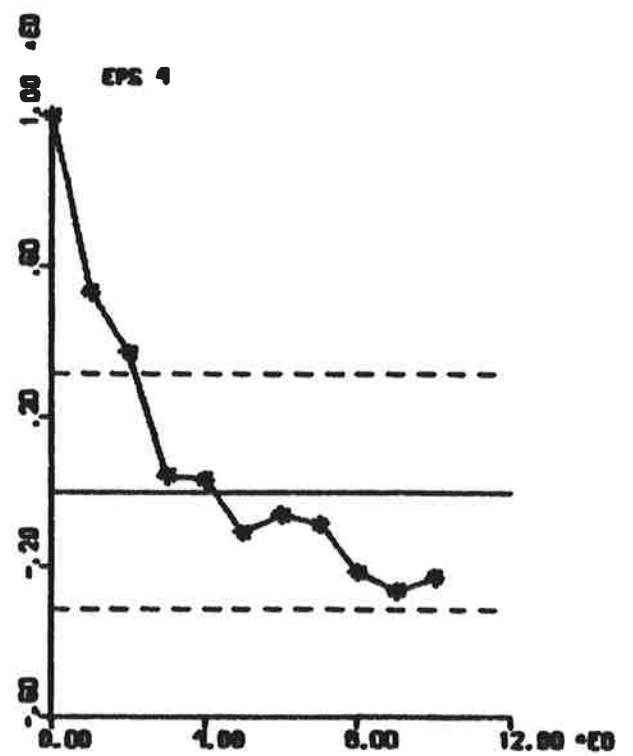
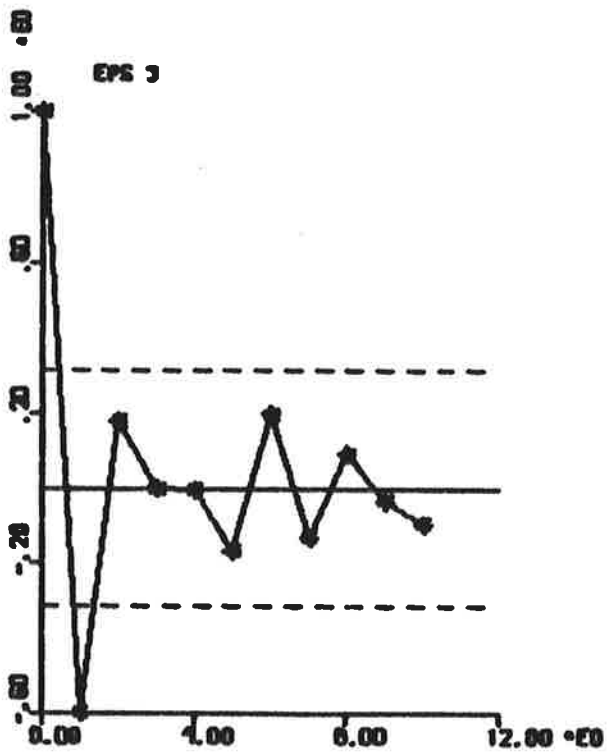
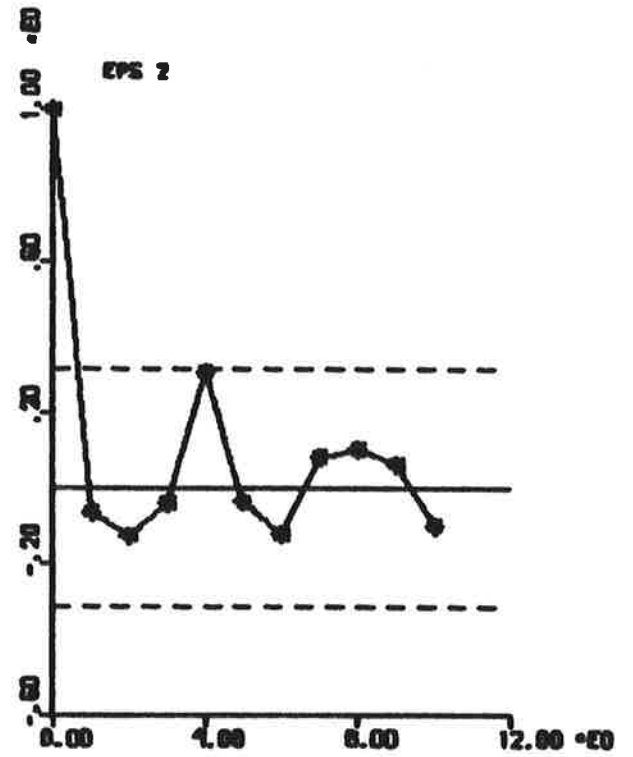
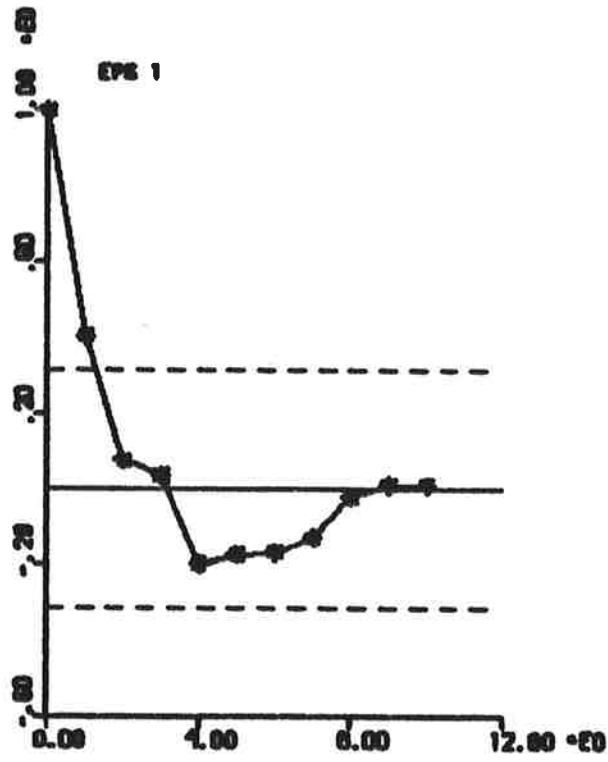


Fig. 3.6 c - Autocorrelation functions of residuals.
The dashed lines are $\pm 2\sigma$ limits.

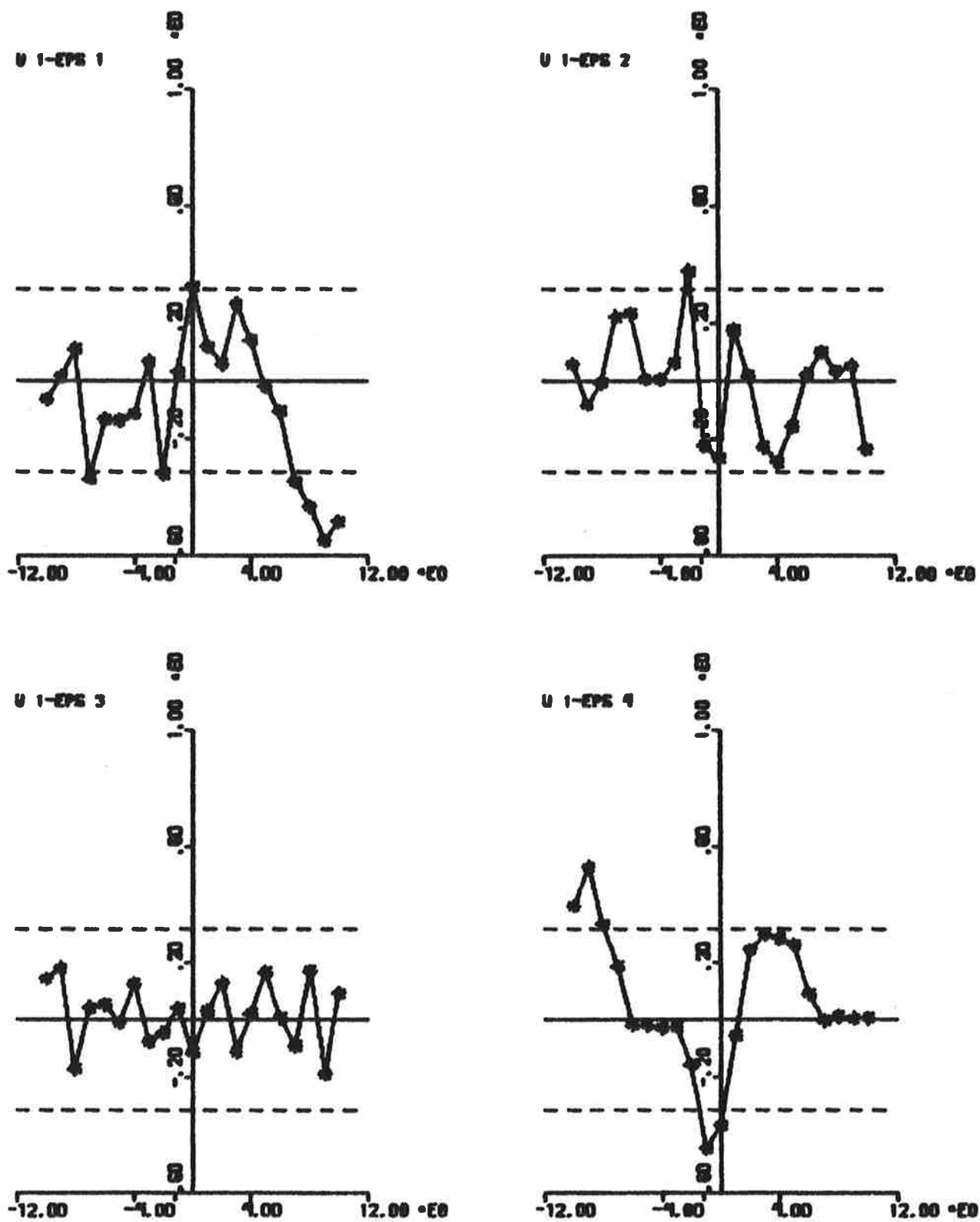


Fig. 3.6 d - Cross correlation functions between rudder input and residuals.
The dashed lines are $\pm 2\sigma$ limits.

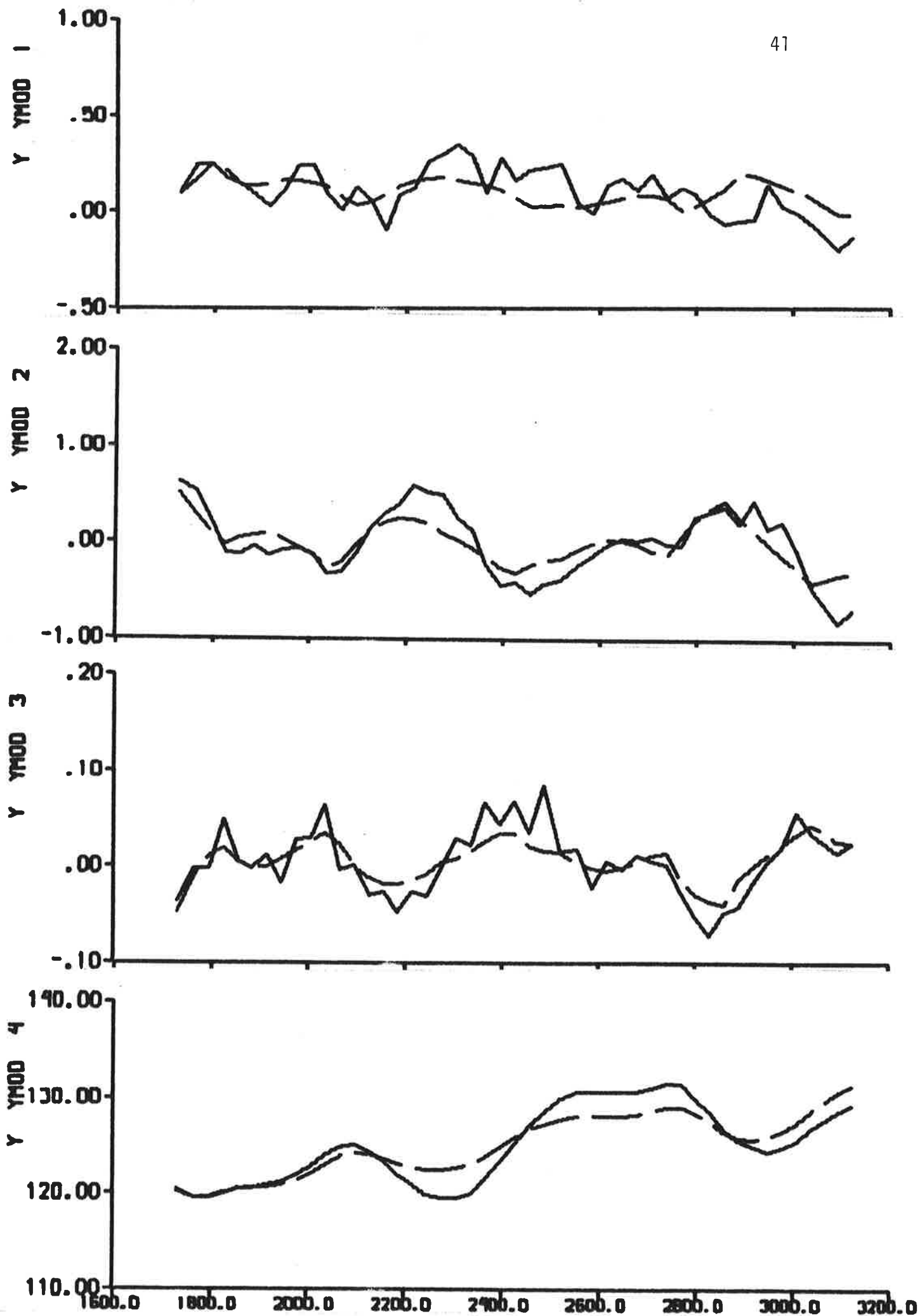


Fig. 3.7 a - Result of output error identification to data from the second part of experiment 1, when the model is fixed to SSPA:s model. The dashed lines are model outputs. Cf. Fig. 2.1.

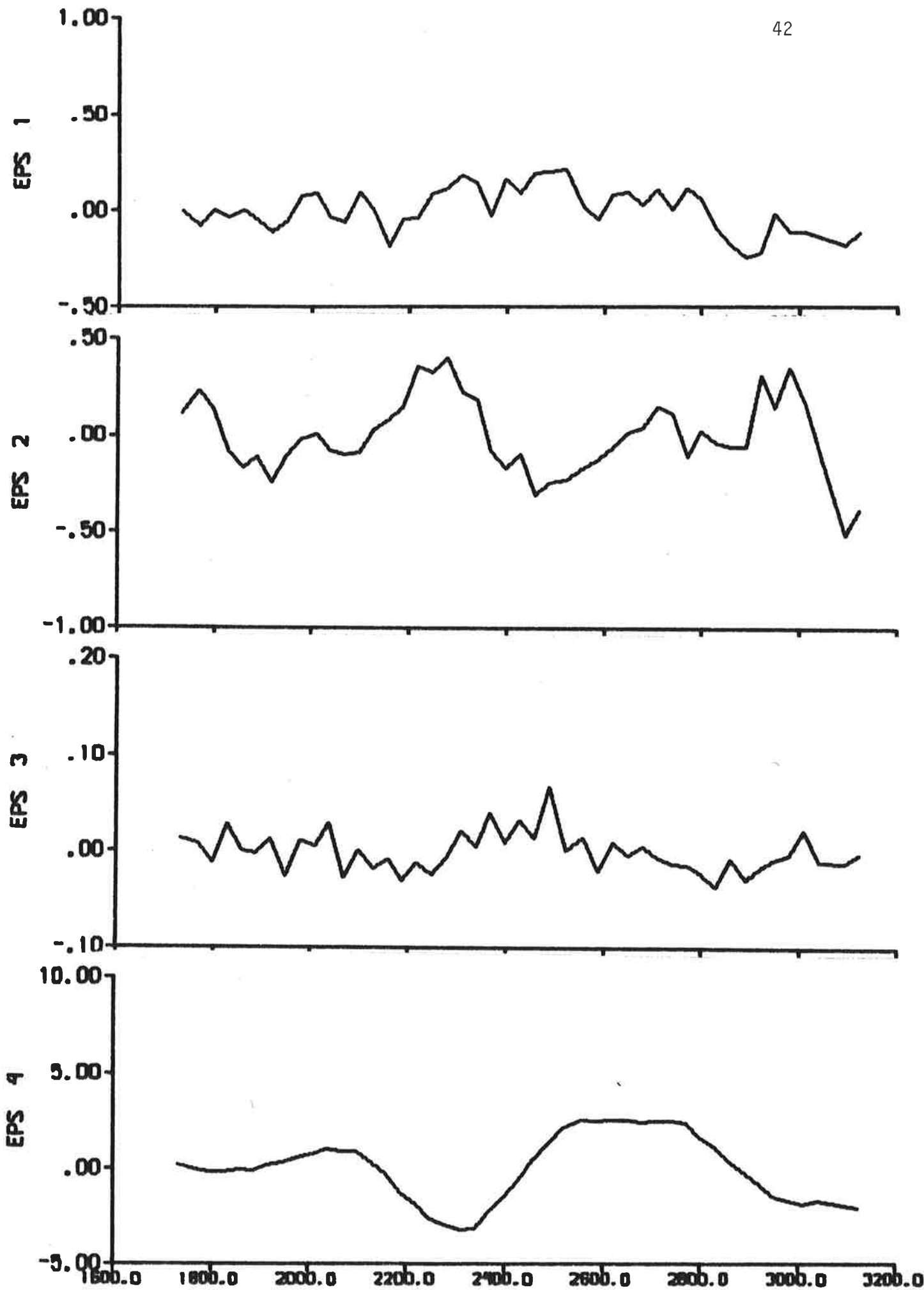


Fig. 3.7 b - Residuals.

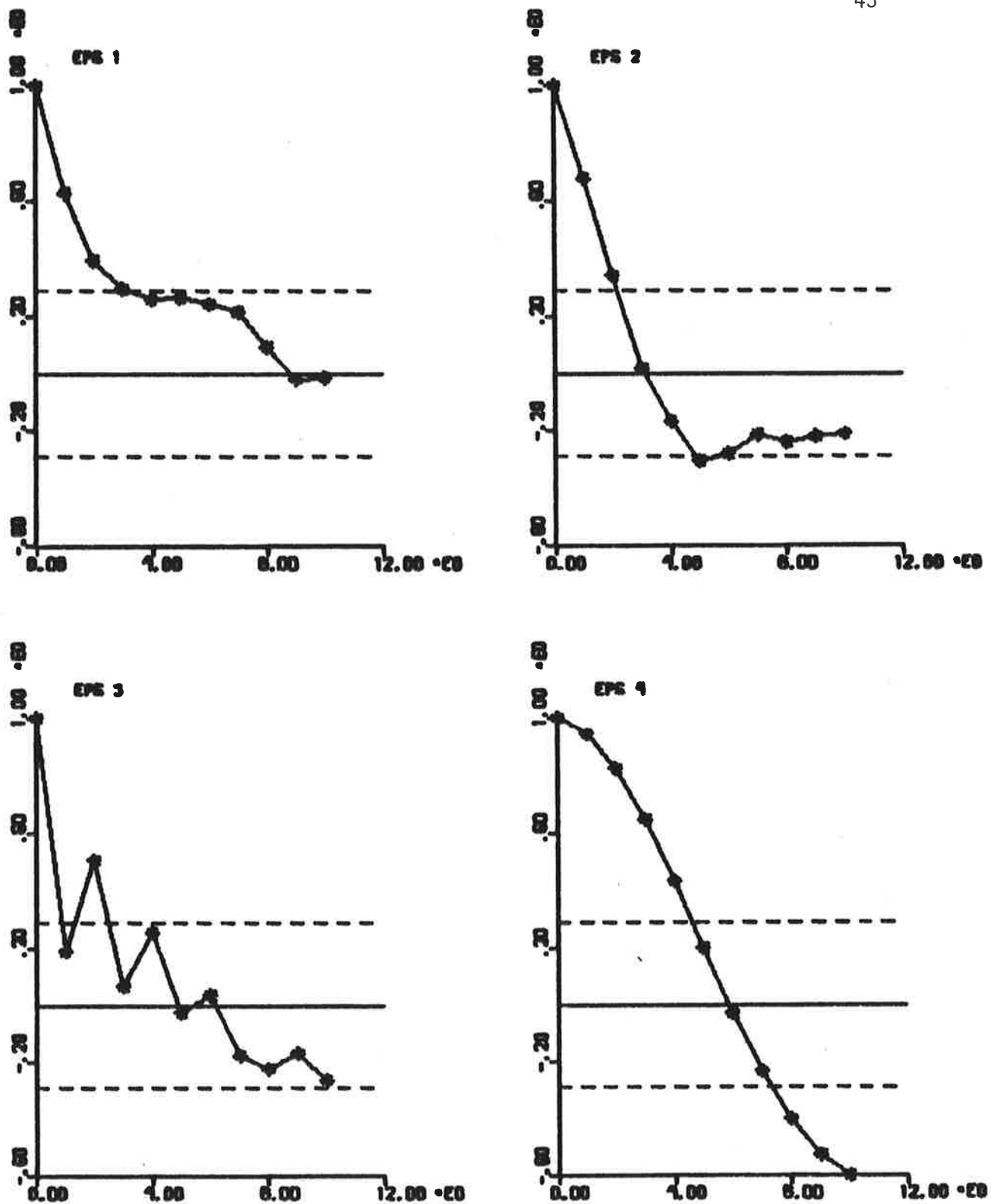


Fig. 3.7 c - Autocorrelation functions of residuals.

The dashed lines are $\pm 2\sigma$ limits.

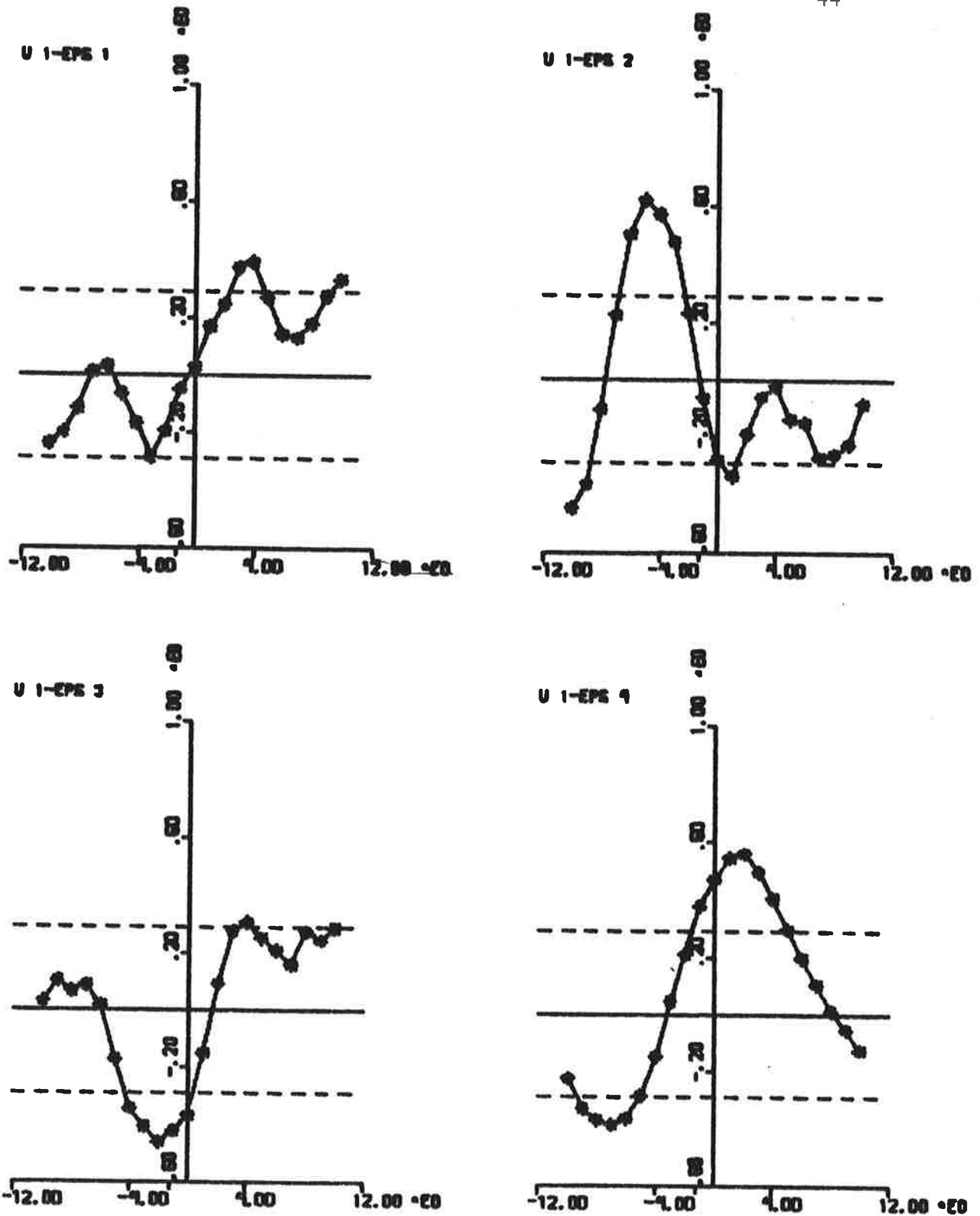


Fig. 3.7 d - Cross correlation functions between rudder input and residuals.
The dashed lines are $\pm 2\sigma$ limits.

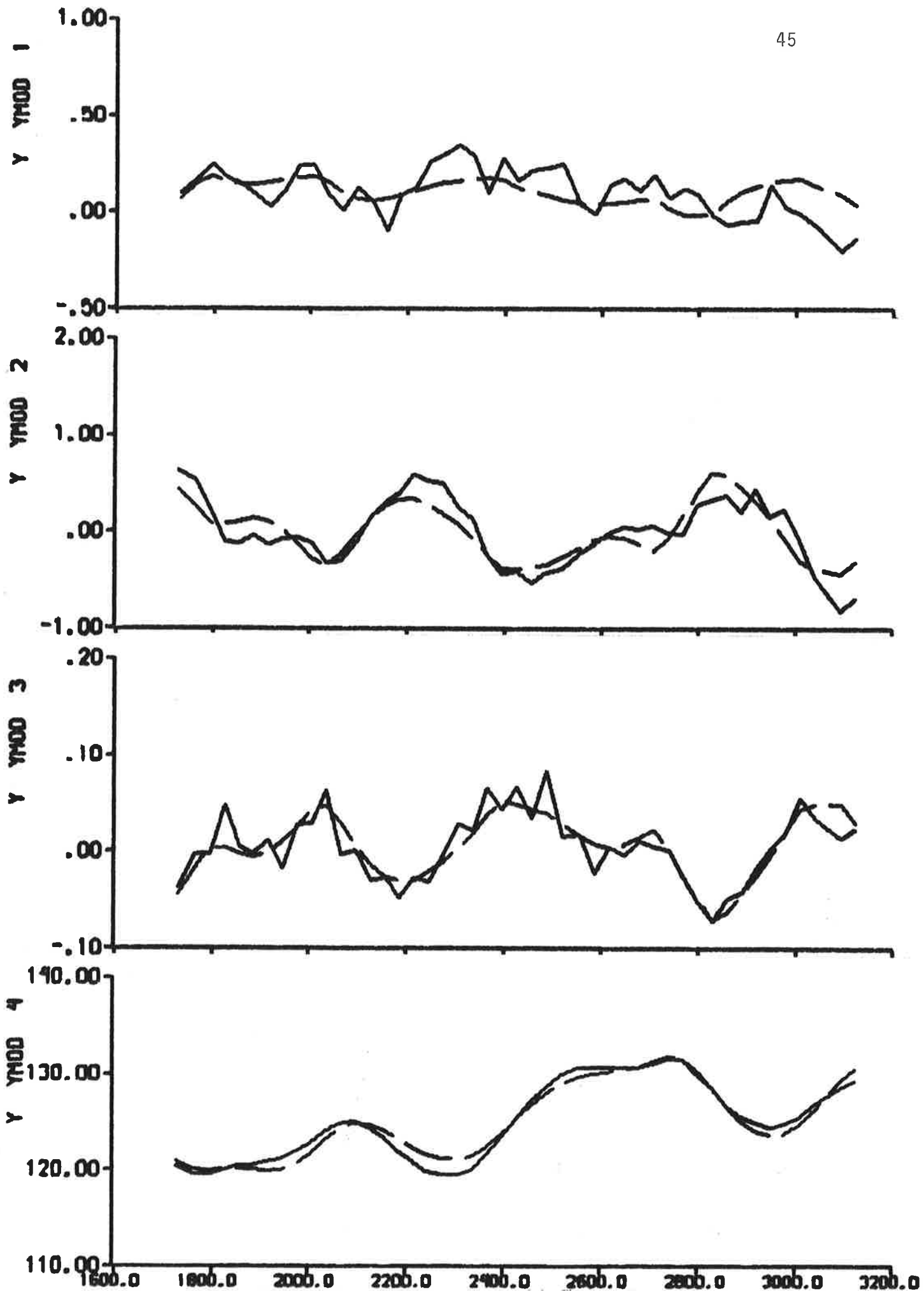


Fig. 3.8 a - Result of output error identification to data from the second part of experiment 1. The dashed lines are model outputs. Cf. Fig. 2.1.

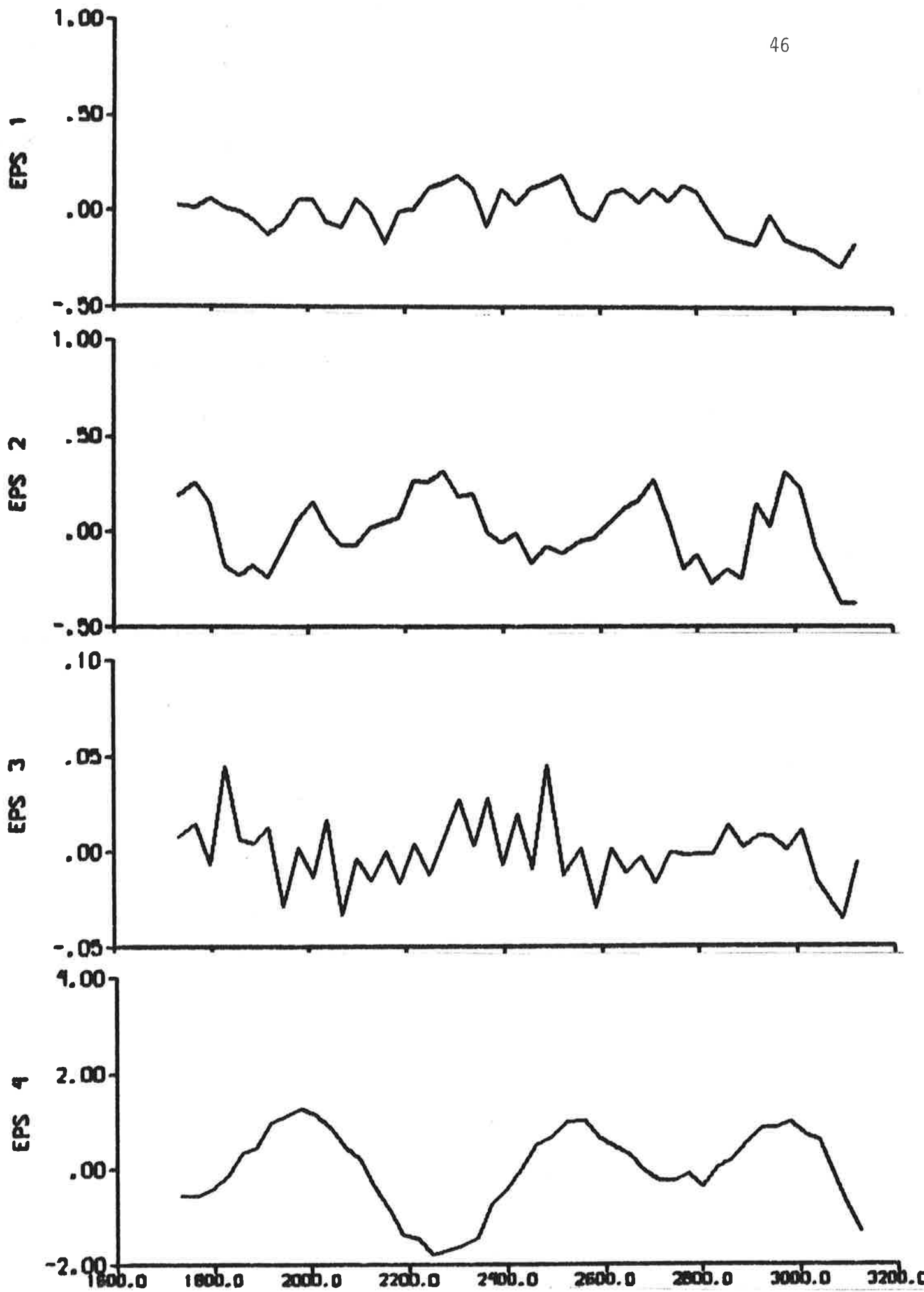


Fig. 3.8 b - Residuals.

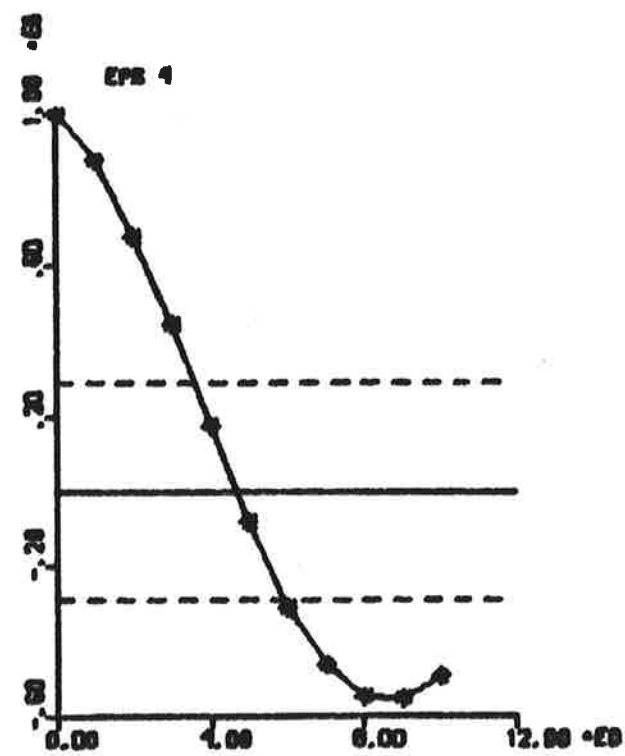
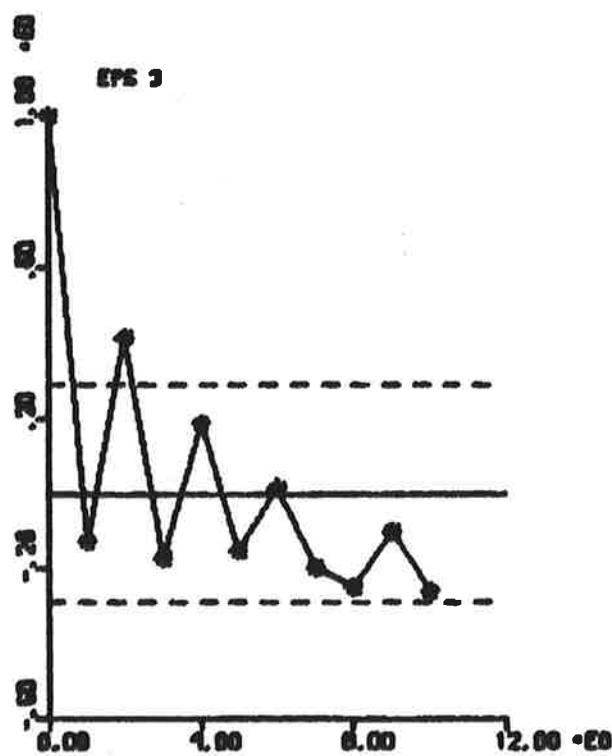
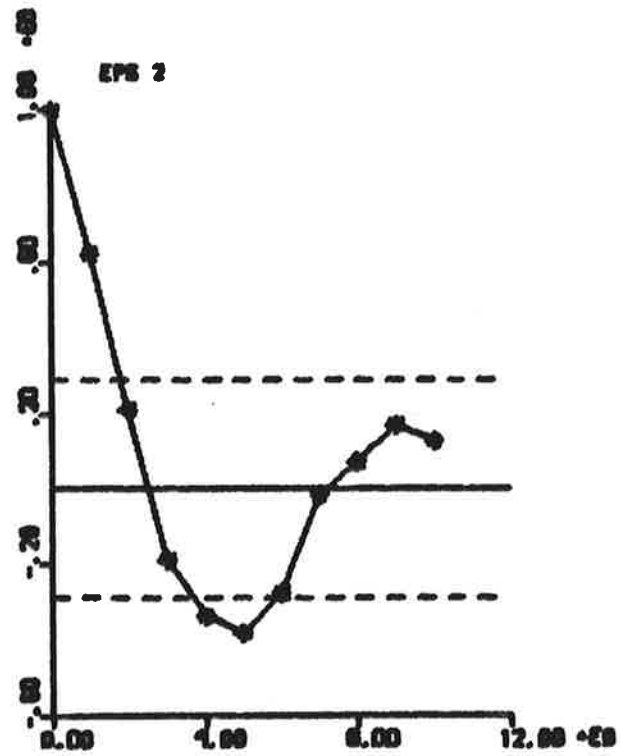
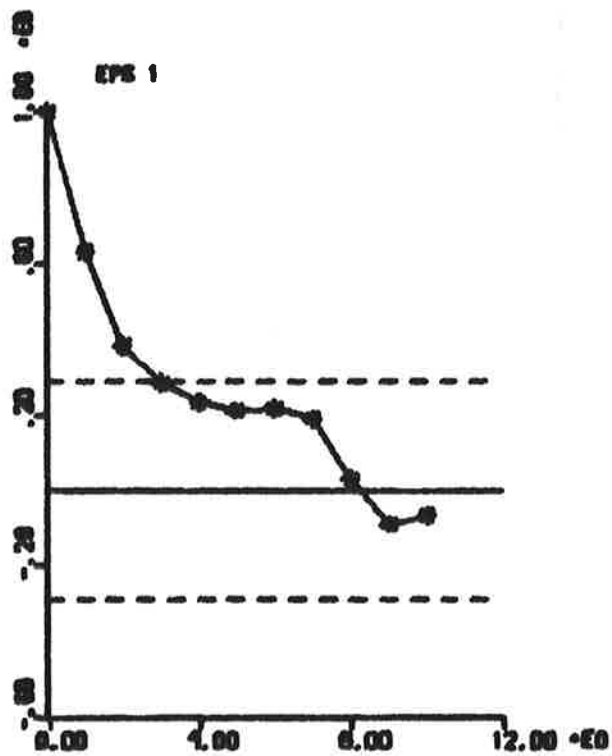


Fig. 3.8 c - Autocorrelation functions of residuals.

The dashed lines are $\pm 2\sigma$ limits.

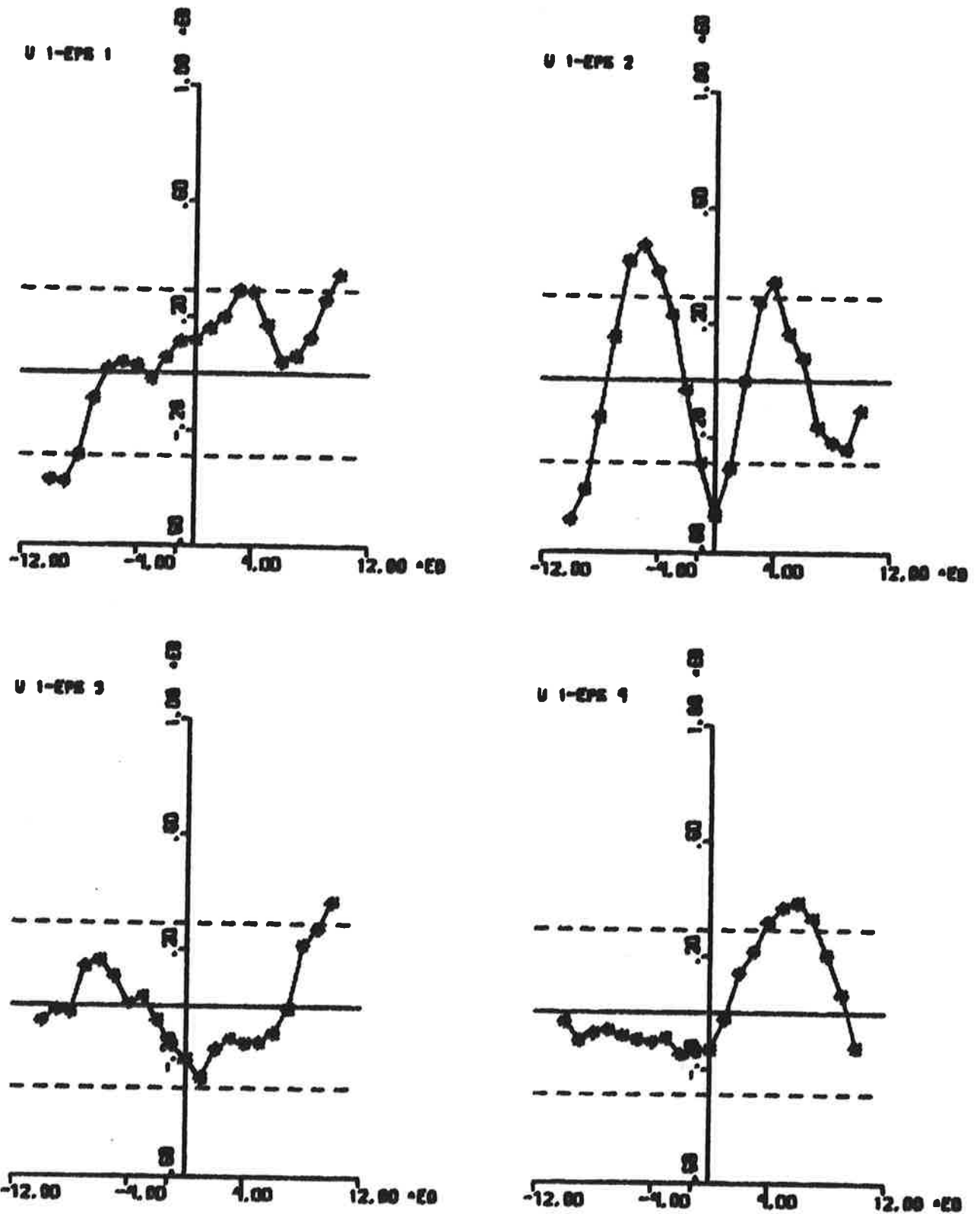


Fig. 3.8 d - Cross correlation functions between rudder input and residuals.
The dashed lines are $\pm 2\sigma$ limits.

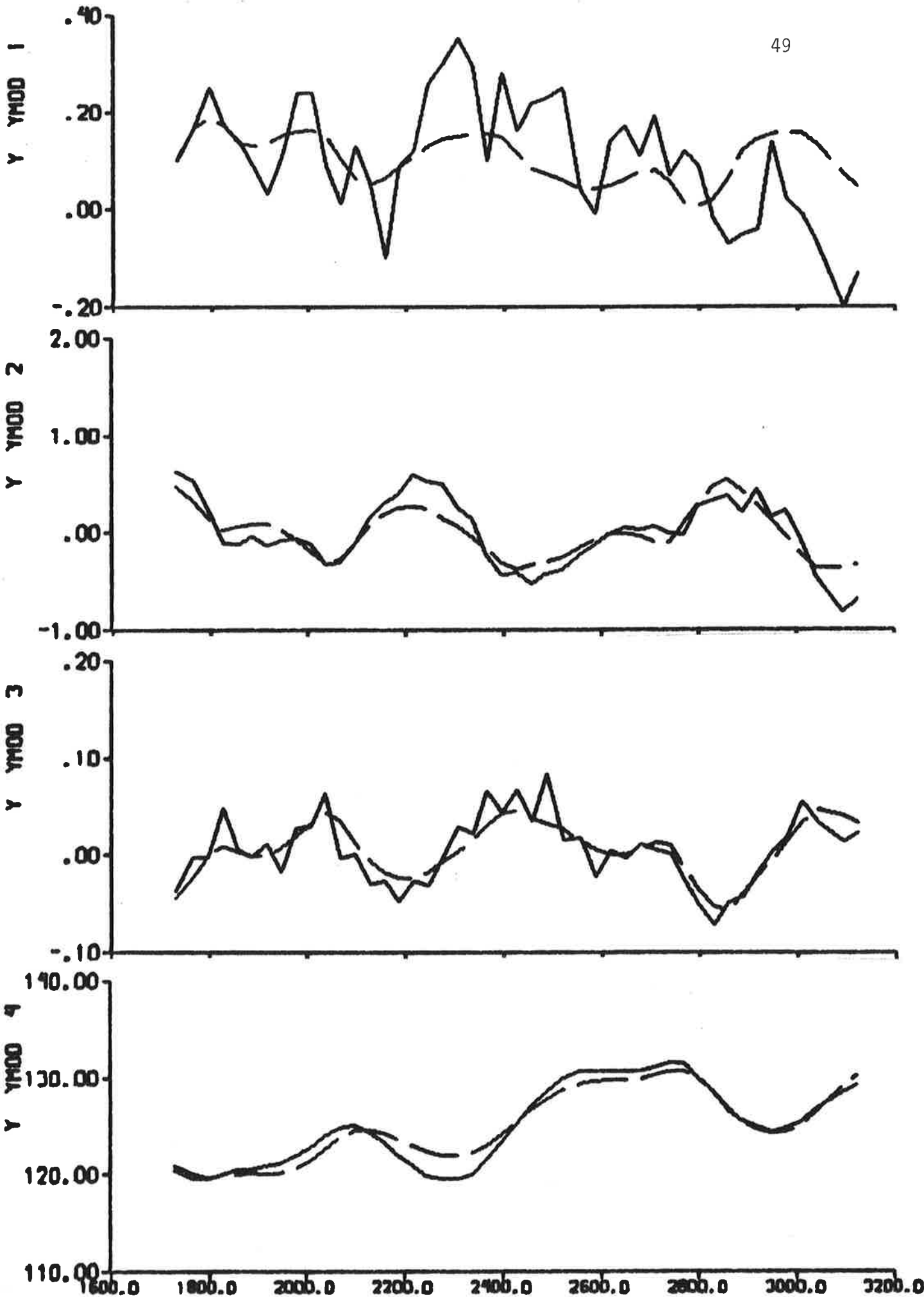


Fig. 3.9 a - Result of maximum likelihood identification to data from the second part of experiment 1. The dashed lines are model outputs. Cf. Fig. 2.1.

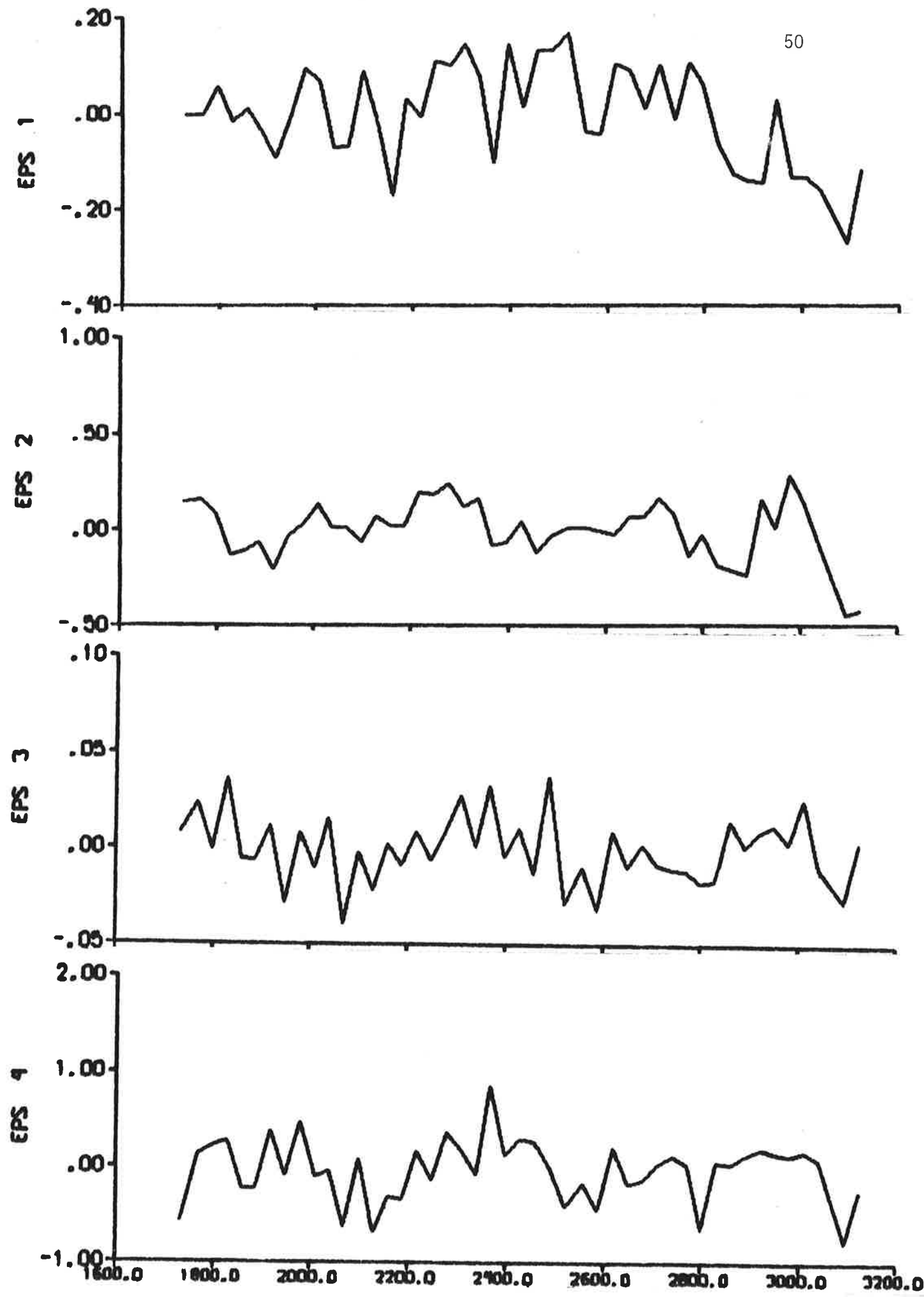


Fig. 3.9 b - Residuals.

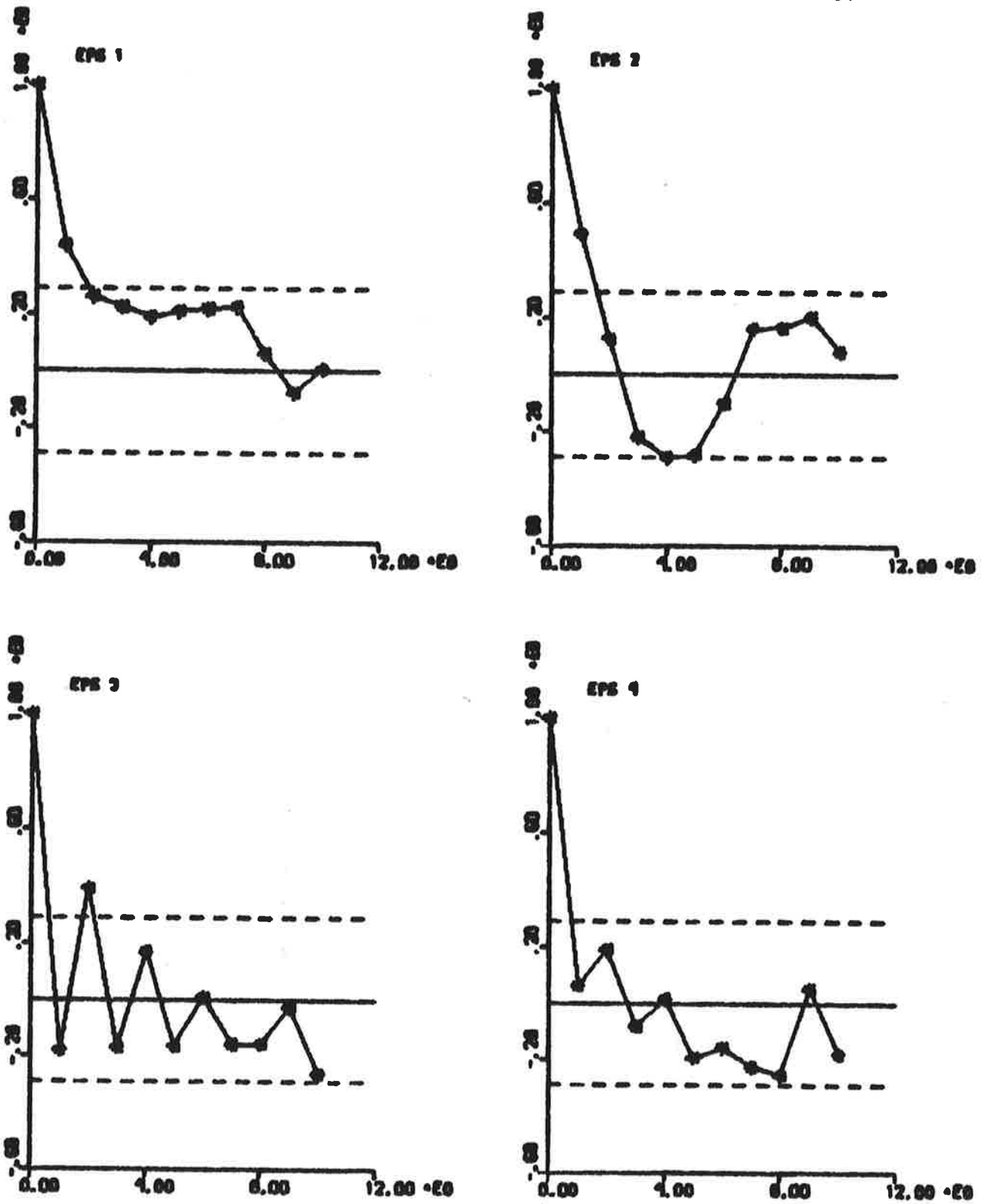


Fig. 3.9 c - Autocorrelation functions of residuals.

The dashed lines are $\pm 2\sigma$ limits.

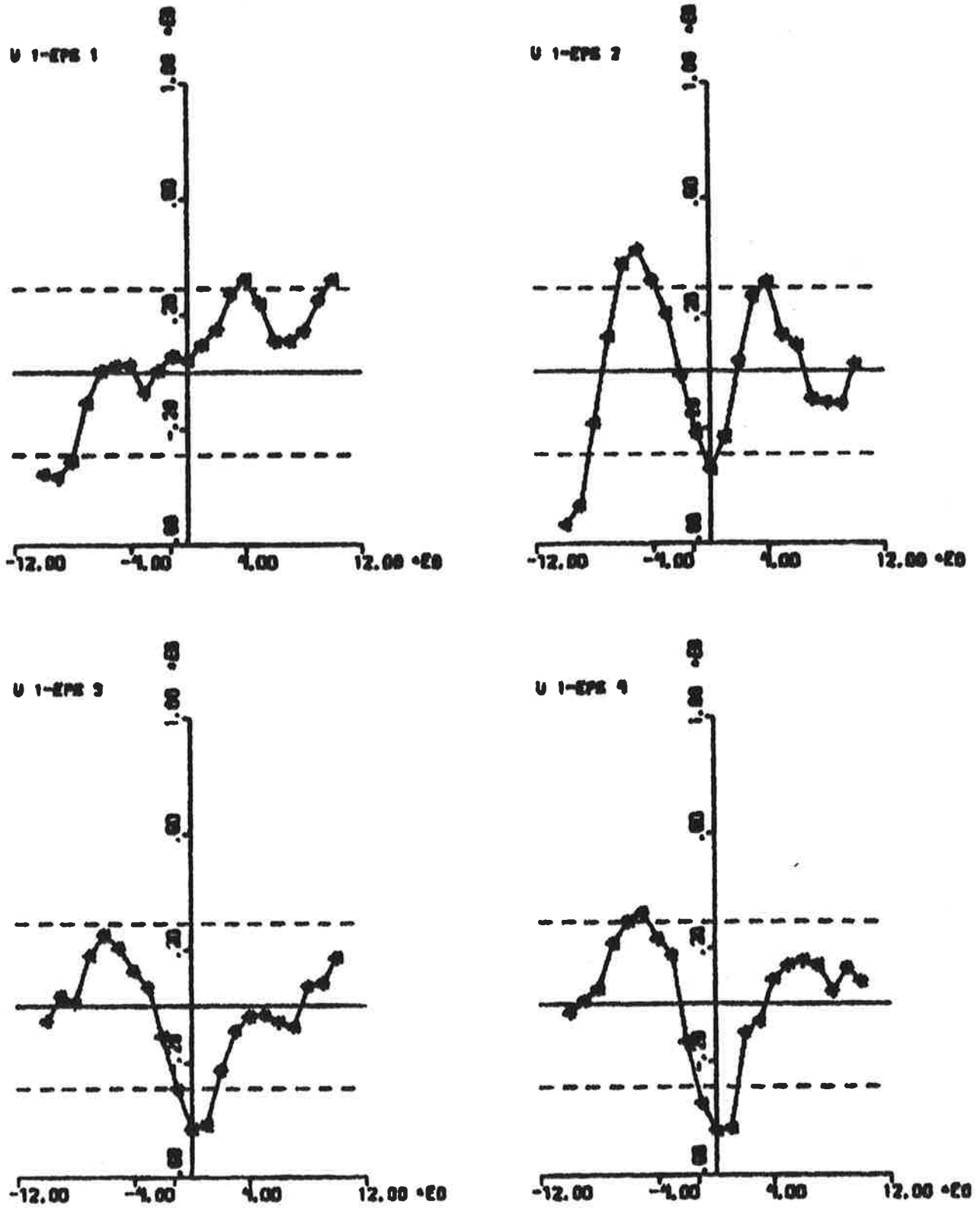


Fig. 3.9 d - Cross correlation functions between rudder input and residuals.
The dashed lines are $\pm 2\sigma$ limits.

Notice that the loss function V_1 (cf. (3.2)) is minimized also when the maximum likelihood method is applied. This means that LISPID transforms the model (3.1) to discrete form with sampling interval $T = 30$ s and computes the innovations representation

$$\begin{aligned}\hat{x}(t+T) &= A\hat{x}(t) + Bu(t) + K\varepsilon(t) \\ y(t) &= C\hat{x}(t) + Du(t) + \varepsilon(t)\end{aligned}\quad (3.9)$$

where the stationary filter gain K is calculated by solving an appropriate discrete, Riccati equation (see Källström, Essebo and Åström (1976) and Åström (1970)). The input vector u , the state vector x and the output vector y are the same as in the model (3.1). The stationary filter gain K obtained from the maximum likelihood identification to data from the first part of experiment 1 is

$$K = \begin{bmatrix} 1.5 \cdot 10^{-2} & 5.8 \cdot 10^{-2} & 5.8 \cdot 10^{-3} & 4.7 \cdot 10^{-3} \\ 1.2 \cdot 10^{-5} & -1.7 \cdot 10^{-4} & 2.3 \cdot 10^{-5} & 2.8 \cdot 10^{-6} \\ 4.7 \cdot 10^{-3} & 7.4 \cdot 10^{-4} & 3.3 \cdot 10^{-3} & 8.4 \cdot 10^{-3} \end{bmatrix} \quad (3.10)$$

and from the second part of experiment 1 is

$$K = \begin{bmatrix} 2.3 \cdot 10^{-2} & 2.4 \cdot 10^{-2} & -3.7 \cdot 10^{-1} & -1.8 \cdot 10^{-2} \\ 6.7 \cdot 10^{-4} & -1.3 \cdot 10^{-4} & 2.1 \cdot 10^{-3} & 9.1 \cdot 10^{-5} \\ 1.6 \cdot 10^{-2} & -1.2 \cdot 10^{-2} & 1.9 \cdot 10^{-1} & 1.9 \cdot 10^{-2} \end{bmatrix} \quad (3.11)$$

The parameters θ_{28} , θ_{29} and θ_{30} of the initial covariance matrix of state estimate errors P_0 were fixed to the following values:

$$\begin{aligned}\theta_{28} &= 0.1 && (\text{m/s})^2 \\ \theta_{29} &= 0.1 && (\text{rad/s})^2 \\ \theta_{30} &= 0.0001 && (\text{rad})^2\end{aligned}$$

Notice that $K = 0$ when the output error method is applied.

The consistency between the outputs from SSPA:s model and the measurements is now quite acceptable for both parts of the experiment (see Figs. 3.4 a and 3.7 a). The estimated hydrodynamic derivatives obtained from output error identifications and maximum likelihood identifications to data from first as well as second part of the experiment are very close to SSPA:s values (see Table 3.5). The model outputs do not differ much from the measurements (see Figs. 3.5, 3.6, 3.8 and 3.9). However, the residuals obtained are not quite uncorrelated to the rudder input and some of the residuals are not white. Akaike's information criterion indicates that the models from the maximum likelihood identifications are advantageous compared to the models from the output error identifications (see Table 3.5). It is difficult to decide which of the models from the maximum likelihood identifications that is to prefer. It is known that the relation $-N_{\delta}' / Y_{\delta}'$ should be approximately 0.5. SSPA:s model gives the value 0.48, and the relations obtained from the maximum likelihood identifications are 0.78 and 0.33 when the data from the first respectively the second part are used. This may indicate that the model obtained from maximum likelihood identification to data from the second part is the best one. It is also concluded that it may be reasonable to fix the relation $-N_{\delta}' / Y_{\delta}'$ when the model (3.1) is used in the future, i.e. to assume that $\theta_{12} \approx 0.5$.

It is also interesting to investigate the performance of the models obtained from the first part of the experiment when they are simulated to the rudder input from the second part, and vice versa. The wind parameters, the biases and the initial state are then fitted to the data by the output error method, but the hydrodynamic derivatives and the time delay are fixed. The results are summarized in Table 3.8 and the plots are shown in Figs. 3.10 - 3.13. The earlier conclusion that the model obtained from maximum likelihood identification to data from the second part is the best one is confirmed (see Fig. 3.13). This is further illustrated by Fig. 3.14, where Figs. 3.9 and 3.13 are combined.

		Second part of data		First part of data	
		Model from output err. ident. to data fr. the first part.	Model from max. likelihood ident. to data fr. the first part	Model from output err. ident. to data fr. the second part	Model from max. likelihood ident. to data fr. the second part
Figure		3.10	3.11	3.12	3.13
Sampling interval T [s]		30	30	30	30
Number of samples N		46	46	39	39
Number of estimated param. ν		10	10	10	10
ISAMP		2	2	2	1
Loss function V_1		0.02383	0.02153	0.00068	0.00050
Akaike's information crit. AIC		-158	-163	-250	-262
Hydrodynamic derivatives ('prime' syst., mass unit $\rho L^3/2$)	Y_V' (θ_5)	-0.0099*	-0.0119*	-0.0131*	-0.0146*
	Y_R' -m' (θ_6)	-0.0068*	-0.0074*	-0.0049*	-0.0057*
	N_V' (θ_7)	-0.0021*	-0.0019*	-0.0017*	-0.0017*
	N_R' -m'x G' (θ_8)	-0.0017*	-0.0014*	-0.0010*	-0.0011*
	Y_δ' (θ_{11})	0.0018*	0.0009*	0.0024*	0.0018*
	N_δ' - ($-\theta_{11}\theta_{12}$)	-0.00067*	-0.00070*	-0.00063*	-0.00060*
Wind parameters	θ_9 [-]	-0.019	-0.030	-0.068	-0.063
	θ_{10} [-]	0.054	0.039	0.037	0.066
Biases	θ_{13} [-]	0.028	0.072	0.065	-0.132
	θ_{14} [-]	0.0017	0.0055	-0.0018	-0.0181
	θ_{15} [knots]	0.26	0.01	0.83	2.61
	θ_{16} [knots]	0.21	-0.04	0.76	2.56
	θ_{17} [deg/s]	-0.0003	-0.0006	0.0014	0.0000
Initial state	θ_{25} [knots]	0.02	0.19	-1.04	-2.87
	θ_{26} [deg/s]	-0.0410	-0.0428	-0.0068	0.0061
	θ_{27} [deg]	121.1	120.9	140.2	140.1
Time delay	T_D ($T-T_{\theta_{34}}$ sin) [s]	21.2*	23.4*	9.2*	23.8*

* = fixed value

Table 3.8 - Parameter values from output error identifications to data from the first and second part of experiment 1. The corresponding hydrodynamic derivatives in the 'bis' system are obtained by dividing with $m' = 0.00918$.

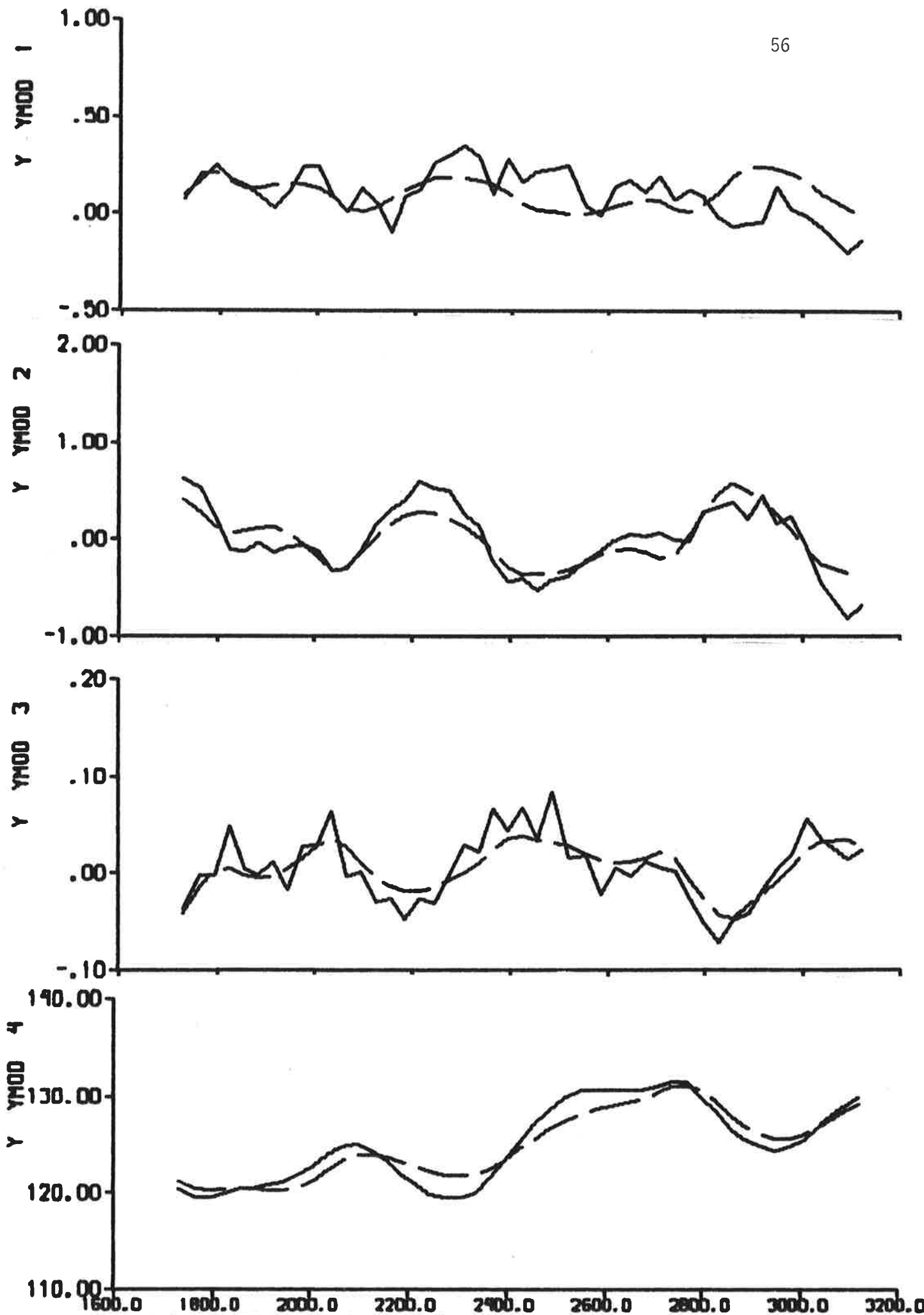


Fig. 3.10 - Result of output error identification to data from the second part of experiment 1, when the model is fixed to the model obtained from output error identification to data from the first part. The dashed lines are model outputs. Cf. Fig. 2.1.

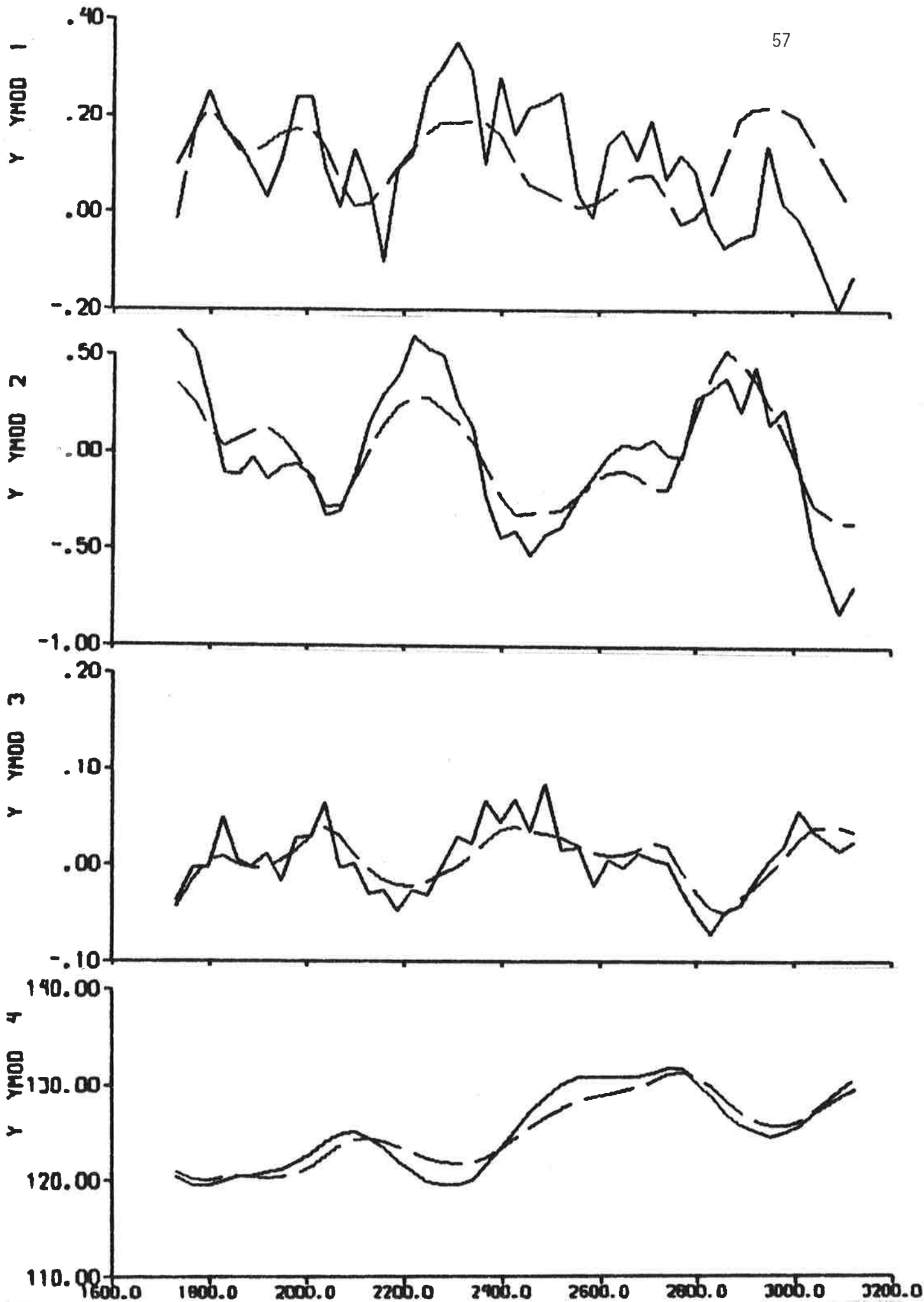


Fig. 3.11 - Result of output error identification to data from the second part of experiment 1, when the model is fixed to the model obtained from maximum likelihood identification to data from the first part. The dashed lines are model outputs. Cf. Fig. 2.1.

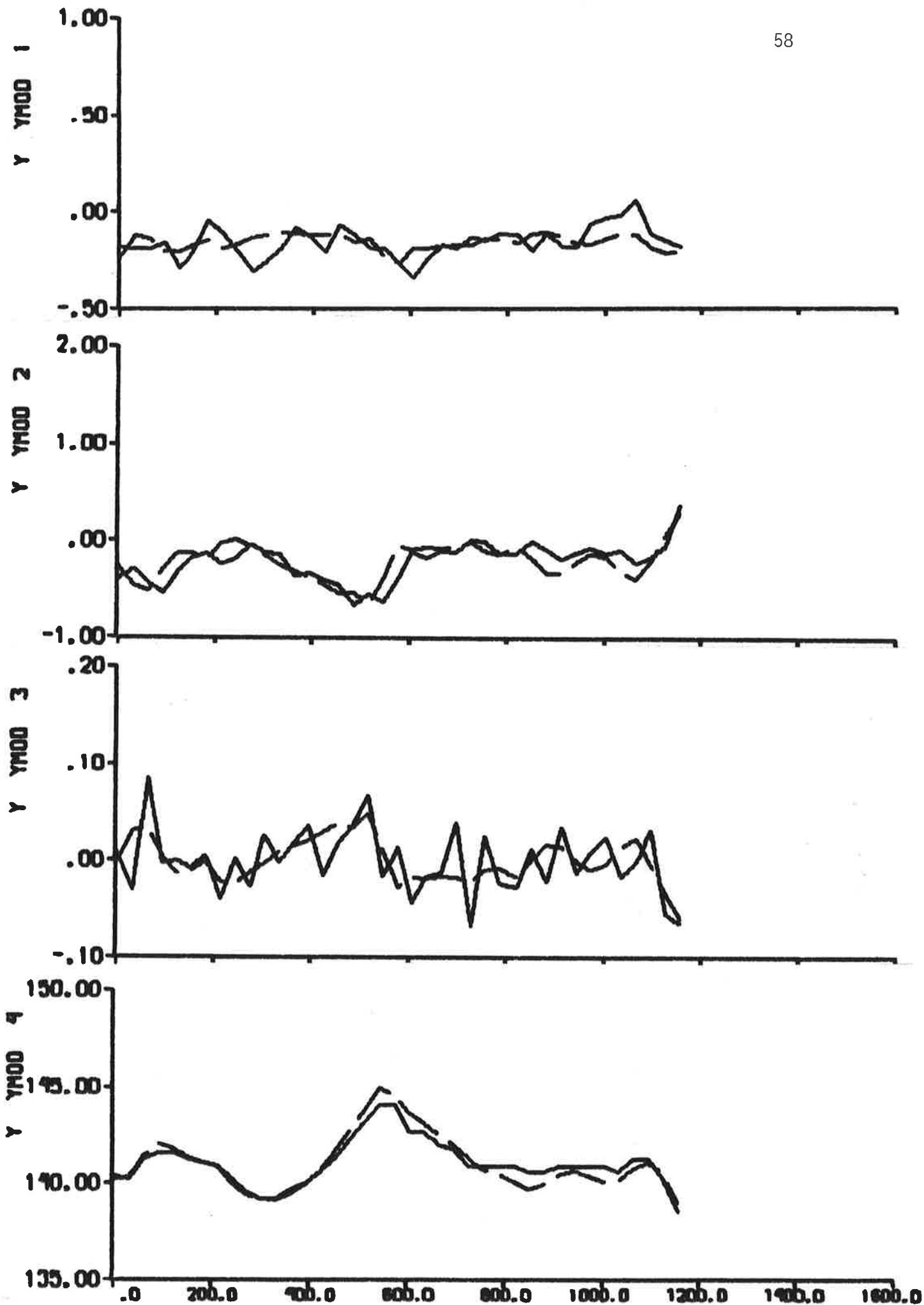


Fig. 3.12 - Result of output error identification to data from the first part of experiment 1, when the model is fixed to the model obtained from output error identification to data from the second part. The dashed lines are model outputs. Cf. Fig. 2.1.

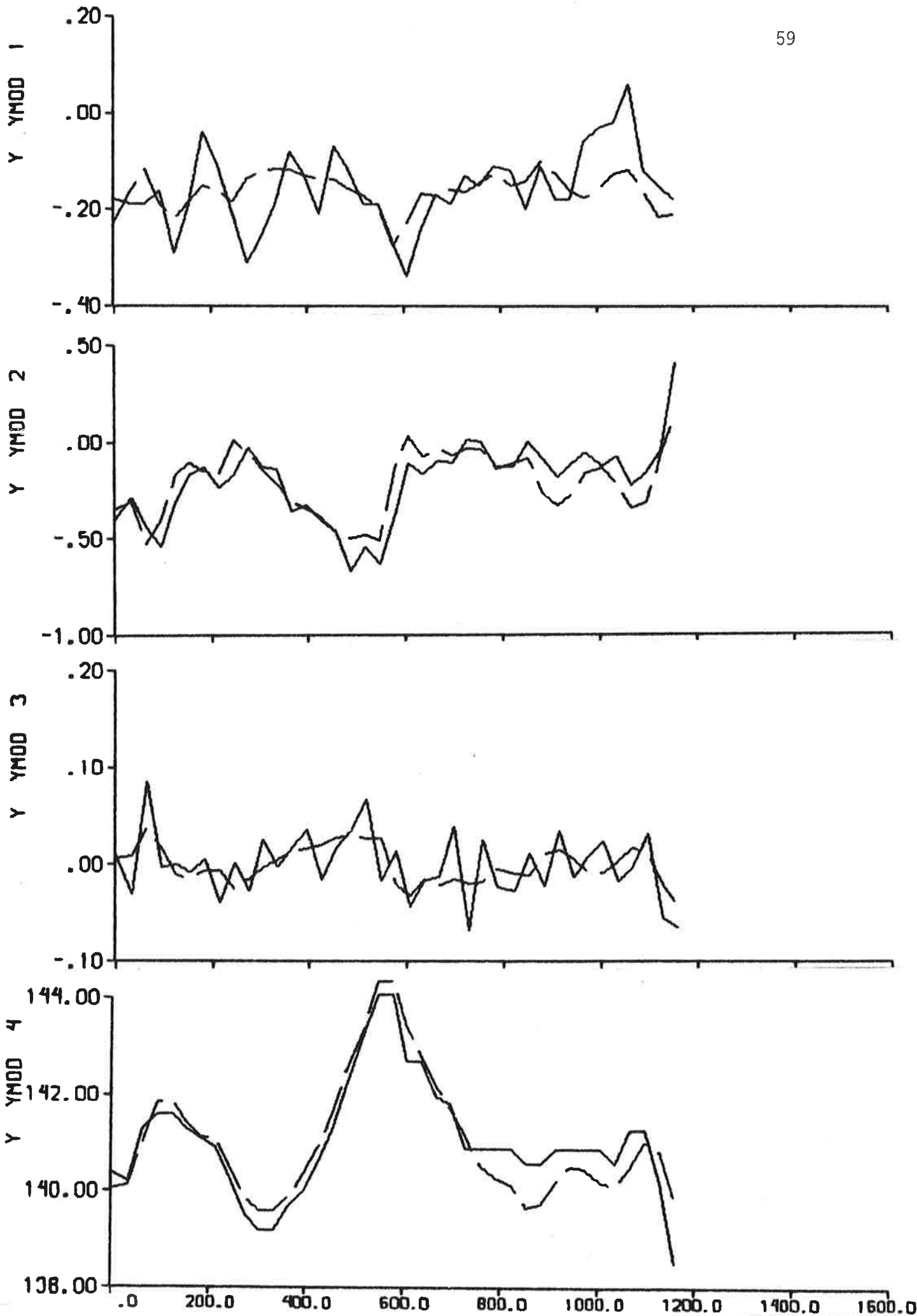


Fig. 3.13 - Result of output error identification to data from the first part of experiment 1, when the model is fixed to the model obtained from maximum likelihood identification to data from the second part. The dashed lines model outputs. Cf. Fig. 2.1.

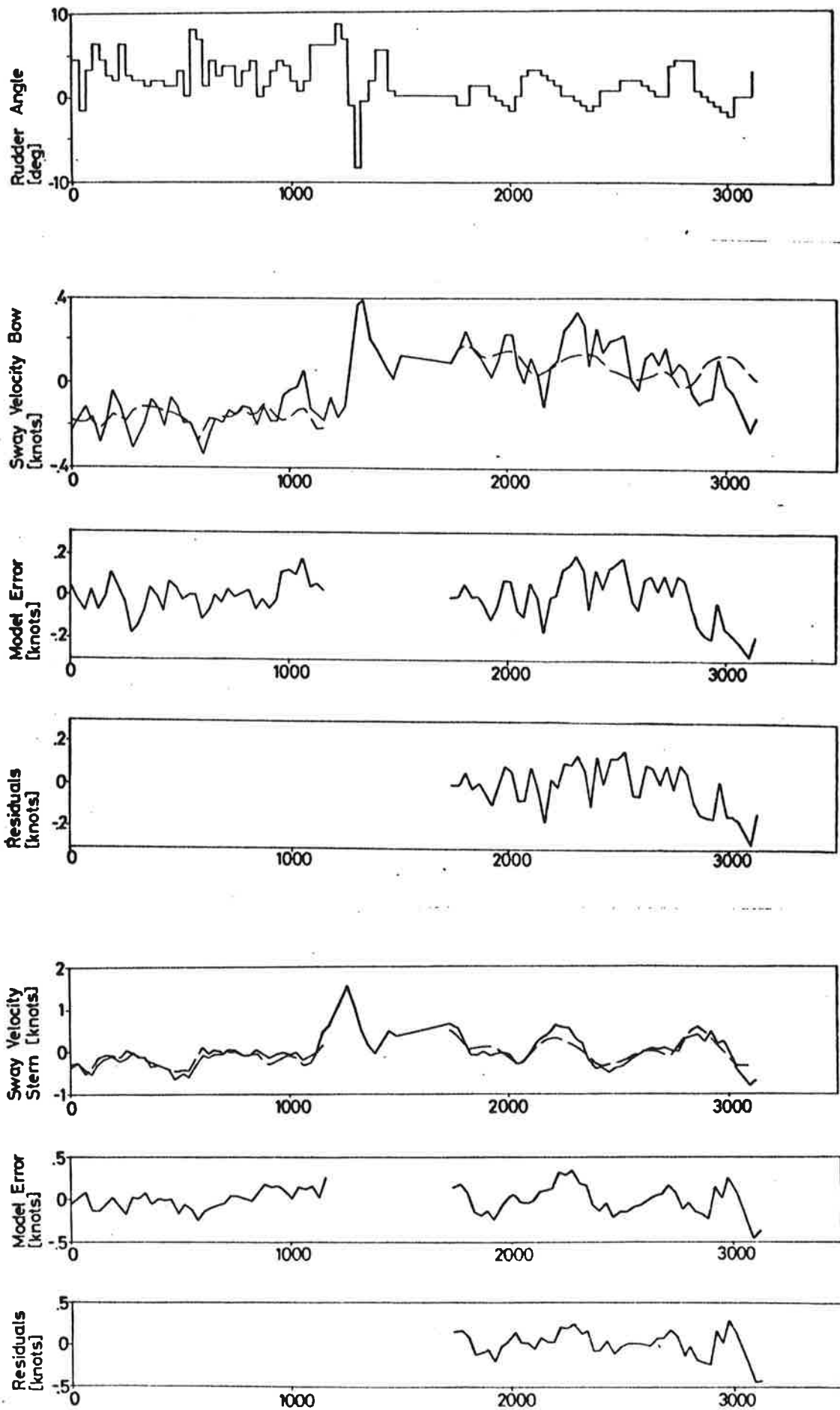


Fig. 3.14 a - Result of maximum likelihood identification to data from the second part of experiment 1 (cf. Fig. 3.9). Simulation of the model to the first part of the rudder input is also shown (cf. Fig. 3.13). The dashed lines are model outputs. Cf. Fig. 2.1.

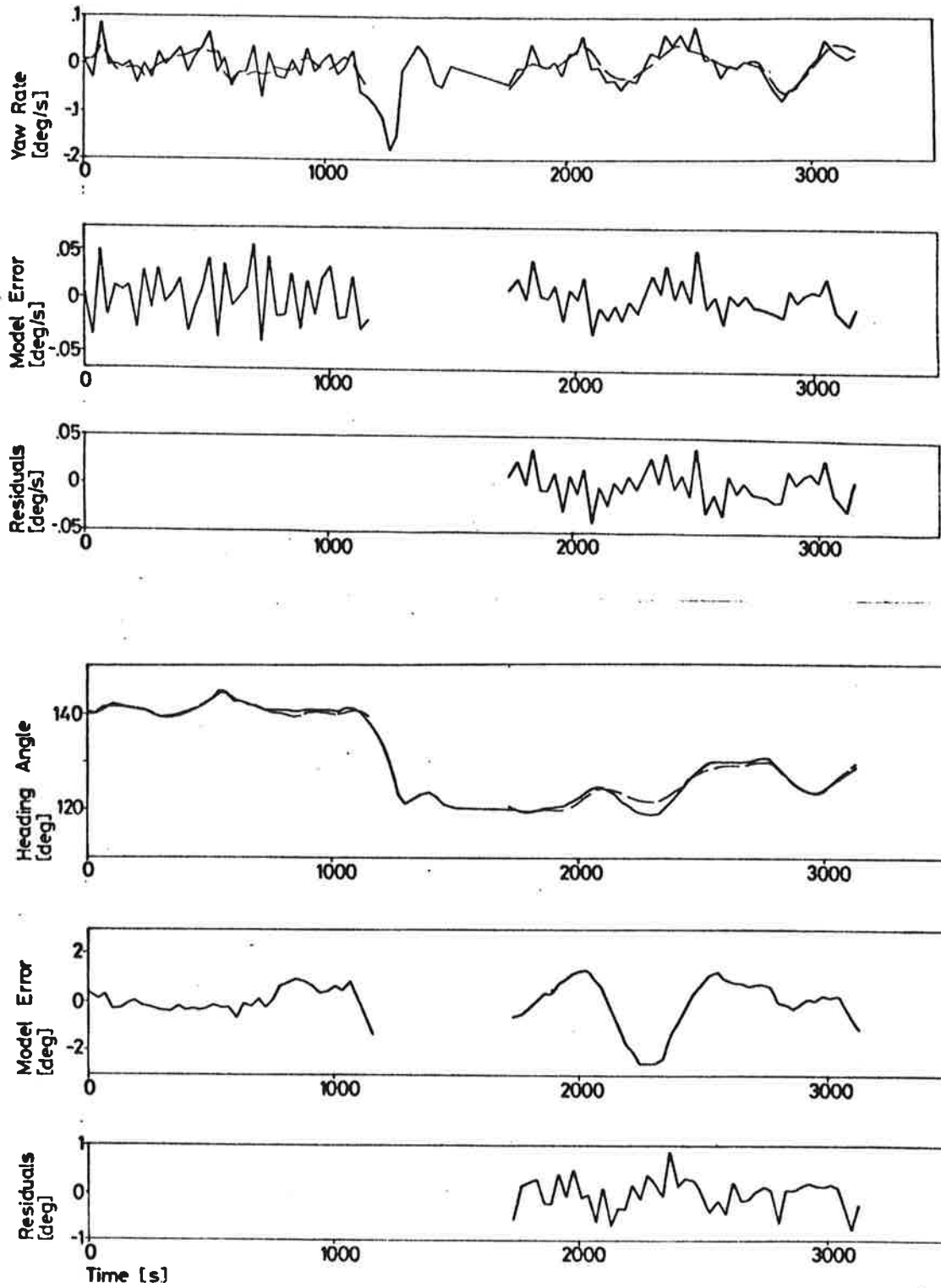


Fig. 3.14 b

4. IDENTIFICATION RESULTS FROM EXPERIMENT 2

It is not possible to determine the hydrodynamic derivatives of the model (3.1) from experiment 2, because the sway velocity was not measured. However, the transfer function relating the heading angle to the rudder angle can be determined, since measurements of headings, and yaw rates, are available.

The identifications with LISPID are based on the following linear model of the steering dynamics (cf. Åström, Norrbin, Källström and Byström (1974) and Åström, Källström, Norrbin and Byström (1975)):

$$\begin{pmatrix} dx_1 \\ dr \\ d\psi \end{pmatrix} = \begin{pmatrix} 0 & 0 & -\frac{v^3}{L^3} \varphi_3 \\ 1 & -\frac{v}{L} \varphi_1 & -\frac{v^2}{L^2} \varphi_2 \\ 0 & 1 & 0 \end{pmatrix} \begin{pmatrix} x_1(t) \\ r(t) \\ \psi(t) \end{pmatrix} dt +$$

$$+ \begin{pmatrix} \alpha_1 \frac{v^3}{L^3} \varphi_5 & \varphi_6 \\ \alpha_1 \frac{v^2}{L^2} \varphi_4 & \varphi_7 \\ 0 & 0 \end{pmatrix} \begin{pmatrix} \delta(t-T_D) \\ U \end{pmatrix} dt + dw$$

(4.1)

$$\begin{pmatrix} r_m(t_k) \\ \psi_m(t_k) \end{pmatrix} = \begin{pmatrix} 0 & 1/\alpha_1 & 0 \\ 0 & 0 & 1/\alpha_1 \end{pmatrix} \begin{pmatrix} x_1(t_k) \\ r(t_k) \\ \psi(t_k) \end{pmatrix} +$$

$$+ \begin{pmatrix} 0 & \varphi_8 \\ 0 & 0 \end{pmatrix} \begin{pmatrix} \delta(t_k-T_D) \\ U \end{pmatrix} + e(t_k)$$

$$k = 0, 1, \dots, N-1$$

$$R_1 = \begin{pmatrix} |\varphi_9| & \sqrt{|\varphi_9| |\varphi_{10}|} \sin \varphi_{11} & 0 \\ \sqrt{|\varphi_9| |\varphi_{10}|} \sin \varphi_{11} & |\varphi_{10}| & 0 \\ 0 & 0 & 0 \end{pmatrix}$$

$$iR_2 = \begin{pmatrix} |\varphi_{12}| & \sqrt{|\varphi_{12}||\varphi_{13}|} \sin \varphi_{14} \\ \sqrt{|\varphi_{12}||\varphi_{13}|} \sin \varphi_{14} & |\varphi_{13}| \end{pmatrix}$$

$$\begin{pmatrix} x_1(t_0) \\ r(t_0) \\ \psi(t_0) \end{pmatrix} = \begin{pmatrix} \varphi_{15} \\ \alpha_1 \varphi_{16} \\ \alpha_1 \varphi_{17} \end{pmatrix}$$

$$P(t_0) = P_0 = \begin{pmatrix} |\varphi_{18}| & \varphi_{21} & \varphi_{22} \\ \varphi_{21} & |\varphi_{19}| & \varphi_{23} \\ \varphi_{22} & \varphi_{23} & |\varphi_{20}| \end{pmatrix}$$

$$T_D = T (1 - |\sin \varphi_{24}|)$$

The following variables are used in (4.1):

Inputs

δ - rudder servo position [deg]

U - artificial unit step input [-]

States

x_1 - linear combination of v, r and ψ [$1/s^2$]

r - yaw rate [rad/s]

ψ - heading angle [rad]

Outputs

r_m - yaw rate [deg/s]

ψ_m - heading angle [deg]

The model (4.1) is provided with the following fixed parameter values:

V - ship speed (8.5 m/s)

L - ship length (329.2 m)

α_1 - conversion factor from degrees to radians (0.01745)

The parameters $\varphi_1 - \varphi_{24}$, or a subset of these parameters, can be estimated in LISPID.

The transfer function relating ψ to δ (in radians) when the time delay T_D is zero is obtained from (4.1):

$$G_{\psi\delta}(s) = \frac{\frac{V^2}{L^2} \varphi_4 s + \frac{V^3}{L^3} \varphi_5}{s^3 + \frac{V}{L} \varphi_1 s^2 + \frac{V^2}{L^2} \varphi_2 s + \frac{V^3}{L^3} \varphi_3} \quad (4.2)$$

If the wind parameter φ_3 is zero, (4.2) becomes (cf. (3.6)):

$$G_{\psi\delta}(s) = \frac{\frac{V^2}{L^2} \varphi_4 s + \frac{V^3}{L^3} \varphi_5}{s [s^2 + \frac{V}{L} \varphi_1 s + \frac{V^2}{L^2} \varphi_2]} = \quad (4.3)$$

$$= \frac{K(1+sT_3)}{s(1+sT_1)(1+sT_2)} = \frac{K_1 (s + \frac{1}{T_3})}{s(s + \frac{1}{T_1})(s + \frac{1}{T_2})}$$

The analysis of experiment 2 is performed with ISAMP = 2 to save computing time, although ISAMP = 3 would be more appropriate. The program LISPID transforms the model (4.1) to discrete form with sampling interval $T = 15$ s and computes the innovations representation (cf. (3.9))

$$\begin{aligned} \hat{x}(t+T) &= A \hat{x}(t) + Bu(t) + K \varepsilon(t) \\ y(t) &= C \hat{x}(t) + Du(t) + \varepsilon(t) \end{aligned} \quad (4.4)$$

where the input vector u , the state vector x and the output vector y are the same as in the model (4.1).

The loss function (cf. (3.2))

$$V_1 = \frac{1}{N} \det \left[\begin{array}{c} N-1 \\ \sum_{k=0} \quad \varepsilon(t_k) \varepsilon^T(t_k) \end{array} \right] \quad (4.5)$$

is then minimized to obtain the maximum likelihood estimates of the unknown parameters. Notice that $K = 0$ in (4.4) when the output error method is applied.

The following parameters of the model (4.1) are always given fixed values:

$$\begin{aligned}
\varphi_{13} &= 0.01 \text{ deg}^2 \\
\varphi_{14} &= 0 \\
\varphi_{18} &= 1 \\
\varphi_{19} &= 1 \\
\varphi_{20} &= 1 \\
\varphi_{21} &= 0 \\
\varphi_{22} &= 0 \\
\varphi_{23} &= 0
\end{aligned}$$

The results of output error identifications and maximum likelihood identifications, when the wind parameter φ_3 is fixed to zero and when φ_3 is estimated, are shown in Figs. 4.1 - 4.4. The parameter estimates obtained are summarized in Table 4.1 and the corresponding transfer function parameters are shown in Table 4.2. Notice that the time delay T_D can be regarded as an approximation of the effective time constant of the rudder machine. The following filter gains (cf. (4.4)) are obtained from the maximum likelihood identifications when $\varphi_3 = 0$ and when φ_3 is estimated, respectively:

$$K = \begin{pmatrix} 4.8 \cdot 10^{-5} & 1.5 \cdot 10^{-5} \\ 2.1 \cdot 10^{-3} & 3.9 \cdot 10^{-4} \\ 5.5 \cdot 10^{-2} & 2.4 \cdot 10^{-2} \end{pmatrix} \quad (4.6)$$

and

$$K = \begin{pmatrix} 3.9 \cdot 10^{-5} & 9.3 \cdot 10^{-6} \\ 3.3 \cdot 10^{-3} & 4.4 \cdot 10^{-4} \\ 7.3 \cdot 10^{-2} & 2.6 \cdot 10^{-2} \end{pmatrix} \quad (4.7)$$

The filter gains are approximately the same, although the covariance matrices R_1 and R_2 differ significantly (see Table 4.1).

		Output error φ_3 fixed	Output error φ_3 est.	Max. like- lihood φ_3 fixed	Max. like- lihood φ_3 est.
Figure		4.1	4.2	4.3	4.4
Sampling interval T [s]		15	15	15	15
Number of samples N		121	121	121	121
Number of estimated parameters ν		11	12	15	16
ISAMP		2	2	2	2
Loss function V_1		0.36699	0.28692	0.00582	0.00588
Akaike's information criterion AIC		7	-21	-486	-483
Normalized ('prime' system) transfer function parameters	φ_1	3.61	3.41	2.95	2.22
	φ_2	0.04	0.15	-0.10	-0.10
	φ_4	-2.68	-2.42	-1.87	-1.57
	φ_5	-1.31	-1.45	-1.31	-0.93
Wind param.	φ_3 [-]	0*	-0.0205	0*	0.0058
Biases	φ_6 [$1/s^3$]	$6.0 \cdot 10^{-7}$	$-5.6 \cdot 10^{-7}$	$5.5 \cdot 10^{-7}$	$7.4 \cdot 10^{-7}$
	φ_7 [rad/s^2]	-0.00303	-0.00041	-0.00152	-0.00017
	φ_8 [deg/s]	0.0053	0.0046	0.0030	0.0025
Covariance matrices	$R_1(1,1) (\varphi_9)$	-	-	$5.1 \cdot 10^{-12}$	$2.6 \cdot 10^{-9}$
	$R_1(1,2)$	-	-	$3.8 \cdot 10^{-11}$	$-4.6 \cdot 10^{-7}$
	$(\sqrt{ \varphi_9 \varphi_{10} } \sin \varphi_{11})$				
	$R_1(2,2) (\varphi_{10})$	-	-	$7.0 \cdot 10^{-8}$	$8.2 \cdot 10^{-5}$
	$R_2(1,1) (\varphi_{12})$ [deg/s] ²	-	-	$1.9 \cdot 10^{-3}$	1.4
Initial state	φ_{15} [$1/s^2$]	0.00317	0.00079	0.00132	-0.00003
	φ_{16} [deg/s]	0.0028	-0.0010	-0.0010	-0.0015
	φ_{17} [deg]	199.6	199.0	198.3	198.3
Time delay	$T_D (T-T \sin \varphi_{24})$ [s]	9.0	7.8	0.8	0.3

* = fixed value

Table 4.1 - Parameter values from identifications to data from experiment 2.

	SSPA:s model	Output error φ_3 fixed	Output error φ_3 estimated	Max. likeli- hood φ_3 fixed	Max. likeli- hood φ_3 estimated
K'	-0.72	-33.02	-9.88	13.01	9.12
K_1'	-0.90	-2.66	-2.40	-1.85	-1.57
T_1'	2.30	90.91	22.93	-29.51	-22.16
T_2'	0.36	0.28	0.30	0.34	0.44
T_3'	1.03	2.05	1.67	1.43	1.68

Table 4.2 - Normalized ('prime' system) transfer function parameters (cf. (4.3) and (3.8)) computed from the models in Table 4.1, when the wind parameter φ_3 is zero.

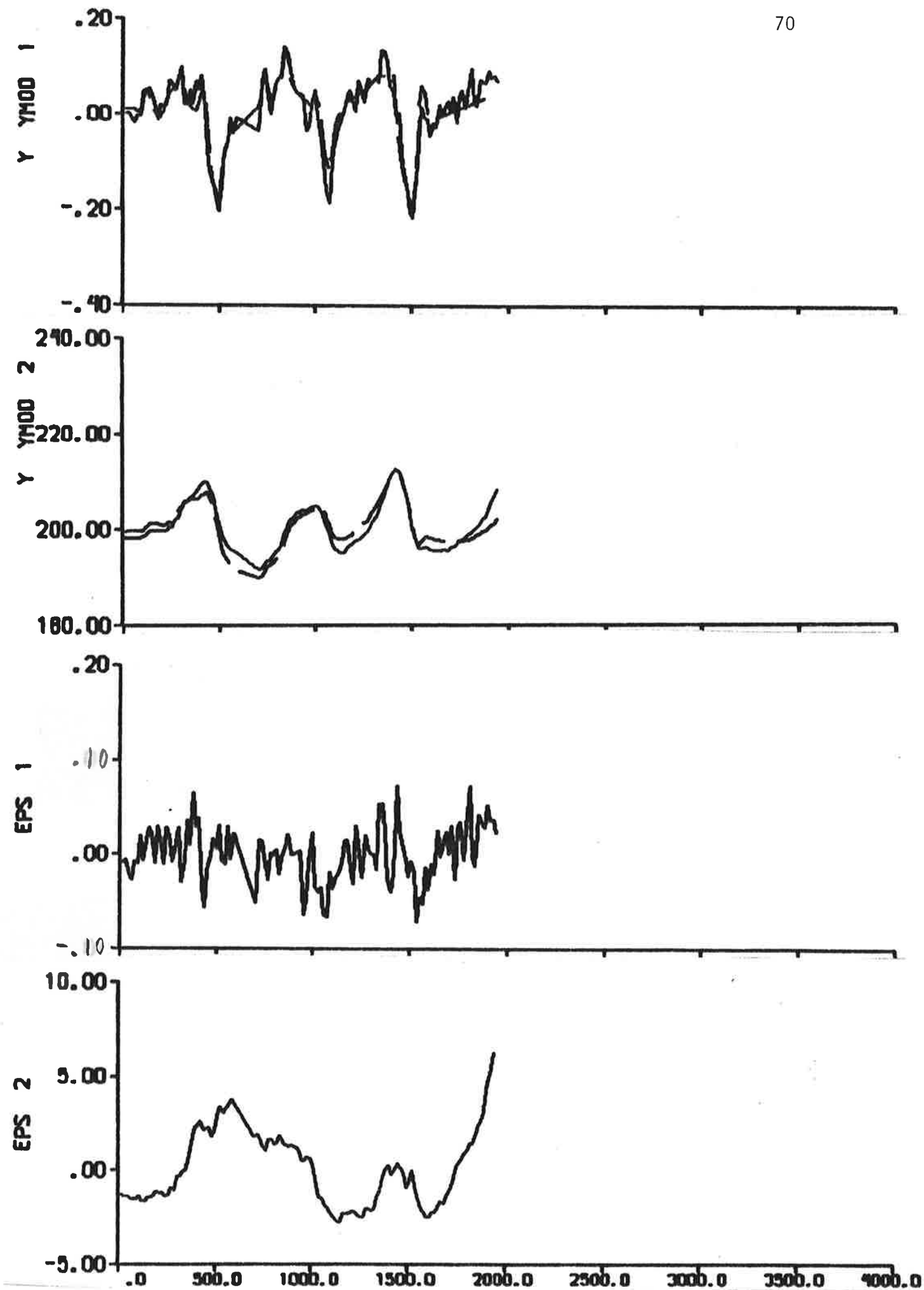


Fig. 4.1 a - Result of output error identification to data from experiment 2, when the wind parameter φ_3 is fixed to zero. The dashed lines are model outputs. Cf. Fig. 2.2.

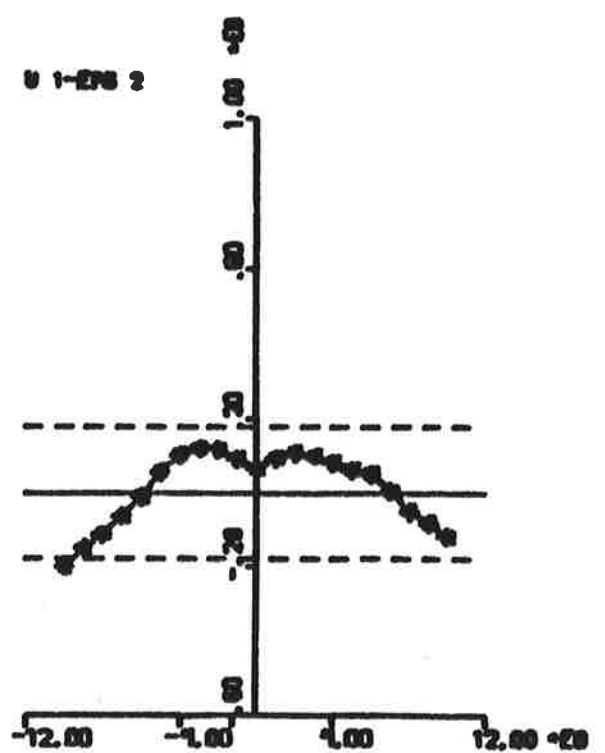
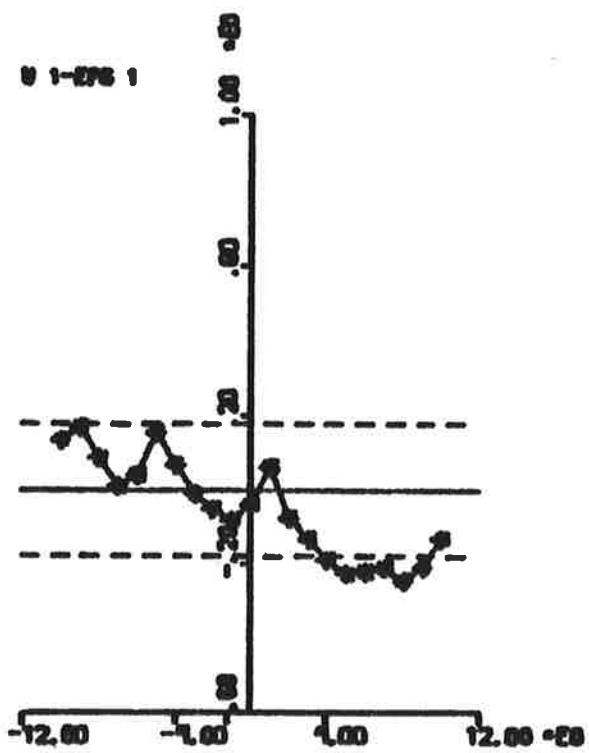
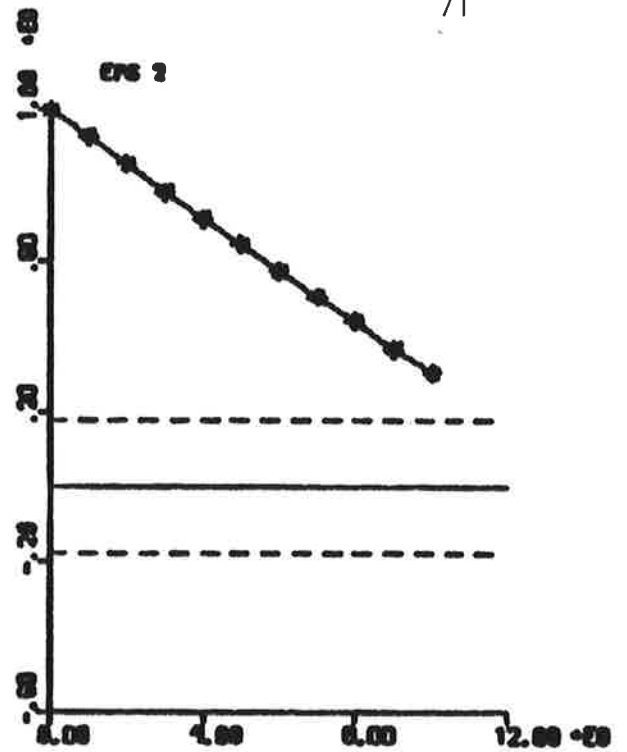
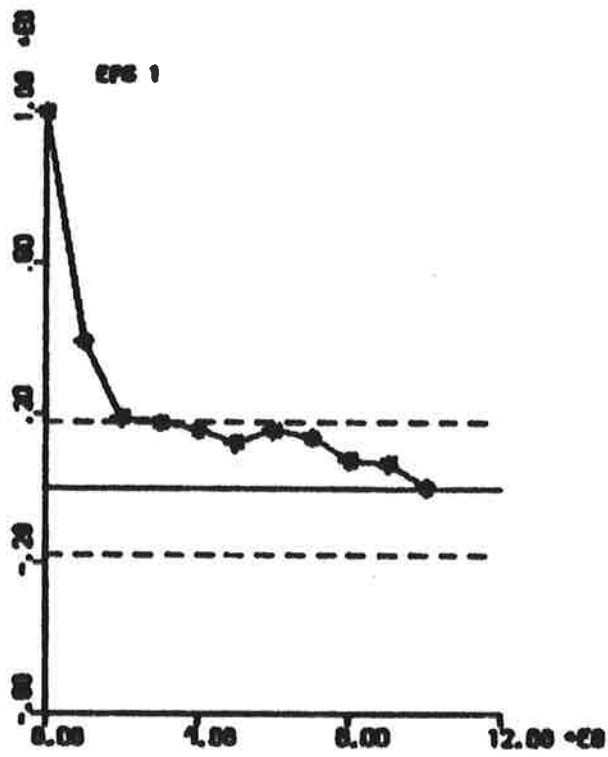


Fig. 4.1 b - Autocorrelation functions of residuals and cross correlation functions between rudder input and residuals. The dashed lines are $\pm 2\sigma$ limits.

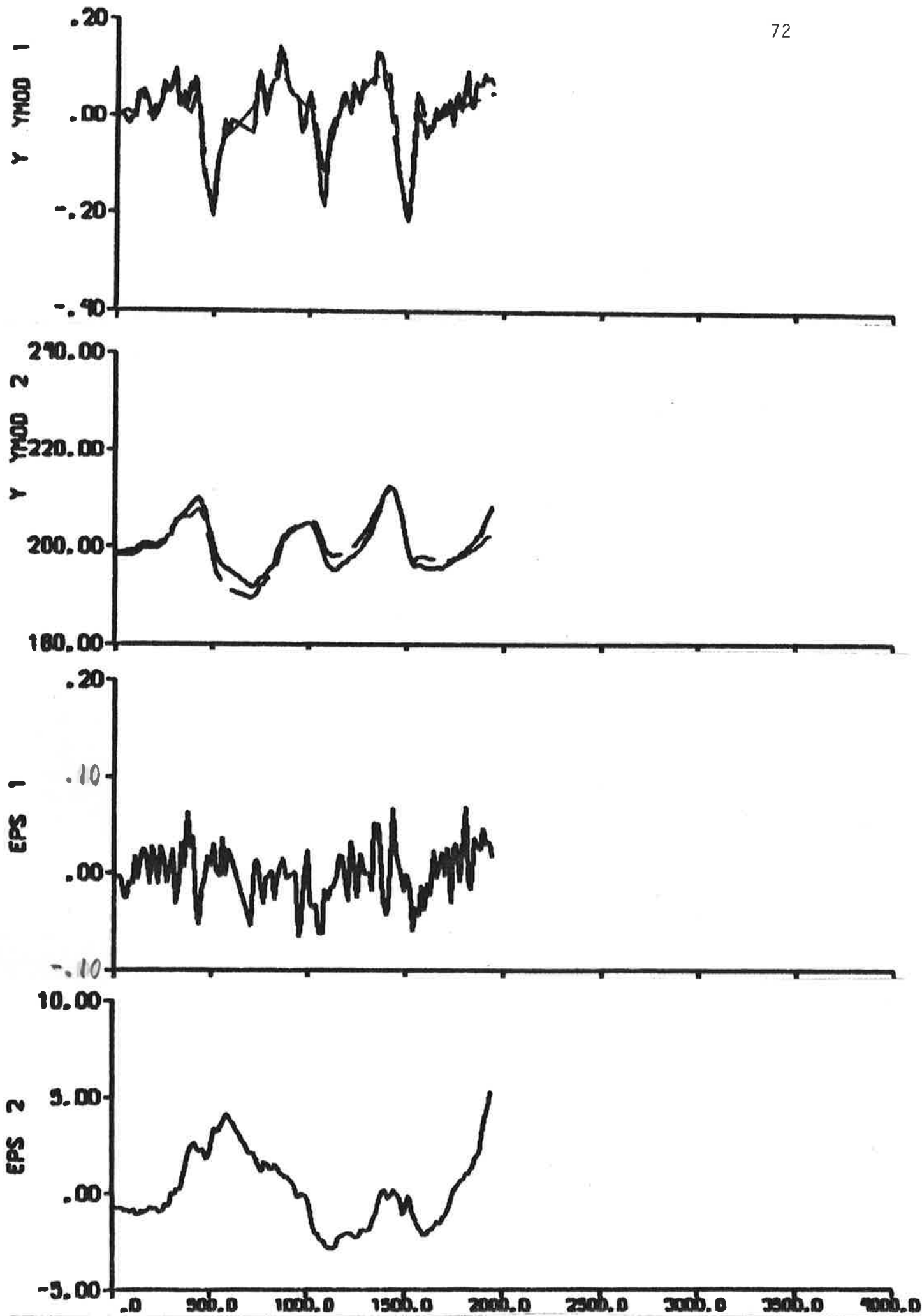


Fig. 4.2 a - Result of output error identification to data from experiment 2, when the wind parameter φ_3 is estimated. The dashed lines are model outputs. Cf. Fig. 2.2.

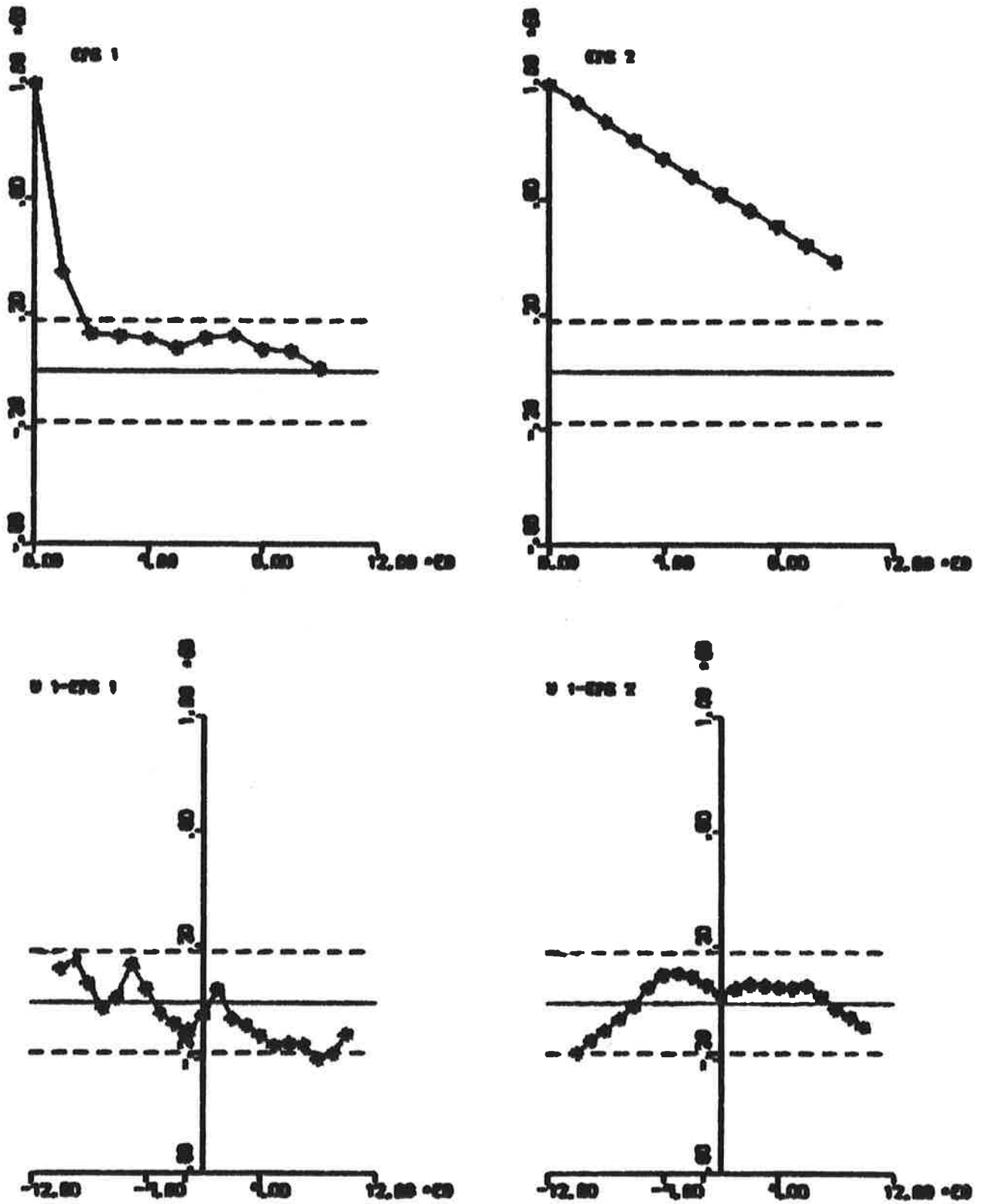


Fig. 4.2 b - Autocorrelation functions of residuals and cross correlation functions between rudder input and residuals. The dashed lines are $\pm 2\sigma$ limits.

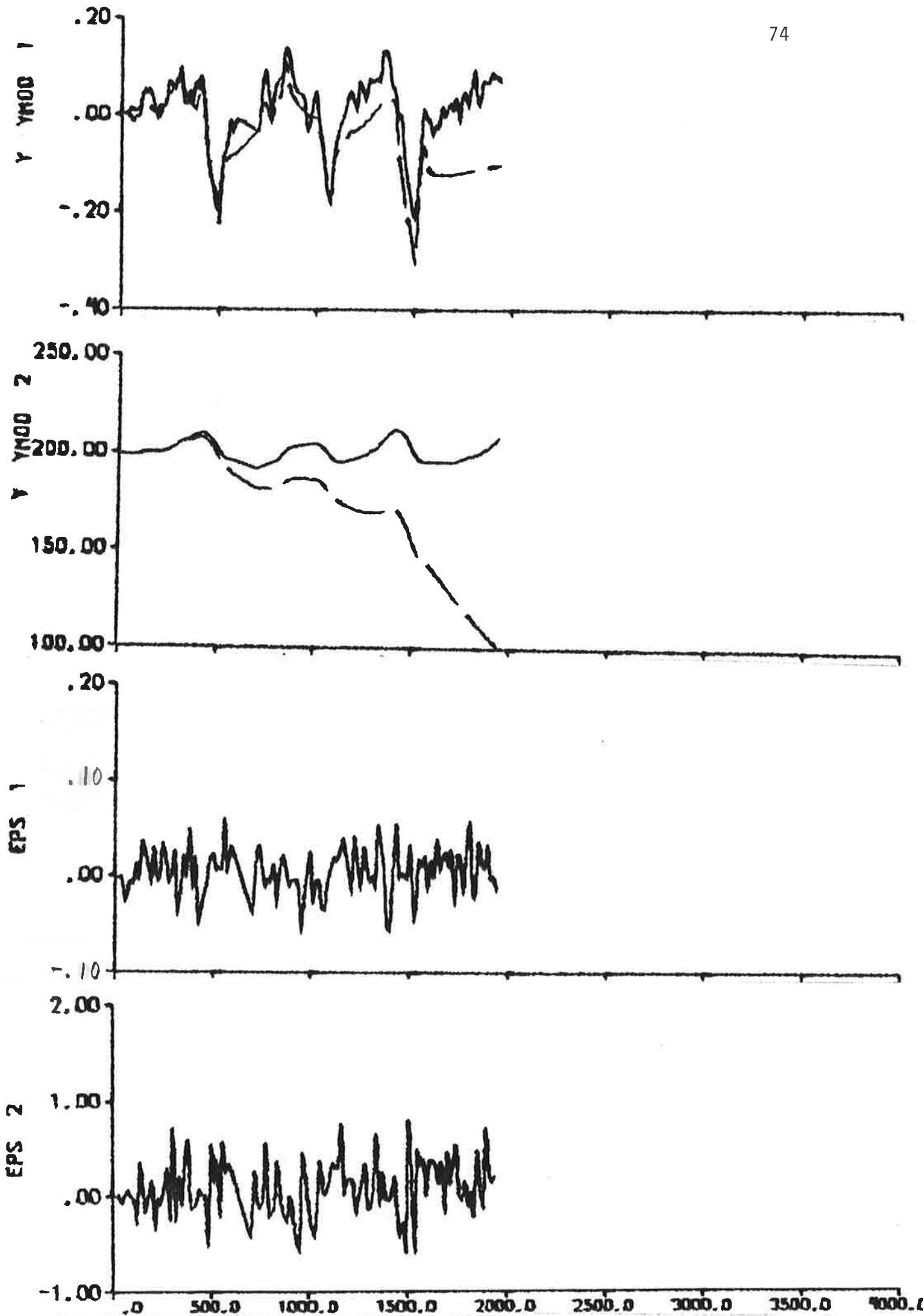


Fig. 4.3 a - Result of maximum likelihood identification to data from experiment 2, when the wind parameter φ_3 is fixed to zero. The dashed lines are model outputs. Cf. Fig. 2.2.

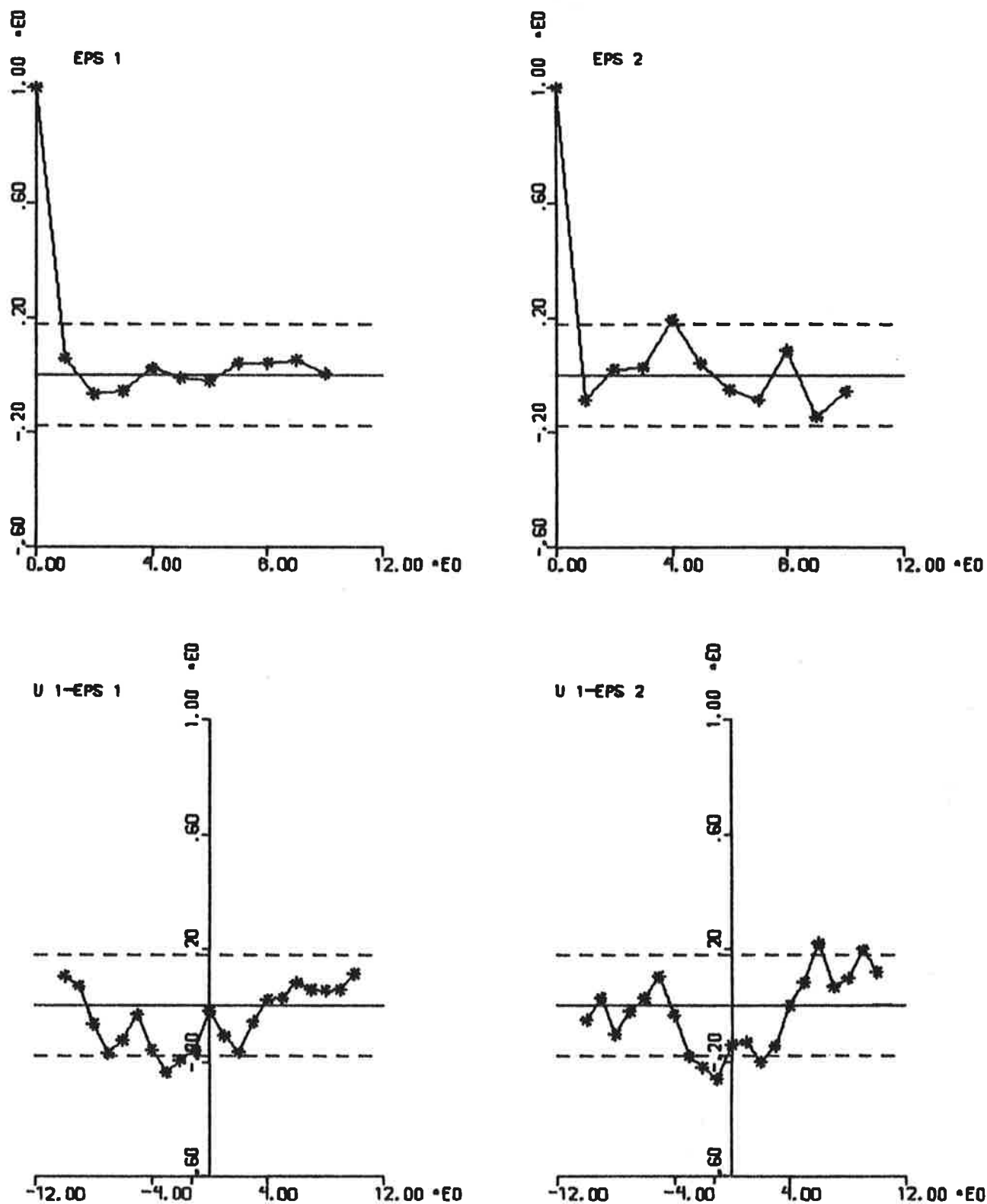


Fig. 4.3 b - Autocorrelation functions of residuals and cross correlation functions between rudder input and residuals. The dashed lines are $\pm 2\sigma$ limits.

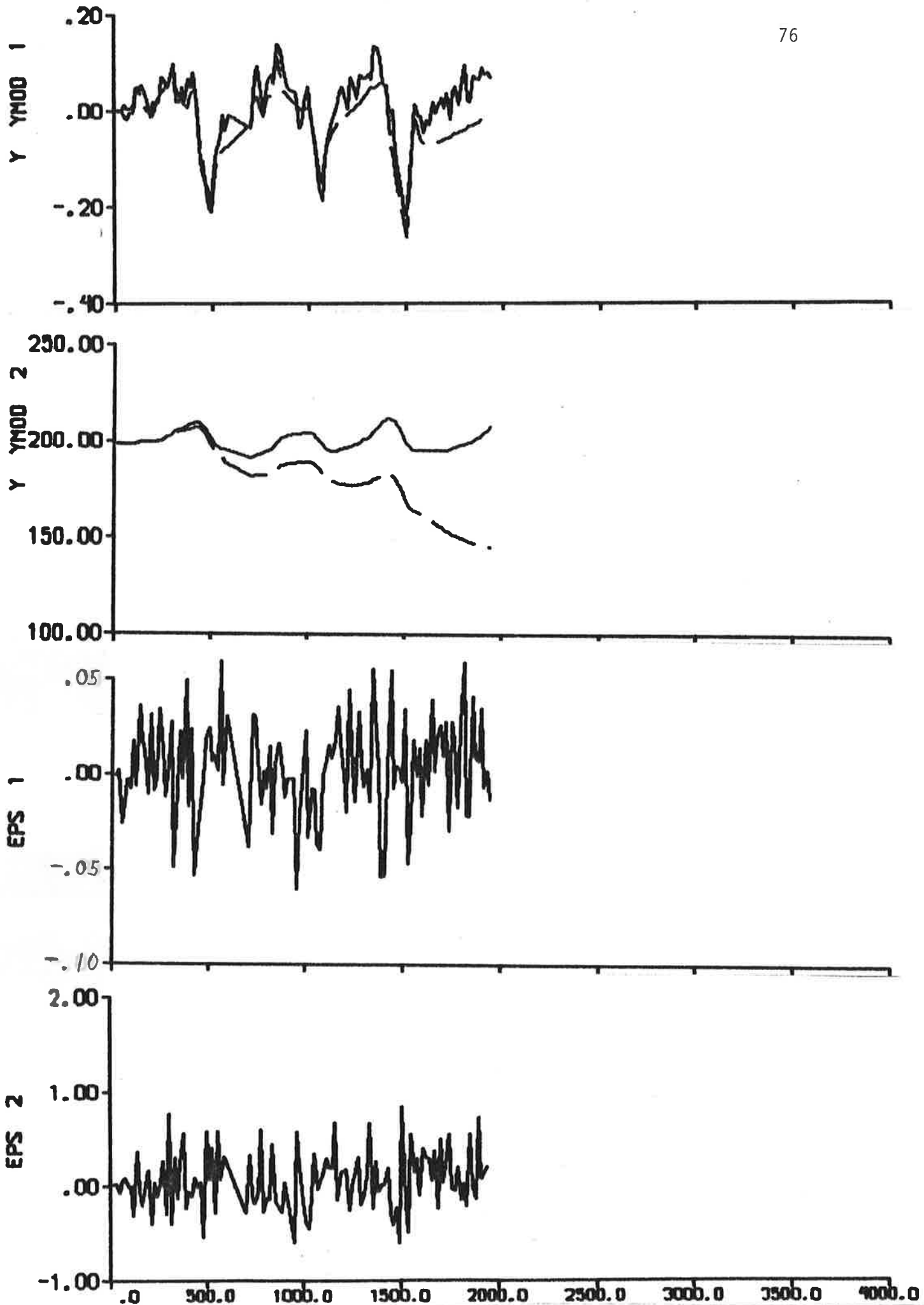


Fig. 4.4 a - Result of maximum likelihood identification to data from experiment 2, when the wind parameter φ_3 is estimated. The dashed lines are model outputs. Cf. Fig. 2.2.

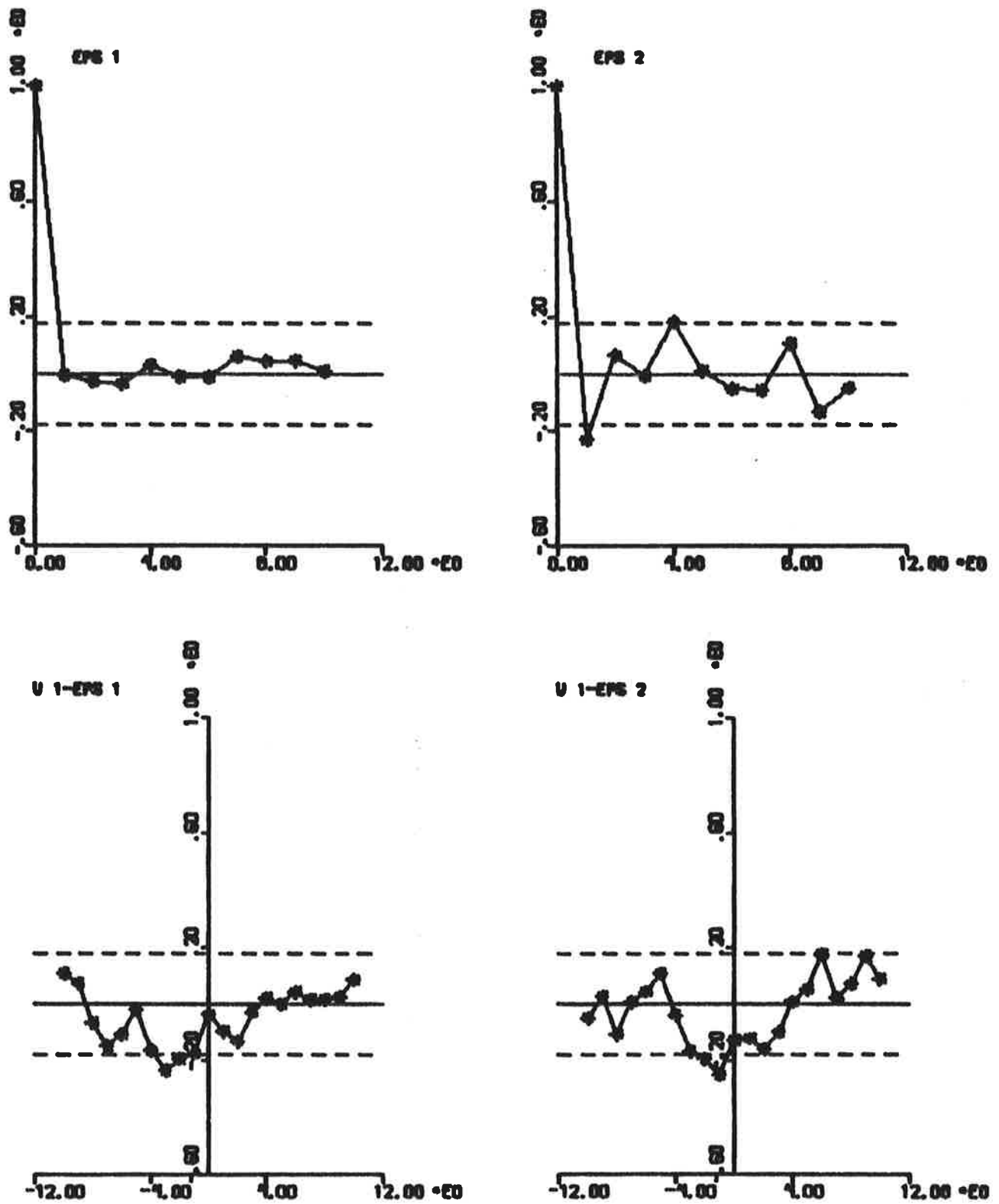


Fig. 4.4 b - Autocorrelation functions of residuals and cross correlation functions between rudder input and residuals. The dashed lines are $\pm 2\sigma$ limits.

It is concluded from Akaike's information criterion that the wind parameter φ_3 should be estimated when the output error method is applied (see Table 4.1). A good consistency between the model outputs and the measurements is obtained (see Fig. 4.2). However, the residuals are not white and the gains and time constants obtained differ significantly from SSPA:s values (see Table 4.2).

When the maximum likelihood identifications are compared it is concluded that the wind parameter φ_3 should not be estimated. The loss function V_1 obtained when φ_3 is estimated is even larger than the value obtained when $\varphi_3 = 0$. This indicates that the minimum value of V_1 was not found when φ_3 was estimated.

The model obtained from maximum likelihood identification when $\varphi_3 = 0$ is the best one according to Akaike's information criterion. However, the model outputs differ significantly from the measurements (see Fig. 4.3 a), but this discrepancy can easily be corrected by readjusting the biases φ_6 - φ_8 . Fig. 4.3 b indicates that the residuals obtained are white and almost uncorrelated to the rudder input. However, the values of K' and T_1' differ significantly from SSPA:s estimates (see Table 4.2), and it is concluded that the model obtained is unstable while SSPA:s model is stable.

There are at least two possible reasons for the difficulties met when experiment 2 is analysed:

- o The influence of non-linear effects.
- o The missing of seven consecutive readings in the middle of the experiment.

Because experiment 2 only lasted for about 30 min was it decided not to divide the experiment.

5. CONCLUSIONS

Two experiments performed on the 255 000 tdw tanker Sea Splendour have been analysed using the identification program LISPID. The output error method and the maximum likelihood method have been applied.

Measurements of sway velocities, yaw rates and headings were available from the first experiment. Since estimates of the acceleration hydrodynamic derivatives were obtained from SSPA, was it possible to determine the other six linear hydrodynamic derivatives from this experiment. A strange model was obtained when the output error method was applied to all data from experiment 1. A more reasonable model was obtained from the maximum likelihood method, but the estimated hydrodynamic derivatives differed very much from the estimates obtained from SSPA. The difficulties were probably due to a course change in the middle of the experiment and to the fact that seven consecutive readings were missed.

It was thus decided to avoid the difficulties by dividing experiment 1 into two parts, one before the yaw and one after. The application of the output error method and the maximum likelihood method to data from the first part as well as from the second part gave estimates of the hydrodynamic derivatives, which were very close to SSPA:s estimates. It was concluded that the models obtained from the maximum likelihood method were advantageous compared to the models from the output error method.

Large measurement biases were sometimes obtained when experiment 1 was analysed. These large biases were compensated by a large initial state, and it was concluded that it may be suitable to fix the measurement biases or the initial state when this model of the steering dynamics is used in the future. It was also concluded that it may be suitable to fix the relation between the rudder derivatives $-N_{\delta}'/Y_{\delta}'$ in the future, because this relation is known to be approximately 0.5.

Measurements of sway velocities were not available from the second experiment, so it was only possible to determine the transfer function relating the heading to the rudder angle. The model obtained from the maximum likelihood method was better than the one obtained from the output error method, if Akaike's information criterion was considered. However, the gain and the long time constant obtained from the maximum likelihood method differed significantly from SSPA:s estimates. The model obtained was even unstable, while SSPA:s model was stable. Two reasons for the difficulties met by using the data from experiment 2 were suggested, namely the influence of non-linear effects during the experiment and the missing of seven consecutive readings.

A wind of about 10 m/s was blowing during the first experiment, while the wind speed was 4-5 m/s during the second experiment. It was concluded from the identifications to data from both experiments that it was questionable if the wind parameters should be estimated. It seems reasonable to fix the wind parameters to zero in the future, when experiments on large tankers performed in wind speeds less than 10 m/s are analysed.

It was thus possible to determine the linear steering dynamics of the Sea Splendour by system identification techniques applied to full-scale experiments, although the analysed data had several defects. Especially the identification results from experiment 1 are very good. The maximum likelihood method has proved to be advantageous compared to the output error method, although the models obtained from the output error method in several cases are acceptable. The identification program LISPID has proved to be a powerful tool to determine the linear steering dynamics of ships.

6. ACKNOWLEDGEMENTS

This work has been supported by the Swedish Board for Technical Development under Contracts 734128 U and 754053.

The author would like to express his gratitude to Kockums Shipyard in Malmö and to the Salén Shipping Companies in Stockholm for their positive attitude to this type of research. The author also thanks Mr. J. Eriksson, Mr. L. Sten and Mr. N.E. Thorell, Kockums, who made the experiments, and Mr. K.I. Andersson, who was captain of the Sea Splendour during the experiments.

7. REFERENCES

Akaike, H. (1972):

Use of an Information Theoretic Quantity for Statistical Model Identification. Proc. 5th Hawaii International Conference on System Sciences, pp 249-250, Western Periodicals Co, North Hollywood, California.

Åström, K.J. (1970):

Introduction to Stochastic Control Theory.
Academic Press, New York.

Åström, K.J. and Källström, C.G. (1973):

Application of System Identification Techniques to the Determination of Ship Dynamics. Proc. 3rd IFAC Symp on Identification and System Parameter Estimation, the Hague/Delft, the Netherlands.

Åström, K.J., Norrbin, N.H., Källström, C. and Byström, L. (1974):

The Identification of Linear Ship Steering Dynamics Using Maximum Likelihood Parameter Estimation. TFRT-3089, Department of Automatic Control, Lund Institute of Technology, Lund, Sweden. Also available as Report 1920-1, Swedish State Shipbuilding Experimental Tank, Gothenburg, Sweden.

Åström, K.J., Källström, C.G., Norrbin, N.H. and Byström, L. (1975):

The Identification of Linear Ship Steering Dynamics Using Maximum Likelihood Parameter Estimation. Publ No 75, Swedish State Shipbuilding Experimental Tank, Gothenburg, Sweden.

Åström, K.J. and Källström, C.G. (1976):

Identification of Ship Steering Dynamics. Automatica 12, pp 9-22.

Källström, C.G., Essebo, T. and Åström K.J. (1976):

A Computer Program for Maximum Likelihood Identification of Linear Multivariable Stochastic Systems. Preprints 4th IFAC Symp on Identification and System Parameter Estimation, Part 2, pp 508-521, Tbilisi, USSR.